STRUCTURAL ARCHITECTURE AND EVOLUTION OF THE HUMBER ARM ALLOCHTHON, FRENCHMAN'S COVE - YORK HARBOUR, BAY OF ISLANDS, NEWFOUNDLAND

CHRISTOPHER R. BUCHANAN

STRUCTURAL ARCHITECTURE AND EVOLUTION OF THE HUMBER ARM ALLOCHTHON, FRENCHMAN'S COVE - YORK HARBOUR, BAY OF ISLANDS, NEWFOUNDLAND

by

A thesis submitted to the School of Graduate Studies in partial fulfillment of the requirements for the degree of Master of Science

Department of Earth Sciences
Memorial University of Newfoundland
January, 2004

St. John's Newfoundland

Abstract

The Frenchman's Cove –York Harbour area provides extensive exposure of a critical structural contact within the Humber Arm Allochthon. The Blow Me Down Ophiolite Massif is exposed in the uppermost structural slice and complexly deformed and dismembered sedimentary rocks of the Humber Arm Supergroup are located in the intermediate slices of the allochthon. The sedimentary rocks are early Cambrian- to early Ordovician-age and represent diverse depositional settings, including early rift-basins, the continental slope of the Cambro-Ordovician carbonate platform, and syntectonic flysch deposits.

Five tectono-stratigraphic domains are distinguished on the basis of lithostratigraphy, the geometries of fold-thrust systems, and overprinting criteria of successive generations of structures. Detailed analysis of the fold-fault systems demonstrates that four phases of deformation affect the area. D_1 forms recumbent F_1 folds and duplex structures, creating regional scale nappe-type structures. A regional scale F_2 antiformal culmination at Frenchman's Cove is associated with thrust faults that dismember folded F_1 duplex structures during D_2. Out-of-sequence D3 fault systems, truncate the antiformal culmination and incorporate slices of volcanic rocks in an east-verging imbricate fan, and locally form discreet mélange zones. D_4 consists of a steep northerly-striking fault system with apparent sinistral strike-slip fault displacements. The complex structural systems mapped in this area demonstrate that careful, detailed

tectono-stratigraphic studies are required to resolve the tectonic history of the allochthon and emplacement mechanisms of the Bay of Islands Ophiolite Complex.

Acknowledgments

I would like to thank my supervisors, Drs. T. Calon and E. Burden for providing both a research project and financial assistance through their grant. Their advice, encouragement, and willingness to share knowledge allowed me to grow in leaps and bounds as a geologist.

This project was supported by the Earth Sciences Sector of Natural Resources Canada through a contribution to Memorial University under the Canadian Geosciences National Mapping Program Appalachian Forelands and Platform architecture project. This support was used to complete field work in the Bay of Islands and provided analysis of palynology samples. I thank Denis Lavoie for his commitment and interest during the span of the project. Through Denis Lavoie the project was provided logistical and equipment support from the Geological Survey of Canada.

Jennifer Young, Melissa Putt, and Allison Cocker worked with me as field assistants during two summer field seasons. I thank them for the tenacity during the often brutal stream and tuck-a-more traverses in the Frenchman's Cove area. Their ability and ideas as geologists were great contributions to the project and I learned a lot about Newfoundland through them.

Mark Childs, Marlaine and Junior Childs, Jerry and Rose Sheppard, and Glen Pennel provided logistical support throughout the project. The hospitality of these generous individuals and their families made our field crews feel welcome in their communities. The quality of seamanship demonstrated by Jerry Sheppard and Glen

Pennel allowed us access to the coastal sections that would have otherwise been unavailable.

Peer support was always available to me at Memorial University. Vanessa Bennett and Don Wright provided scientific, educational, and personal support. Dr. J. Waldron, Amber Henry, and James Bradley of the University of Alberta provided many helpful discussions during field work. Exposure to their field area, ideas, and expertise on the geology of the Humber Zone was a great benefit to myself and helped to develop my knowledge of the Humber Arm Allochthon.

Finally I thank my wife, Debra Buchanan, for her fortitude, patience, and support. Without her I could not have finished this thesis. We knew it would be a crazy time in Newfoundland and it was. If we can manage this, then we can manage anything.

Table of Contents

Abstract ii

Acknowledgments iv

Table of Contents vi

List of Figures ix

List of tables xii

Chapter one: Introduction 1

1.0 Introduction 1

1.1 Study area and location 2

1.2 Regional geology of the external Humber Zone 6

1.2.1 Geology of the autochthon 6

1.2.2 Geology of the Humber Arm Allochthon in Bay of Islands 8

1.3 Purpose and scope of the project 9

1.4 Methodology 11

Chapter two: Evolution of geological thoughts on the Humber Arm Allochthon 13

2.1 Previous work in the Frenchman's Cove – York Harbour area 13

2.2 Emplacement mechanisms for the Bay of Islands Ophiolite Complex 21

2.3 Mélange development 24

Chapter three: Lithostratigraphy 28

3.1 Lithostratigraphy of the Frenchman's Cove - York Harbour area. 30

3.1.1 Blow Me Down Brook formation 30

3.1.2 Irishtown formation 31

3.1.3 Cook's Brook formation 33

3.1.4 Middle Arm Point formation 34

3.1.5 Eagle Island formation 36

3.1.6 Wood's Island and Frenchman's Cove volcanics 38

3.2 Paleontology and Palynology occurrences in study area 41
3.2.1 *Oldhamia* Occurrences 43
3.2.2 Palynology of strata of the Humber Arm Allochthon 44
3.2.3 Thermal alteration patterns from processed palynology samples 48

Chapter four: Tectono-stratigraphic domains 51

4.1 Domain 1 52

4.2 Domain 2 53

4.3 Domain 3 55

4.4 Domain 4 56

4.5 Domain 5 57

Chapter five: Fold systems 60

5.1 F_1 fold system 60

5.2 F_2 fold systems 65
5.2.1 Domain 1 65
5.2.2 Domain 2 69
5.2.3 Domain 3 74
5.2.4 Domain 4 78
5.2.5 Domain 5 82

5.3 F_3 fold systems 90

5.4 Interference patterns formed by superposition of fold generations 94

Chapter six: Cleavage development 103

6.1 S_1 cleavage 103

6.2 S_2 Cleavage 108

6.3 Cleavage development in the Blow Me Down Brook formation 111

Chapter seven: Fault systems 112

7.1 F_1 thrust faults 113
7.1.1 Domains 1, 2, and 5 113
7.1.2 Shear zone at boundary of Domains 4 and 5 115

7.2 F_2 thrust faults 118
7.2.1 Domains 1 and 5 118
7.2.2 Domain 2 119
7.2.3 Domain 3 121
7.2.4 Domain 4 125

7.2.5 Domain 5 127
7.3 F_3 thrust system 130
7.3.1 West of Frenchman's Cove 131
7.3.2 Wood's Island 133
7.3.3 South of Frenchman's Cove 134
7.5 Post F_3 faults 138
7.6 Mélange in the Frenchman's Cove-York Harbour area 141

Chapter eight: Sequence and timing of structural events in the Frenchman's Cove - York Harbour area 146
8.1 Determination of regional deformation events 146
8.2 Phases of deformation 152
8.2.1 D_1 deformation 152
8.2.2 D_2 deformation 157
8.2.3 D_3 deformation 162
8.2.4 D_4 deformation 165
8.3 Mélange vs. dismemberment and mixing during polyphase deformation 167
8.4 Proposed tectonic setting 172
8.5 Conclusions 174

References cited 179

Appendix A - Sample lists 188

Appendix B - Field stations 201

Appendix C - Geochemistry analysis 215

Insert I Geology of the Frenchman's Cove - York Harbour area, Bay of Islands, Newfoundland ..... pocket

Insert II Cross-sections for Domains 1, 2, and 3 ..... pocket

Insert III Cross-sections for Domains 4 and 5 ..... pocket

Insert IV Locations of Field Stations ..... pocket

List of Figures

Figure 1.1 Major lithotectonic zones of Newfoundland (after Williams, 1973) and the lithotectonic components of the Humber Zone (after Waldron and Stockmal, 1994). ... 3

Figure 1.2 Regional geology in the vicinity of the study area from Williams and Cawood (1989). ... 5

Figure 2.1 Development of stratigraphy in western Newfoundland and the Bay of Islands (after Botsford, 1988). ... 17

Figure 2.2 Regional cross-section through the Little Port Complex, Blow Me Down Ophiolite Massif, and the western limb of the Cook's Brook Syncline (from Williams and Cawood, 1989). ... 18

Figure 2.3 Raymond's (1984) classification for mélanges. This chart divides the continuum of dismemberment into four stages with sub-divisions based on tectonic origin. ... 26

Figure 3.1 Lithostratigraphic chart of the sedimentary rocks in the Humber Arm Allochthon. After Botsford (1988). See also Figure 2.1 for tectono-stratigraphic relationships. ... 29

Figure 3.2 Lithological sections of the Blow Me Down Brook formation. Arrow indicates younging direction of the beds. ... 32

Figure 3.3 Lithological sections of the Cook's Brook formation. Arrow indicates younging direction of the beds. ... 35

Figure 3.4 Typical lithologies of the Middle Arm Point formation. ... 37

Figure 3.5 Lithological sections of the Eagle Island formation. Arrows indicate younging direction of the beds. ... 39

Figure 3.6 Rock type and tectonic setting discrimination plots using trace elements. 42

Figure 3.7 Location of samples processed for palynology in study area. ... 45

Figure 5.1 Common morphological expression of F_1 folds in Domains 1 and 2. ... 62

Figure 5.2 Morphological expressions of F_1 folds in Domain 3. ... 64

Figure 5.3 Morphological expressions of F_2 folds in Domain 1. ... 67

Figure 5.4 Lower hemisphere, equal area projections for orientation data defining the F_2 fold-thrust system in Domain 1. ... 68

Figure 5.5 Morphological expressions of F_2 folds in Domain 2. ... 70

Figure 5.6 Lower hemisphere, equal area projections for orientation data defining the F_2 fold-thrust system in Domain 2 (Insert II, sections E-E', F-F', and G-G'-G"). ... 72

Figure 5.7 Lower hemisphere, equal area projections for orientation data defining the F_2 fold-thrust system in Domain 2b (Insert II, Section H-H'). **73**

Figure 5.8 Gently east-plunging F_2 fold in thick-bedded sandstones within Domain 3b (Insert IV, station J1001) **75**

Figure 5.9 Lower hemisphere, equal area projections for orientation data defining the F_2 fold-thrust system in Domain 3b (Insert II, Section K-K'). **77**

Figure 5.10 Lower hemisphere, equal area projections for orientation data defining the F_2 fold-thrust system in Domain 3c (Insert II, Section L-L'). **79**

Figure 5.11 Lower hemisphere, equal area projections for orientation data defining the F_2 fold-thrust system in Domain 4, on Wood's Island and Seal Island (Insert III, sections M-M' and N-N'). **81**

Figure 5.12 Lower hemisphere, equal area projections for orientation data defining the F_2 fold-thrust system in Domain 5 (Insert III, Section O-O'). **84**

Figure 5.13 Lower hemisphere, equal area projections for orientation data defining the F_2 fold-thrust system in Domain 5 (Insert III, sections P-P' and Q-Q'). **85**

Figure 5.14 Lower hemisphere, equal area projections for orientation data defining the F_2 fold-thrust system in Domain 5 (Insert III, sections R-R'-R" and S-S'). **87**

Figure 5.15 Recumbent F_2 fold related to a southwest-verging backthrust in the F_2 fold-thrust system in Domain 5 (Insert III, Section S-S'). **89**

Figure 5.16 Lower hemisphere, equal area projections for orientation data defining the F_2 fold-thrust system in Domain 5 (Insert III, Section T-T'-T"). **91**

Figure 5.17 A broken F_3 fault-propagation fold in a sandstone succession of the Blow Me Down Brook formation (Insert II, Section I-I'). **93**

Figure 5.18 Lower hemisphere, equal area projections for orientation data defining the F_3 fold-thrust system in Domain 3c (Insert II, sections I-I' and J-J'). **95**

Figure 5.19 Spectrum of interference patterns developed by the superposition of fold systems with different orientations (from Ramsay and Huber, 1987). **97**

Figure 5.20 Examples of the dominant fold interference patterns developed by the superposition of F_1 and F_2 fold systems in the map area. **99**

Figure 5.21 Possible asymmetries of mushroom-type structures, depending on the trend of the F_1 fold system at the time of F_2 superposition. **101**

Figure 6.1 F_1 folds demonstrating cleavage fanning around the hinge due to the development of longitudinal strain fields in the competent limestone beds (Insert III, Section R-R'). **106**

Figure 7.1 F_1 shear zone at the base of the Wood's Island Volcanics and the associated kinematic indicators (Insert III, Section N-N', Detail B). **116**

Figure 7.2 Style of F_2 thrust faults in Domain 3. ..... **122**

Figure 7.3 Stereoplots presenting fault plane and fault kinematic data for the late, northerly striking fault population, which overprints the area. **124**

Figure 7.4 Kinematic indicators developed in the brittle-ductile fault zone at the top of the Wood's Island Volcanics. Arrows depict the shear sense. **135**

Figure 7.5 An east-verging F_3 thrust fault separating listwanite in the hanging wall from dismembered shale and sandstone in the footwall (Insert I, station 486)..... **136**

Figure 7.6 Stereoplots presenting fault plane and fault kinematic data for the late, northerly striking fault population, which overprints the area. **140**

Figure 7.7 Fabrics and exotic blocks of mixed lithologie set in a strongly cleaved shale matrix in the mélange zone on Wood's Island (Insert III, Section T'-T"). **144**

Figure 8.1 Schematic sections depicting the evolution of broken, recumbent F_1 folds, which develop nappe-type structures. The brittle-ductile style of deformation is the result of progressive loading during the emplacement of the Blow Me Down Brook formation and Blow Me Down Ophiolite massif in the D_1 deformation event (not to scale). **155**

Figure 8.2 Schematic sections depicting the evolution of the F_2 antiformal culmination in D_2. Note the high density of F_2 thrust faults and accommodation faults in the core of the culmination, which re-imbricate the folded F_1 duplex structures (not to scale). Detailed, accurate cross-sections are presented on Insert II, sections A to H. General form of the Cook's Brook syncline is adapted from other workers (Stevens, 1965; Waldron et al., 2003)..... **160**

Figure 8.3 Schematic sections depicting the out-of-sequence F_3 fold-thrust system truncating the F_2 antiformal culmination during D_3. The F_3 faults inherit the volcanic rocks by re-imbricating D_1 duplex structures, which are re-folded by the F_2 fold system (not to scale). See Insert II, section I to J and Insert III, Section N-N', Detail C for accurate and detailed sections of the F_3 fold-thrust system. General form of the Cook's Brook syncline is adapted from other workers (Stevens, 1965; Waldron, et al., 2003). **164**

List of tables

Table 3.1 Summary of palynology results correlated to each formation of the Humber Arm Supergroup in the study area. 47

Chapter one:

Introduction

1.0 Introduction

Western Newfoundland has been of interest to geologists for over one hundred years. Some of the earliest investigations of the rocks in this region were completed by Logan (1863), helping to form his ideas about the geology of eastern Canada. The deformed rocks of eastern Canada and Newfoundland were recognized by Logan (1863) to be a part of the Appalachian Mountains of the southeastern United States. During this early time the distribution of igneous, continental and marine sedimentary rocks and their deformation patterns in orogenic belts were modelled as geosynclines (Kay, 1951). Geosyncline theories do not provide an adequate mechanism to account for the kinematics and styles of orogenic deformation, although, the models remained popular for almost a century (Reading, 1986).

In the second half of the twentieth century the rocks of western Newfoundland provided significant evidence in support of plate tectonic theory. The recognition that the

Newfoundland Appalachians contained all the components of a complete Wilson Cycle (Wilson, 1966) revolutionized geological understanding of the Appalachian Orogenic Belt. Oceanic spreading and subduction processes of plate tectonic theory provide deformation mechanisms which account for orogenic belts along plate margins and the presence of oceanic lithosphere in these belts (Bird and Dewey, 1970; Church and Stevens, 1971; Dewey and Kidd, 1974). Williams (1964 and 1979) established four northeasterly trending lithotectonic belts on the island of Newfoundland, each distinguished by characteristic stratigraphic, petrologic, and structural elements (Figure 1.1). Together the Humber, Dunnage, Gander, and Avalon zones represent the development of a stable, Laurentian continental margin, growth and collapse of the Iapetus Ocean, accretion of an exotic terrane and ultimately the docking of an outboard continental plate. These processes occurred during three phases of deformation: the Taconic, Acadian, and Alleghanian orogenies.

The Humber Zone contains the remnants of the Laurentian margin. The Hare Bay and Humber Arm allochthons preserve the distal components of the margin, providing structural windows into the architecture of the margin. The complex internal structure of the Humber Arm Allochthon contains the history of the Laurentian margin. Careful, detailed geological studies can unravel this history and describe the tectonic processes which formed western Newfoundland

1.1 Study area and location

The study area is located on the west coast of Newfoundland forty kilometres west of Corner Brook (Humber Arm 12 G\01 NTS sheet). The southern boundary of the

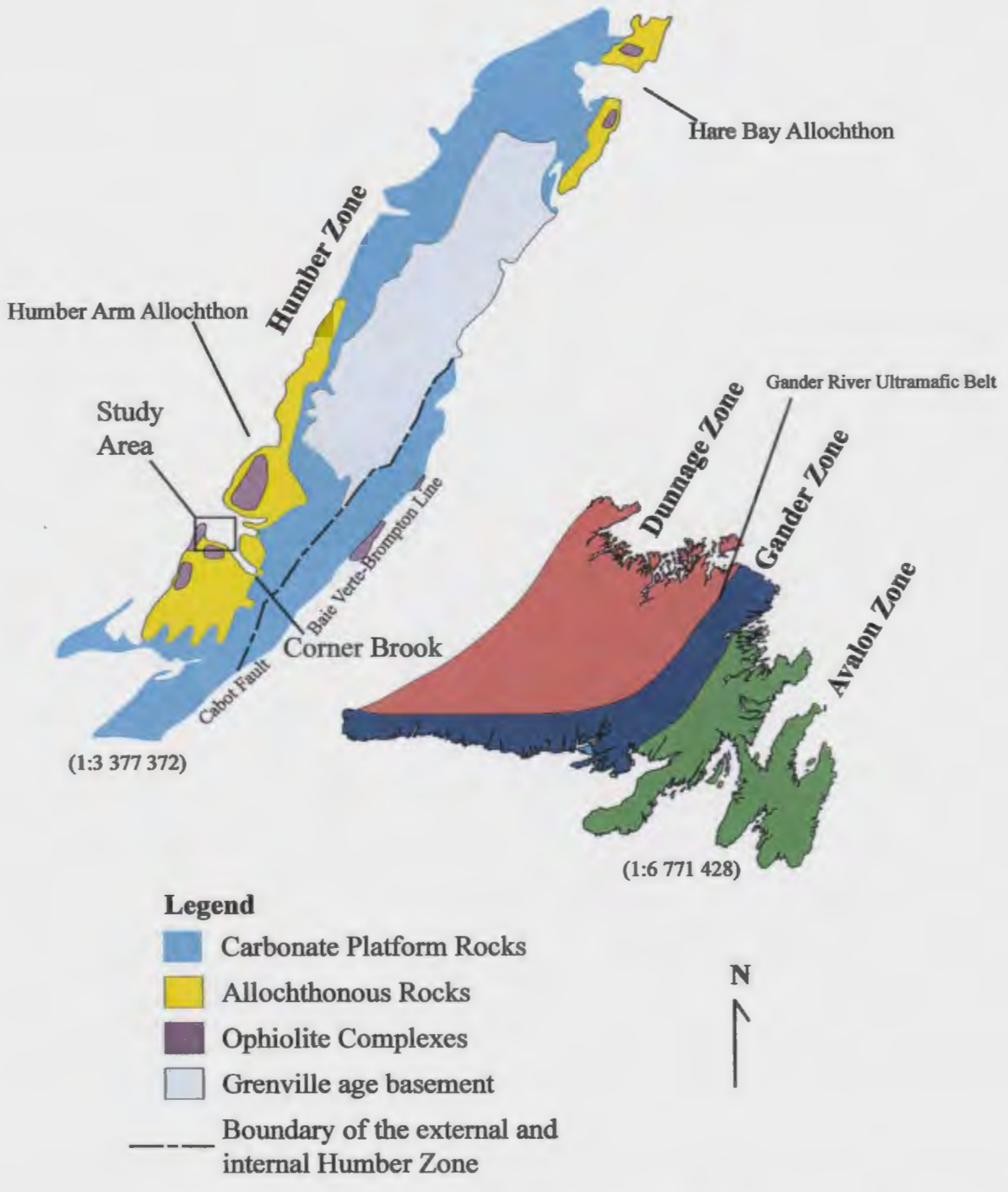

Figure 1.1 Major lithotectonic zones of Newfoundland (after Williams, 1973) and the lithotectonic components of the Humber Zone (after Waldron and Stockmal, 1994)

study area follows the northern edge of the Blow Me Down Ophiolite Massif (Figure1.2). The area also includes Governor's Island, Seal Island, and the southern shoreline of Wood's Island.

Access to the area is provided by Highway #450 on the southern shore of Humber Arm and Bay of Islands. Shoreline traverses can be started at several locations, where side roads lead to beach cabins. Boats are necessary for access to the islands and several coastal locations where sea cliffs prevent shoreline access. Submerged boulders, reefs, and rocky shorelines limit landing points and these traverses are best undertaken at low tide and when the wind is down. Experienced boatmen and dories can be hired in the communities of Frenchman's Cove, York Harbour, and Lark Harbour.

The terrane is rugged and traverses away from shoreline exposures are difficult. Vegetation covers 100% of the area, ranging from grass meadows and bog at higher elevations to tuckamore and thick second growth forest at lower elevations. In thickly vegetated areas outcrop is limited to streambeds and cliff faces on the higher hills. At York Harbour the Brooms Bottom Lowlands, a wet bog, extends south to the Serpentine River between Blow Me Down Mountain and Virgin Hills. Scree and boulder fields shed from the ophiolite massif, cover bedrock close to the massif.

Sea cliffs provide the best exposure of the deformed sedimentary rocks. Eighty to ninety percent of the twenty-seven kilometres of shoreline has exposed cliff faces and occasional wave cut platforms. Unfortunately, many of the three-dimensional relationships of the structural geology in this area are only partially displayed by largely two-dimensional exposures. Relief of the sea cliffs is generally limited to between ten

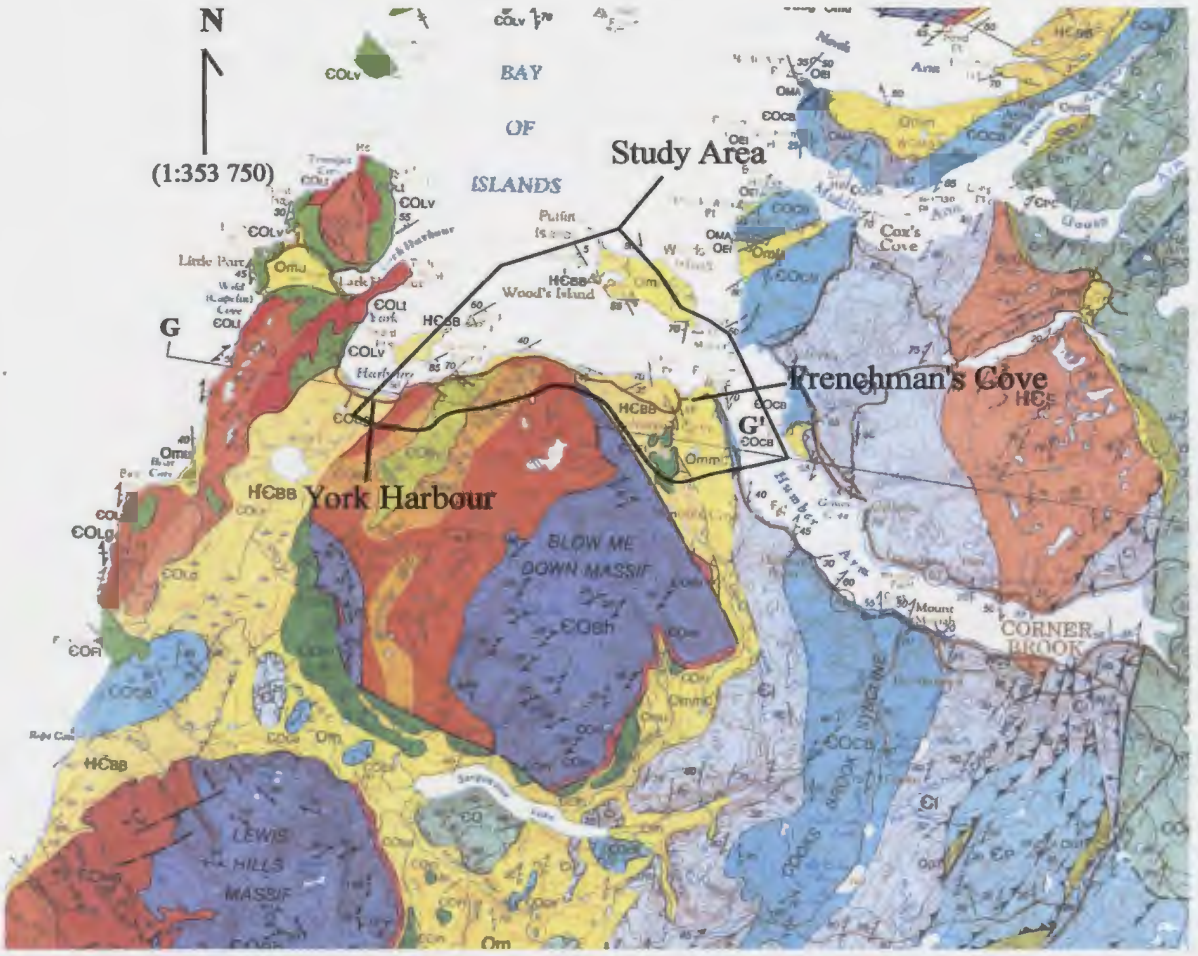

Geology Legend (from Williams and Cawood, 1989)

COL	Little Port Island Arc Complex
COFI	Fox Island River Group
COB	Blow Me Down and Lewis Hills ophiolite massifs
Om	Melange
Ommc	"Companion Melange"

Humber Arm Supergroup

HCBB	Blow Me Down Brook formation
HCs	Summerside formation
CI	Irishtown formation
CO	Platform sequence - undivided
COcb	Cook's Brook formation
OMA	Middle Arm Point formation
OEI	Eagle Island formation

Figure 1.2 Regional geology in the vicinity of the study area from Williams and Cawood (1989).

and twenty metres and rarely exceeds thirty metres, the elevation of a regionally prominent glacial terrace bordering much of the coast line.

1.2 Regional geology of the external Humber Zone

The Humber Zone (Figure 1.1) is the western lithotectonic zone of the Newfoundland Appalachians (Williams, 1979). It is characterized by two allochthonous terranes, capped by ophiolite and igneous complexes and emplaced onto the autochthonous carbonate platform during telescoping of the Laurentian margin (Figure 1.1). The western boundary of the Humber Zone is coincident with the western limit of Appalachian deformation. The intensity of deformation and metamorphism increases to the east across the zone and forms the external and internal subzones (Williams, 1975). Structural styles also change in response to the metamorphic gradient, gradually becoming more ductile. A prominent cleavage fan in the eastern portions of the allochthon is a notable feature formed because of the increasing metamorphic grade (Williams, 1975; Waldron et. al., 1998). These gradual changes in deformation regimes across a narrow belt reflect the complex deformation history of the Humber Zone during both the Taconic and subsequent orogenic events (Williams, 1975; Cawood and Botsford, 1991).

1.2.1 Geology of the autochthon

The lowest stratigraphic sequences of the autochthon are the clastic successions of the Precambrian to Middle Cambrian Labrador Group, which are deposited nonconformably on Grenville age basement of the Laurentian Margin (Williams and

Stevens, 1974; Cawood Nemchin, 2001; Waldron et al., 1998). Volcanic flows that overlie and cut these sedimentary successions have been dated at 550 Ma (Bostock et al., 1983; Krogh, 1982; McCausland et al., 1997), and suggest that initial rifting of the Laurentian margin occurred between 570 Ma and 550 Ma (McCausland and Hodych, 1998). The transition from active rifting to oceanic spreading occurred in the middle Cambrian and is marked by the stratigraphic transition from shallow water clastic sedimentary rocks to deep water shale facies of the rift fill sedimentary rocks (Williams and Hiscott, 1987; Lavoie et al., 2003). Development of an expansive, stable continental margin during a phase of oceanic spreading represents a relatively quiescent tectonic period.

The Middle Cambrian carbonate platform conformably overlies Early Cambrian rocks of the Labrador Group (Williams and Stevens, 1974). In Newfoundland the carbonate platform is subdivided into the Middle to Upper Cambrian Port au Port Group, Upper Cambrian to Lower Ordovician St. George Group, and the Middle Ordovician Table Head Formation (Waldron et. al., 1998). The presence of algal mounds, desiccation cracks, and local erosional disconformities indicates that the platform formed in a shallow water carbonate environment (James et al., 1987). A significant erosional disconformity is present between the Lower Ordovician St. George Group and the Middle Ordovician Table Head Formation (Williams and Stevens, 1974; Waldron et al., 1998). This disconformity is widespread across the autochthon, but is not distinguished in the deeper water continental slope facies preserved in the allochthons.

1.2.2 Geology of the Humber Arm Allochthon in Bay of Islands

Located in the external Humber Zone, the Humber Arm Allochthon is a strongly deformed, but largely unmetamorphosed, terrane of sedimentary and igneous rocks (Williams, 1973; Williams, 1975). The Bay of Islands provides a classic cross-section through the allochthon and frontal portion of the Appalachian Orogenic Belt, demonstrating the telescoping of oceanic crust, outer shelf and slope sedimentary rocks, and tectonic emplacement onto the shallow-water carbonate platform of the autochthon (Williams and Stevens, 1974; Williams and Cawood, 1989).

The allochthon contains four major thrust slices comprised of the Humber Arm Supergroup (Figure 1.2) and the Bay of Islands Ophiolite and Little Port complexes (Williams, 1973; Williams and Cawood, 1989). The lower slices contain the distal margin rocks of the lower to middle Cambrian Curling Group and the middle Cambrian to Tremadoc Northern Head Group. Isolated within the intermediate slice is the coarse, rift-related sandstone of the lower Cambrian Blow Me Down Brook formation. The Arenig-Llanvirn Eagle Island formation, a syntectonic flysch, is found at several structural levels of the allochthon. Igneous rocks of the Bay of Islands Ophiolite and Little Port complexes form the uppermost structural slices, lying as klippen on the sedimentary rocks of the Humber Arm Allochthon.

Structural boundaries between successive slices of the allochthon have been mapped as tectonic mélange by previous workers (e.g., Stevens, 1970; Williams and Godfrey, 1980; Waldron, 1985; Williams and Cawood, 1989; Waldron et al., 1998). Polyphase folds, penetrative cleavage, and exotic blocks in these belts form strong

structural fabrics with a chaotic appearance. The "Companion Mélange" at Frenchman's Cove (Figure 1.2) is considered to be a critical exposure of mélange at the contact between the igneous and sedimentary slices of the allochthon.

1.3 Purpose and scope of the project

Previous work in the Humber Arm Allochthon has focused on resolving the stratigraphy and structure of the Humber Arm Supergroup in the northern and eastern portions of the allochthon. Although the Blow Me Down Brook formation has been the subject of stratigraphic studies (e.g., Stevens, 1965; Quinn, 1988; Palmer et al., 2001), the allochthonous sedimentary rocks in the western portions of Bay of Islands have received little detailed research into their structural and stratigraphic architecture.

The southern shoreline of the Bay of Islands from Frenchman's Cove to York Harbour provides exposure through a steep, poly-deformed structural belt at the contact between the upper and intermediate slices of the allochthon. Within this belt, the sedimentary rocks of the Humber Arm Supergroup are overprinted by successive fold generations, related fabrics, and faults.

The main purpose of this thesis is to provide a detailed analysis of the structural architecture and deformation history in this portion of the allochthon. In light of the re-assignment of the Blow Me Down Brook formation to the Early Cambrian (e.g., Lindholm and Casey, 1989), lithostratigraphic aspects of the allochthon were re-visited in this area. Palynology samples were collected to provide new biostratigraphic data in an attempt to refine the age and stratigraphic position of stratigraphic units in the allochthon, particularly the Blow Me Down Brook formation. Previously many of the rocks in the

Frenchman's Cove - York Harbour area were assigned to mélange. However, the presence of coherent stratigraphic successions contained in fine-scale structural domains allows these rocks to be correlated with the stratigraphy of the allochthon.

A comprehensive set of structural data was collected across the boundaries of the belt. The data depicts the nature and geometry of the boundaries and structural systems developed during the emplacement and deformation of the allochthon. Detailed maps and cross-sections (Inserts I, II, and III) were compiled from continuous logs of the shoreline and delineate distinct domains of unique stratigraphy and structural relationships. The stratigraphic-structural architecture indicates that four phases of deformation have affected the Humber Arm Allochthon. The diverse nature of the documented fold\fault systems further challenges current models that this highly deformed belt is a mélange developed in a horizontal shear zone at the base of the Bay of Islands Ophiolite Complex (e.g., Williams, 1975; Waldron, 1985; Wojtal, 2001).

The tectono-stratigraphic domains are a core component of this thesis and the organization of this thesis reflects the significance of the domains. Chapter two is a review of previous work in the Frenchman's Cove area, emplacement mechanisms for the Bay of Islands Ophiolite Complex, and aspects of mélange formation. Descriptions of the lithostratigraphic units utilized to develop the structural architecture and the results of preliminary palynology studies are presented in Chapter three. An overview and descriptions of the tectono-stratigraphic domains is presented in Chapter four. Chapters' five to seven present the structural data and detailed descriptions of individual structural systems in each of the domains. Chapter eight considers the structural architecture and

deformation history developed in this thesis and its implication to current geological models of the Humber Arm Allochthon and the formation of mélange.

1.4 Methodology

The data collection for this thesis utilized standard geological field techniques. Orientation data was collected using a Freiburg fabric compass and was recorded in field books using dip\dip-direction convention. However, planar structural data is presented in the thesis using the right-hand rule (e.g., strike\dip RH - 120\45 RH)). Coastal exposures were mapped by sketching a series of continuous strip-sections of the exposed sea cliffs. The sketches are anchored approximately every fifty metres using a Garmin GPS unit. Outcrop discovered during inland traverses was located using a Garmin GPS unit and then plotted onto a regional base map using MapInfo. All collected GPS stations, structural measurements, and collected samples were entered in a Microsoft Access database.

MapInfo was used to manipulate data in the Access database and compile the final geological map (Insert I). The cross-sections (Inserts I and II) were constructed using standard structural techniques. Lower hemisphere, equal area plots of orientation data were used to analyse the geometry of the fold systems mapped in each of the structural domains. The stereographic plotting was completed using a program called GEOrient. The cross-sections are oriented perpendicular to the trend of the second generation fold-thrust systems, except in Section N-N' (Insert II), this section is an up-plunge profile of the large anticline on Wood's Island. Although fold profiles are typically constructed as down-plunge views, an up-plunge view was chosen for this

profile in order to present the geometry of the fold in the same orientation as it is viewed along the shoreline outcrop (i.e., looking north). GEOcalculator was used to convert the orientation of measured planar features (e.g., bedding, cleavage, faults, and axial surfaces) to pitches on the plane of each cross-section or fold profile. Cross-sections were chosen over fold profile sections, because the cross-sections are more visually representative of cliff exposures present in the map area. Because the F_2 folds systems are generally gently plunging the error in bed-thickness and angular relationships is not that large. Furthermore, the strong dismemberment and imbrication of the stratigraphic successions in the eastern portions of the map area limits the degree to which the fold systems can be reconstructed. Standard fold reconstruction techniques are used where it is possible to constrain the geometry of individual folds or fold trains with detailed bedding and cleavage measurements. The most notable use of these techniques are presented on Insert II, sections I to J and Insert III, Section N-N' where the extensive sections were reconstructed using Kink method techniques (Marshak and Mitra, 1988).

The textbook, titled "Basic methods of structural geology" by Marshak and Mitra (1988), presents detailed treatments of cross-section construction, fold reconstruction techniques, and techniques and methods used to analyse and manipulate orientation data on lower hemisphere, equal area plots. GEOrient and GEOcalculator are shareware programs written by Dr. R.H. Holcombe at the Department of Earth Science, The University of Queensland.

Chapter two:

Evolution of geological thoughts on the Humber Arm Allochthon

2.1 Previous work in the Frenchman's Cove – York Harbour area

The first geological surveys of western Newfoundland were broad, regional studies encompassing large areas and focusing primarily on traverses of the extensive coastal exposures. Murray and Howley (1881) and Howley (1907) produced the earliest geological maps of western Newfoundland, correlating the abundant shale and sandstone successions with the Silurian successions in Quebec.

Schuchert and Dunbar (1934) undertook an extensive geological survey of western Newfoundland in the 1920s. Based on lithology and fossil assemblages Schuchert and Dunbar (1934) grouped the shale, sandstone and carbonate sequences into seven series (Figure 2.1A). At Curling, a graptolite occurrence constrains the top of their stratigraphic succession, the Humber Arm Series (Figure 2.1A), to the Middle Ordovician. Schuchert and Dunbar's (1934) stratigraphy was a marked departure from

earlier correlations with Silurian sedimentary rocks in Quebec (Logan, 1863; Murray and Howley, 1881; Howley, 1907)

Applying the models of geosyncline development, Schuchert and Dunbar (1934) described the geological evolution of western Newfoundland as an elongate geosyclinal trough. They identified three periods of deformation related to tectonic upheaval and igneous intrusions. In the Bay of Islands Schuchert and Dunbar (1934) considered the igneous complex to be the result of middle Ordovician intrusive activity culminating with the intrusion of Devonian gabbro laccoliths. Intense folding and faulting observed in the Humber Arm Series was attributed to intrusion of the laccoliths (Schuchert and Dunbar, 1934).

Cooper (1936) and Smith (1958) recognized that the igneous rocks were over-thrust on the sedimentary rocks, but still considered the complex to have a local plutonic origin associated with volcanic rocks of region. Amphibolite grade metamorphic rocks were considered a basal aureole imprinted on the surrounding sedimentary rocks during emplacement of the complex (Cooper, 1936; Smith, 1958; Williams, 1971). Cooper (1936) named the suite of igneous rocks the Bay of Islands Igneous Complex

A series of investigations by Walthier (1949), Weitz (1953), and Lilly (1963) attempted to develop the regional stratigraphy, but due to the localized nature of the studies their stratigraphic divisions did not easily extrapolate beyond the study areas. Kindle and Whittington (1958) collected extensive graptolite and trilobite assemblages along the coast and constructed a depositional time frame ranging in age from the late Cambrian to middle Ordovician. Kindle and Whittington (1958) also described the

depositional environments of the sedimentary successions, relating them to the deep water edge of the western carbonate platform identified by Johnson (1941) and Kay (1945; 1951).

In a then revolutionary paper, Rodgers and Neale (1963) suggested that all of the allochthonous deep-water sedimentary rocks were emplaced, from the east, onto an autochthonous carbonate platform, similar to the klippe in the Taconic region of New York. This model of westerly transported terranes became the basic component for all later tectonic models in western Newfoundland (Stevens, 1965; Bruckner, 1966; Lilly, 1967; Williams, 1975). The allochthons of Rodgers and Neale (1963) consisted of the sedimentary rocks mapped by Schuchert and Dunbar (1934) as the Humber Arm Series, the Cow Head Breccia, and the Bay of Islands Igneous Complex.

The advent of the theories of continental drift, plate tectonics (Dewey, 1969) and oceanic cycles (Wilson, 1966) in the 1960's had a profound impact on the geological understanding of western Newfoundland. Plate tectonics allowed the synthesis of the Humber Zone geology into a holistic model involving a progression of tectonic settings. Departing from the igneous intrusion models of Cooper (1936) and Smith (1958), the Bay of Islands Igneous Complex was recognized as a remnant of oceanic lithosphere (Stevens, 1970; Dewey and Bird, 1971), a fundamental leap in the understanding of the geological evolution of western Newfoundland.

Stevens (1970) formalized the stratigraphy of the allochthon as the Humber Arm Supergroup containing the Cow Head and Curling groups. In the Humber Arm region, the Curling Group was subdivided into three flysch units derived from the carbonate

platform to the west, and from the advancing Taconic thrust sheets in the east (Figure 2.1D). Stevens (1970) included Bruckner's (1966) stratigraphy of the allochthon as informal formational units of the Curling Group. This informal stratigraphy is commonly used in current literature and includes the following formations: the Irishtown (Stevens, 1965), Summerside (Stevens, 1965), Cook's Brook (Stevens, 1965), Middle Arm Point (Stevens, 1965), and Blow Me Down Brook (Lilly, 1967). The Bay of Islands Ophiolite Complex was, for the first time, considered to be a far travelled thrust slice emplaced at the highest structural level of the Allochthon (Stevens, 1970).

Strongly deformed sedimentary rocks in Frenchman's Cove, previously mapped as chaotic zones, were interpreted as tectonic mélange at the contact of successive structural slices of the allochthon (Stevens, 1970). Each of the structural slices was bound by mélange formed during the transportation and assembly of the allochthon (Stevens, 1970; Williams, 1973). Regional mapping by Williams (1973), Comeau (1972), Schillereff and Williams (1979), Godfrey (1982) and Williams and Cawood (1989) delineated a broad belt of strongly deformed sedimentary rocks of the Curling Group. Rare "knockers" of volcanic and ultramafic rocks, mostly in close proximity to the ophiolite massifs, were used to define the complex belt as tectonic mélange (Williams and Godfrey, 1980; Williams and Cawood, 1989). The mélange was considered to be the tectonic contact between the Bay of Islands Ophiolite Complex and lower slices of the allochthon (Williams and Godfrey, 1980; Waldron, 1985; Williams and Cawood, 1989). The position of mélange at the boundaries of each thrust sheet is illustrated in Figure 2.2, a regional cross-section produced by Williams and Cawood (1989). The section

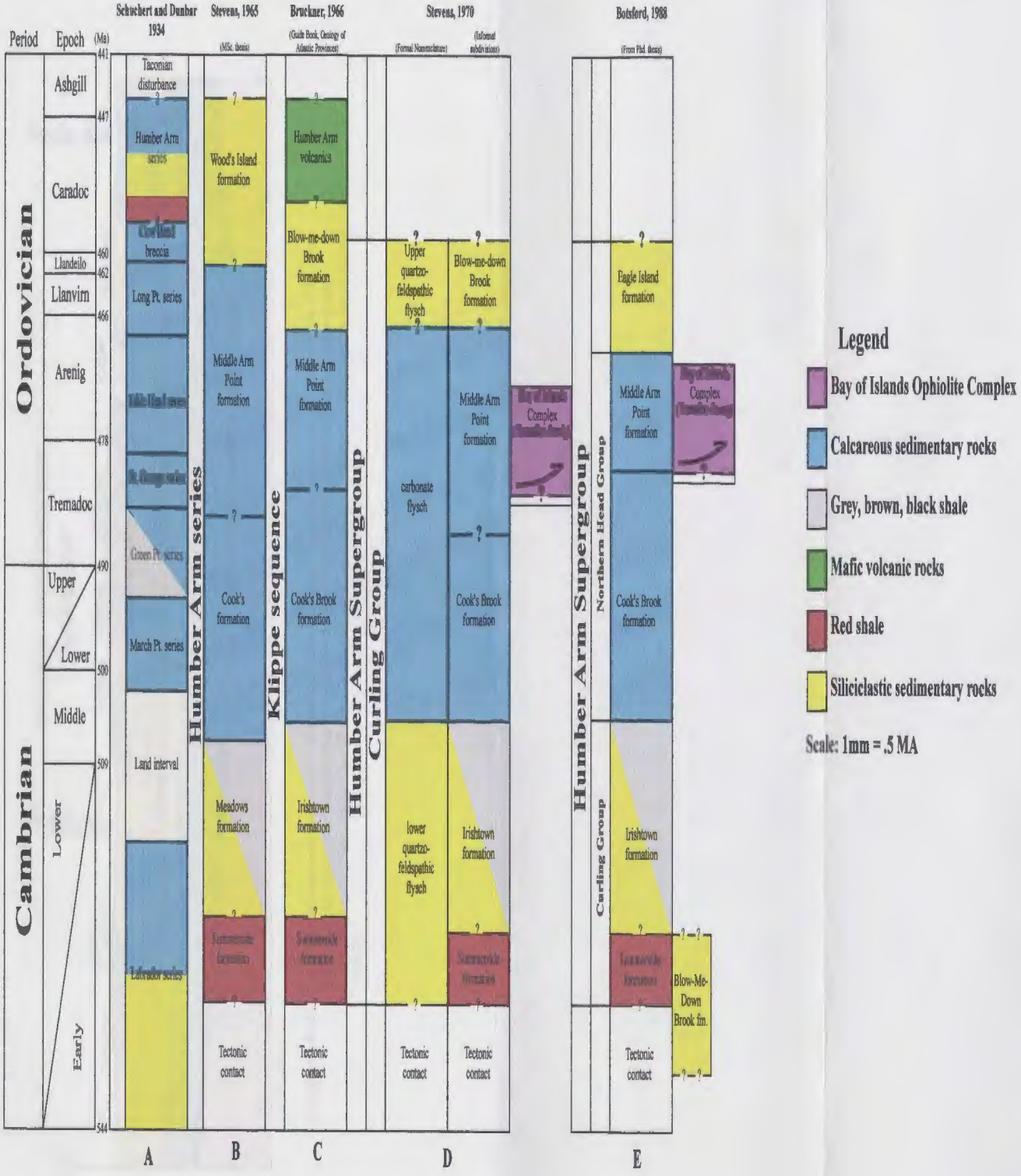

Legend

- Bay of Islands Ophiolite Complex
- Calcareous sedimentary rocks
- Grey, brown, black shale
- Mafic volcanic rocks
- Red shale
- Siliciclastic sedimentary rocks

Scale: 1mm = .5 MA

Figure 2.1 Development of stratigraphy in western Newfoundland and the Bay of Islands (after Botsford, 1988).

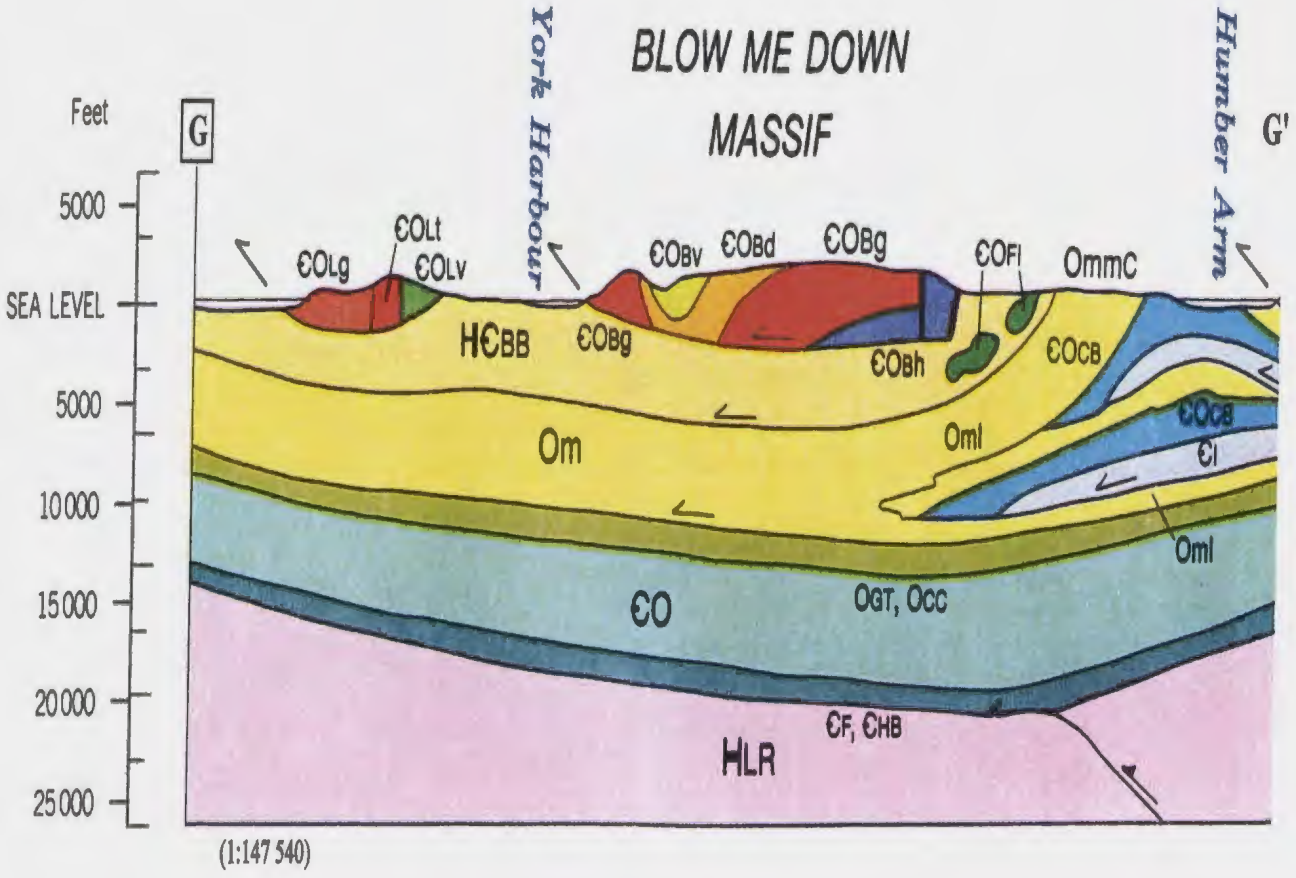

Figure 2.2. Regional cross-section through the Little Port Complex, Blow Me Down Ophiolite Massif, and the western limb of the Cook's Brook Syncline. Location of Section G-G' is shown on Figure 1.2 (from Williams and Cawood, 1989)

depicts sub-horizontal structural contacts between the Blow Me Down Brook Ophiolite Massif, mélange, and the lower, sedimentary slices of allochthon. In this configuration the ophiolite massifs must lie as klippen in the uppermost levels of the allochthon.

At Frenchman's Cove the "Companion Mélange" is an extensive belt of dismembered and polyphase deformed sedimentary rocks of the Humber Arm Supergroup, considered to be the best exposure of mélange in the area (Stevens, 1970; Williams, 1973; Williams, 1975; Waldron, 1985). Criteria used to identify mélange include shale injection, quartz filled tension gashes perpendicular to bedding, isolated fold hinges, scaly cleavage, and broken formation (Waldron, 1985). Bosworth (1984) introduced the concept of structural slicing to account for the development of rhomboidal, lens-shaped blocks during dismemberment of the stratigraphic succession. Structural slicing produces small-scale fault systems with the same geometry as larger scale thrust systems, progressively dismembering coherent bedding. Bosworth (1984) interpreted the development of mélange at Frenchman's Cove as the result of overprinting of first generation folds by a slaty cleavage associated with the development of later, second generation, east-verging folds and thrusts. Waldron (1985) also identified two generations of folds in the eastern portion of the Humber Arm, but does not discuss the implications of second generation asymmetry. Waldron et al. (1988) relates the formation of mélange to the olistostromal style slumping of poorly lithified and water-saturated sedimentary rocks of an over steepened accretionary wedge. In contrast, Wojtal (2001) interpreted fault arrays in the mélange to have developed during

thrusting in a general non-coaxial shear environment. The orientation of the fault arrays are similar to the development of conjugate Riedel shears and indicate northwest-verging shear, consistent with regional shortening in the Bay of Islands (Wojtal, 2001).

Botsford (1988) completed a detailed stratigraphic study of the carbonate flysch units in Steven's (1970) Curling Group, but this nomenclature has never been formalized in literature. Using graptolite assemblages Botsford (1988) restricted the siliciclastic Summerside and Irishtown formations to the early Cambrian Curling Group and separated the calcareous Cook's Brook and Middle Arm Point formations into the new, middle Cambrian to early Ordovician Northern Head Group (Figure 2.1). Occurrences of the Arenig graptolite *Isograptus victoriae victoriae* marked the upper boundary of the Middle Arm Point formation and established the depositional age of the Eagle Island formation, a siliciclastic Ordovician flysch unit. Lindholm and Casey (1989) discovered the Cambrian trace fossil *Oldhamia* in the shale components of the Blow Me Down Brook formation. This made it possible to separate coarse sandstone units of the Blow Me Down Brook formation from the Arenig Eagle Island formation. The revisions to the depositional age of the formations are reflected in the work of Williams and Cawood (1989). However, this map compilation does not consider the impact of these new ages to the regional distribution of each formation or the structural architecture of the allochthon.

Quinn (1992) compared occurrences of Ordovician flysch units across the Humber Arm Allochthon and described in detail the sedimentology of the Lower Head Formation and Goose Tickle Group. In this study Botsford's (1988) Eagle Island

formation was considered to be part of the Lower Head Formation (Quinn, 1992). Quinn (1995) proposed a depositional model based on the input of syntectonic sediment input via submarine canyons. The large number of sub-environments in this model accounts for the lithological diversity observed in each of the Ordovician flysch units (Quinn, 1995).

Recent mapping initiatives in the Bay of Islands area have focused on resolving the stratigraphy, regional distribution, and the structural architecture of the Humber Arm Supergroup. In the eastern portions of the allochthon Palmer et al. (2001) completed detailed surveys and measured several stratigraphic sections of the Curling Group and Blow Me Down Brook formation in an attempt to define type sections for these stratigraphic packages. The nature of deformation in the area limits the available exposures of the units and it was not possible to establish type sections (Palmer et al., 2001). Based on this mapping, Waldron et al. (2002) identified north-south striking belts formed by an imbricate stack of the Humber Arm Supergroup. In the western extent of the allochthon Burden et al. (2001) and Calon et al. (2002) demonstrated that mélange in the vicinity of the Little Port Complex can be subdivided into mappable stratigraphic units. The regional distribution and extent of these units indicate that it is possible to resolve the complex internal structure of the Humber Arm Supergroup and the allochthon.

2.2 Emplacement mechanisms for the Bay of Islands Ophiolite Complex

Ophiolite complexes in the Appalachians represent tracts of oceanic lithosphere obducted onto the Laurentian Margin (Dewey, 1969; Malpas and Stevens, 1979). In

Newfoundland prominent ophiolite belts occur in the Humber Zone and along the western boundary of the Dunnage Zone, the Baie-Verte Brompton Line (Figure 1.1). The Gander River Ultramafic Belt on the eastern boundary of the Dunnage Zone (Figure 1.1) is possibly a third ophiolite occurrence (Williams, 1975). In the Humber Zone, ophiolite complexes are incorporated in allochthonous terranes formed during the Taconic Orogeny (Williams, 1975). The source of the Humber Zone ophiolites remains enigmatic, though proximity to the Dunnage Zone suggests this eastern terrane may be a possible source. Occurrences of Early Ordovician ophiolites along the Baie Verte-Brompton Line are associated with volcanic rocks of island arc affinity (Williams, 1975). This suggests that extensive volcanic arc development occurred prior to the Taconic Orogeny (Williams, 1982). Back-arc spreading in the arcs is a possible source for creating the oceanic lithosphere represented by the ophiolite complexes. Complex structural geology, metamorphism, and poor exposure limits the extent to which this tentative link between the Dunnage and Humber zone ophiolites can be demonstrated.

Early emplacement models for the Bay of Islands Ophiolite Complex utilized gravity sliding as the primary tectonic mechanism (Rodgers and Neale, 1963, Stevens, 1970, Williams, 1975). These models suggest that each structural slice of the allochthon slides down-slope from the east, progressively building the Humber Arm Allochthon (Williams, 1975). In order to create the potential energy required for gravity slides continuous uplift must occur in the hinterland of the orogen, moving each successive slice into a structurally elevated position and providing "tectonic head" (Malpas and Stevens, 1979). Furthermore, to generate a failure with displacement in a particular

direction the uplifted rock units must dip in that general direction. Sustained orogenic uplift has not been documented during the middle to late Ordovician; limiting the possibility of gravity sliding as a mechanism for the development of the regionally extensive Humber Arm Allochthon.

Malpas and Stevens (1979) proposed the concept of tectonic underplating to describe the stacking sequence of the allochthons and the styles of deformation observed in Bay of Islands. This model suggests that the Grenville basement of the Laurentian margin is subducted eastwards beneath oceanic lithosphere and the developing island arc system (Malpas and Stevens, 1979). As subduction continues foreland propagating thrust faults detach slices of the continental margin, adding the slices to the base of the obducting plate. Mélange formed along the boundaries of the structural slices is considered to be due to the increase in hydrostatic pressure during the underplating process. In this fashion the structural stacking order of the Humber Arm Allochthon is created and the relative transport distances of the slices are preserved (Malpas and Stevens, 1979), not unlike the models proposed for the development of accretionary wedges (e.g., Karig, 1980; Charvet and Ogawa, 1994).

Ophiolite obduction during trench rollback is suggested by Cawood and Suhr (1992) as the primary mechanism for emplacement of Bay of Islands Ophiolite Complex. Trench rollback requires the presence of old, heavy oceanic crust to generate high rates of subduction. Cawood and Suhr (1992) suggest that this dense oceanic lithosphere was preserved between promontories and re-entrants of the Laurentian margin. Extensional zones are created within the outboard arc complex as the obducting plate thins to keep

pace with the retreating hinge-line of the subduction zone, generating younger oceanic lithosphere. In the extensional zones strike-slip/transform fault systems associated with active spreading centres form pop-up structures and thrust-belts that result in the initial displacement of oceanic lithosphere (Karig, 1980; Sylvester, 1988; Cawood and Suhr, 1992). In the final stages of this model continuing subduction consumes the older oceanic lithosphere and a more conventional foreland propagating accretionary wedge will develop during collision between the Laurentian continent and the younger outboard portion of the island arc systems created at the western margin of the Dunnage Zone (Cawood and Suhr, 1992). Final emplacement and transport of the ophiolites occurs in this compressional environment and assemblage of the Humber Arm Allochthon is controlled by the development of fold and thrust systems in the accretionary wedge.

2.3 Mélange development

The term mélange was first used to by Greenly (1919) at Anglesey to describe chaotic rock bodies containing igneous, metamorphic, and sedimentary blocks in a fine-grained matrix. The term was revived in the 1960's to describe similar fabrics formed in a broad range of tectonic and sedimentary settings. Tectonic settings that have been suggested included subduction complexes (Hsu, 1974; and Cloos, 1984), fore- and back-arc basins (Cowan, 1985), transform faults (Saleeby, 1979), continental slopes (Jacobi, 1984), and strike-slip complexes (Karig, 1980). Raymond (1984) suggested a narrow definition of the term mélange in order to limit application of the term to an end member of a dismemberment continuum. His definition requires that mélange units be mappable, lack coherent stratigraphic contacts, and include blocks of all sizes of both exotic and

native rock types embedded in a finer-grained matrix (Raymond, 1984). Raymond (1984) proposed a classification of mélange based on the degree of dismemberment and the inclusion of exotic material (Figure 2.3). The scheme divides the spectrum of dismemberment into four stages and sub-divides the classification based on the origin of the mélange, tectonic or olistostrome. This classification provides a simple method of identifying and describing mélange occurrences, but does not constrain the deformation paths required to create a mélange.

Mélange presents a difficult structural problem; the chaotic appearance of the fabrics requires persistent, detailed observation to unravel the structural relationships that reveal its deformation history. Two views exist regarding the strain paths required to produce these fabrics: coaxial (Cowan, 1985; Waldron, 1985) versus non-coaxial strain (Byrne, 1984; Bosworth, 1984, Needham, 1987). Coaxial strain fields require extension to occur in mutually perpendicular directions. Chocolate tablet structures and extensional veins perpendicular to bedding are often considered to have formed in coaxial strain fields (Byrne, 1984). However, it has been demonstrated that all of the fabrics observed in mélanges may also be formed in non-coaxial strain fields during the formation of multiple fold generations (Byrne, 1985; Bosworth, 1985; Needham, 1987). The transposition of early fabrics by later folding events is a common feature of polydeformed belts (Hobbs et al., 1976). The deformation of an existing planar element during transposition is dependent upon its orientation relative to the strain field of the folding event (Ramsay and Huber, 1987). As a result individual limb domains of early folds can be subjected to compression, extension or both and the fabrics characteristic of

<table>
<tr><th></th><th>Coherent Units</th><th>Broken Units</th><th>Dismembered Units</th><th>Mélanges</th></tr>
<tr><td></td><td>Stratigraphic units with internal stratal continuity</td><td>Stratigraphic units with locally broken internal stratal continuity</td><td>Rock bodies without internal stratal continuity and exotic blocks</td><td>Rock bodies without internal stratal continuity, but with exotic blocks</td></tr>
<tr><td>Diapiric and Tectonic units</td><td rowspan="2"></td><td rowspan="2">Broken formations or complexes (S or T)</td><td rowspan="2">Dismembered formation or complex</td><td>Diapiric Mélange</td></tr>
<tr><td>Tectonic Mélange</td></tr>
<tr><td>Igneous or sedimentary units</td><td>Formation (S) or Complex (i)</td><td>Endolistostrome</td><td>Polygenetic Mélange
Allolistostrome</td></tr>
</table>

Figure 2.3 Raymond's (1984) classification for mélanges. This chart divides the continuum of dismemberment into four stages with sub-divisions based on tectonic origin.

mélanges will be developed during strong transposition. Structural slicing is a second process which occurs in non-coaxial strain fields and can develop contemporaneously with transposition (Bosworth, 1984; Needham, 1987). This process develops micro- to small macro-scale fault systems with geometries identical to large scale thrust systems (Bosworth, 1984). The geometries of these fault systems are analogous to the development of conjugate riedel-type fractures and P-fractures described by Petit (1987) during brittle deformation in a simple shear environment. Structural slicing progressively dismembers a rock body with coherent stratigraphy, eventually creating broken formation. The similarity in the geometries of small scale faults created by structural slicing and thrust fault systems suggests that this process mimics regional thrust systems on a small scale within the individual regional faults.

In Humber Arm mélange is limited to discrete intervals associated with significant faults. This is interpreted to indicate formation in a non-coaxial strain field associated with both the polyphase fold and thrust systems. Igneous "knockers" in Humber Arm mélanges consist of rock types present within the Humber Arm Allochthon. This relationship is taken to suggest the mélange may have been formed late in the deformation history of the allochthon.

Chapter three:

Lithostratigraphy

The southern shorelines of Humber Arm and Bay of Islands provide extensive exposure of deformed sedimentary successions of the Humber Arm Supergroup. Five distinctive lithostratigraphic units are present in the Frenchman's Cove-York Harbour area, and are correlated with Botsford's (1988) informal stratigraphy of the Humber Arm Supergroup (Figure 3.1). These include rocks of the Blow Me Down Brook, Irishtown, Cook's Brook, Middle Arm Point, and Eagle Island formations.

Strata in the study area are highly imbricated and continuous stratigraphic sections are not present. A steep structural belt at Frenchman's Cove separates lithologies of the Curling and Northern Head groups in the east from a broad, belt of the Blow Me Down Brook formation in the west. This chapter presents lithological descriptions for each formation and the results of a preliminary palynology study of the area. By understanding the stratigraphy and paleontology of the area, the rocks can be used as a tool to help delineate structural boundaries and determine the deformation history of the area.

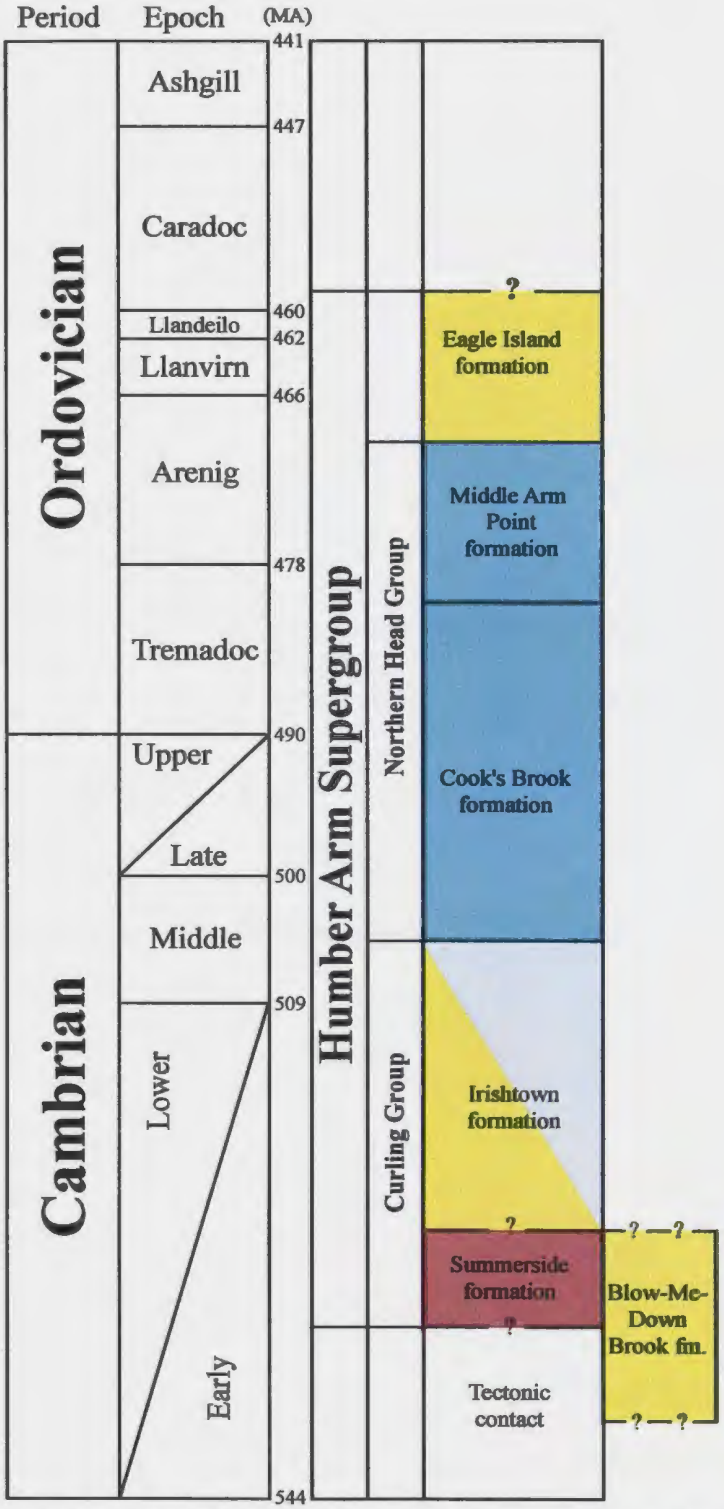

Figure 3.1 Lithostratigraphic chart of the sedimentary rocks in the Humber Arm Allochhton. After Botsford (1988). See also Figure 2.1 for tectono-stratigraphic relationships.

3.1 Lithostratigraphy of the Frenchman's Cove - York Harbour area.

3.1.1 Blow Me Down Brook formation

Lilly (1967) originally identified the Blow Me Down Brook formation and proposed a type section along Blow Me Down Brook (Insert I). Thick sandstone beds of this formation outcrop extensively in the western portions of the study area. Thrust faults and an array of northeasterly striking sub-vertical faults have broken the Blow Me Down Brook formation in to numerous, short stratigraphic sections. The Blow Me Down Brook formation is in structural contact with other components of the Humber Arm Supergroup; stratigraphic relationships with over and underlying units are obscured by the strong structural overprint.

A coarse-grained sandstone, consisting of individual, 2 to 3 metre thick, amalgamated sandstone beds is the predominant lithology of the Blow Me Down Brook formation (Figure 3.2a). Individual beds can be divided into three basic components: a basal conglomerate, massive main body, and an upper section with dewatering pipes and current depositional structures.

Each bed has a distinctive basal granule and pebble conglomerate, which lies on a scour into the underlying bed. Typically, granule and pebble conglomerate beds fine upwards into the thick (2-3m), main sandstone body. Internally the conglomerate is poorly sorted and clast supported. Clasts of angular granite, feldspar, quartz, and intraformational sub-rounded shale pebbles range in size from 2 to 20 millimetres. The

matrix of the conglomerate beds is composed of medium to fine grained quartz and feldspar grains.

The main sandstone body is poorly sorted and grain-sizes range from coarse sand to granules and small, isolated pebbles. Quartz is the primary constituent of the sandstone. Variable quantities of feldspathic fragments define a lithological range between arkosic and quartzose sandstone. The main body of the sandstone is commonly green, but ranges from greenish-grey to buff in colouration. Sedimentary structures are rare in the mostly massive sandstone bodies. Occasionally graded beds and planar and cross-laminations are present in the upper 10 to 15 centimetres of a sandstone bed. Dish-like and sheeted dewatering structures are abundant in the main sandstone. The intensity and frequency of the dewatering structures increases towards the top of the sandstone beds and are often deformed by compaction and deposition of subsequent sandstone bodies at the top of the beds.

Shale intervals within the Blow Me Down Brook formation (Section N - N') consist of 6 to 10 metres of rusty black shale with lesser amounts of red and green shale interbedded with 10 to 50 centimetre thick sandstone beds (Figure 3.2b). The sandstone interbeds are moderately sorted, often arkosic, and have abundant low-angle cross-bedding. It is within these intervals where the early Cambrian trace fossil *Oldhamia* is found.

3.1.2 Irishtown formation

The Irishtown formation, an interval of thick bedded black shale and minor, interbedded sandstone, is limited to a single imbricate slice located on the western side of

a. Predominant lithology of the formation, thick, coarse, green sandstone beds (Section N-N')

b. Thin to medium bedded sandstone shale succession. Oldhamia traces are present on the black shale beds (Section N-N').

Figure 3.2 Outcrop sections of the Blow Me Down Brook formation. Arrow indicates younging direction of the beds.

Frenchman's Cove (section H-H', Insert II).

The shale is strongly cleaved, but thin beds of the original bedding are readily apparent. Individual beds are 1 to 2 centimetres thick and packages of thin beds are 30 to 40 centimetres thick. The stratigraphic thickness of the shale exposed in this section is approximately thirty metres. Interbedded with the shale is a southwest striking, thin (8 cm), white, quartzose sandstone bed. The sandstone consists of well-sorted, fine to medium-grain quartz sand grains. The bed is discontinuous, but extends for several metres across the exposure. Small-scale ripple laminations near the top of the sandstone indicate the bed is upright; younging to the northwest. Cleavage is steeper than bedding at this locality which is consistent with the younging direction. The bedding\cleavage relationship also indicates the bedding forms the south-eastern limb of a syncline (section H-H', Insert II).

3.1.3 Cook's Brook formation

The Cook's Brook formation is characterized by ribbon-like bands of medium to thick bedded limestone and shale successions. Intervals of distinctive limestone-clast conglomerate punctuate the formation at several stratigraphic levels (Figure 3.3a). The ribbon limestone units range in thickness from 1 to 10 centimetres and are composed of very fine grained, grey limestone. Thicker, 5 to 50 centimetre calcarenite beds are commonly interbedded with the ribbon limestone successions. Lithologically the calcarenites are typically fine grained and grey in colour; some beds contain oolites. Massive beds, cross beds, convolute beds, and parallel-laminations are common sedimentary structures in the calcarenite. Sedimentary structures are typical of the B and

C Bouma sequence, suggesting the ribbon limestone and calcarenite successions in the Frenchman's Cove-York Harbour area were deposited by turbidity currents (Bouma, 1962).

Conglomerate intervals observed in the Cook's Brook formation are a distinctive and diagnostic lithology of the formation. The conglomerate beds consist of randomly oriented limestone fragments set in a carbonate matrix. The conglomerates are poorly sorted and clasts are sub-rounded to angular. Clast size is proportional to bed thickness and range in size from pebbles to large cobbles. The clasts are commonly tabular in shape, suggestive of an intraformational source. In the study area the conglomerate beds range from 15 centimetres to 2 metres in thickness. The most extensive exposure of the Cook's Brook conglomerate occurs in the hinge zone of an F2 fold located at station A2509 (Insert II, Section B-B').

Black, rusty-black, and green shale units are interbedded with the calcareous components of the Cook's Brook formation (Figure 3.3b). The thickness of the shale intervals ranges from a few centimetres to several metres. Thin (1 – 3 cm) beds of calcareous siltstone are common in the shale components of the formation. Pyrite nodules form rusty, pyrite rich lenses in thicker shale units. Patchy silicification is associated with the green shale successions, but is not extensive or limited to the Cook's Brook formation shales.

3.1.4 Middle Arm Point formation

The Middle Arm Point formation is distinguished from the Cook's Brook formation by an increase in the ratio of shale to carbonate beds and the appearance of

a. East-verging F_2 fold in a thick succession of ribbon to thick bedded limestone. The prominent thick bed is Cook's Brook Conglomerate (Section E-E', station A2509).

b. West-verging F_2 fold in ribbon bedded limestone (Section S-S', station 281).

Figure 3.3 Outcrop sections of the Cook's Brook formation. Arrow indicates younging direction of the beds.

dolostone beds (Figure 3.4a). Thin to thick dolostone beds, weathered yellow-brown, and interbedded with thick successions of green, black, and red shale characterize the Middle Arm Point formation in the area. Thickness of the dolostone bedding ranges from a 1 centimetre to 50 centimetres. Thick stratigraphic sections of thin ribbon-like beds of dolostone are common in the formation. The thicker beds commonly display crossbedding, planar laminations, and massive beds. These sedimentary structures are typical of B and C Bouma sequences (Bouma, 1962) and the successions have been interpreted as deep-water turbidite deposits by previous workers (Botsford, 1988). Figure 3.4b shows a typical dolomite bed from the Middle Arm Point formation.

Shale intervals often dominate the stratigraphy of the formation, containing variable proportions of green, black, minor red shale and few carbonate beds. Successions range in thickness from centimetres, interbedded with carbonate, to tens of metres of massive shale. Weak to moderate silicification of the shale successions is common. Pyrite nodules in are abundant in the black shale successions and commonly these intervals have a rusty appearance. Rare limestone, chert, and clastic sandstone beds are interbedded within the Middle Arm Point formation. The presence of these lithologies may indicate proximity to the stratigraphic boundaries of the formation with the Cook's Brook and Eagle Island formations.

3.1.5 Eagle Island formation

In the study area the Eagle Island formation is characterized by 1 centimetre to 2 metre beds of poorly sorted, medium to coarse grained sandstone. Quartzose sandstone is the most common lithology, but arkosic beds are occasionally present in the formation.

a. Folded and faulted succession of medium dolomite beds, black, and green shale (section E-E').

b. 35 cm thick bed of dolomitized calcarenite with convolute, planar, and massive bedding (section E-E'). Arrow indicates younging direction of the beds.

Figure 3.4 Typical lithologies of the Middle Arm Point formation.

Ribbon sandstone successions are a common occurrence in the Eagle Island formation (Section H-H' and Section Q-Q'). Lenses of polylithic conglomerate composed of granitic and shale clasts fills scours in the underlying beds and are common at the base of thicker sandstone beds. The colour of the sandstone does not show a correlation to bed thickness and ranges from buff to pale green. Sandstone of the Eagle Island formation is commonly carbonate cemented. Grey, black, and occasionally red shale units are interbedded with the sandstones (Figure 3.5a and b).

Current and biogenic structures are common in the Eagle Island formation. These structures include: climbing ripples, cross-laminations, planar laminations, flutes, and scours. Load casts and fluid escape structures are ubiquitous soft sediment deformation features in the sandstone. In thicker beds pillar and sheet structures are regularly formed. Spherical concretions, Quinn's (1992) 'cannonball concretions', are frequent in sandstone beds and seem to be unique to the Eagle Island formation as they do not occur in other siliciclastic units within the study area. Biogenic structures at the base of finer grained sandstone beds are abundant. These fossils cannot be assigned to a source fauna, but are useful for determining the younging direction.

3.1.6 Wood's Island and Frenchman's Cove volcanics

Two significant occurrences of pillow basalts are present in the area: The Wood's Island and Frenchman's Cove volcanics. The Wood's Island Volcanics are a prominent ridge of red pillow basalts which outcrop on the southern shore of Wood's Island and strike inland to the north. The volcanics form distinct flows of pillows that dip to the southwest. The form of the pillows is such that the pointed base of each pillow layer is

a. Ribbon to thick bedded calcareous sandstone of the Eagle Island formation (section H-H', station S0204).

b. Thin to very thick bedded sandstone succession of the Eagle Island formation (section R'-R", station 279).

Figure 3.5 Outcrop sections of the Eagle Island formation. Arrows indicate younging direction of the beds.

pointed to northeast, indicating the flows are upright. The upper and lower contacts of the volcanic pile are complex structural zones. The Frenchman's Cove Volcanics occur south of the town forming a series of large hills and ridges. Exposure of the hills is limited to large cliff faces with poor access. The basalts flows consist of large, well formed pillows. Indirect observation of the flows suggests they have a sub-vertical attitude. The Frenchman's Cove Volcanics are dark green to black in colour and do not show the same degree of hematite alterations as seen on Wood's Island.

The volcanics are fine grained and strongly altered to hematite, forming the distinctive colour. In many parts of the outcrop the pillows are hematite altered to the core. Individual pillows are easily recognized in the pile. The pillows have well developed chilled margins with small vesicles. Joints perpendicular to the circumference of the pillow are common in the chilled margin and terminate against the more massive core of the pillow. Interbedded parallel to the volcanic flows are thin, discontinuous beds of grey limestone. The grey limestone also fills interstitial spaces between adjacent pillows. Carbonate veins are common features cutting the pillow volcanics.

The results of analysis by ICP-XRF of a sample from the Wood's Island Volcanics are presented in Appendix C. Although the usefulness of the chemistry is limited by the lack of a statistical sample set it does present some interesting results which require further research. A discrimination plot of Nb/Y vs. $Zr\backslash TiO_2$ (Winchester and Floyd, 1977) indicates the samples lies near the boundary between basalt and sub-alkaline basalt (Figure 3.6a). Previous workers have included Wood's Island Volcanics in the Blow Me Down Brook formation and correlated the volcanics to the late

Precambrian, rift related Skinner Cove Formation (Williams, 1975; Palmer et al, 2001). Figure 3.6b is a tectonic discrimination plot (Meschede, 1986) modified from McCausland and Hodych (1998). It plots chemistry data collected by Baker (1979) for the Skinner Cove Formation. This data forms a distinct population on the Nb side of the ternary diagram, indicating the volcanic rocks of the Skinner Cove Formation are intraplate alkali basalts (McCausland and Hodych, 1998). In contrast, the Wood's Island sample is depleted in Nb and plots near the base of the ternary diagram and falls within the field that represents volcanic arc basalts or mid-ocean ridge basalt. The depleted Nb is a feature of volcanic rocks associated with island arcs and suggests these volcanics are arc related and have not been generated in a rift setting.

Due to the limited sample population the chemistry of the Wood's Island Volcanics is not conclusive. However, it does indicate that the correlation with the Precambrian Skinner Cove and Blow Me Down Brook formations may be incorrect. The possibility of an island arc origin for the Wood's Island and Frenchman's Cove volcanics should be investigated as an alternative hypothesis for the origin of these volcanic rocks.

3.2 Paleontology and Palynology occurrences in study area

Macrofossils have traditionally been used to provide ages for the stratigraphic successions in western Newfoundland. Common fossils found in the allochthon include middle Cambrian to Ordovician graptolites, trilobites, and distinctive, early Cambrian trace fossils. Conodonts are used extensively to correlate Ordovician strata of the autochthon, but the use of micropaleontology is becoming an increasingly common tool within the allochthon too. Acritarch assemblages are abundant in fine-grained

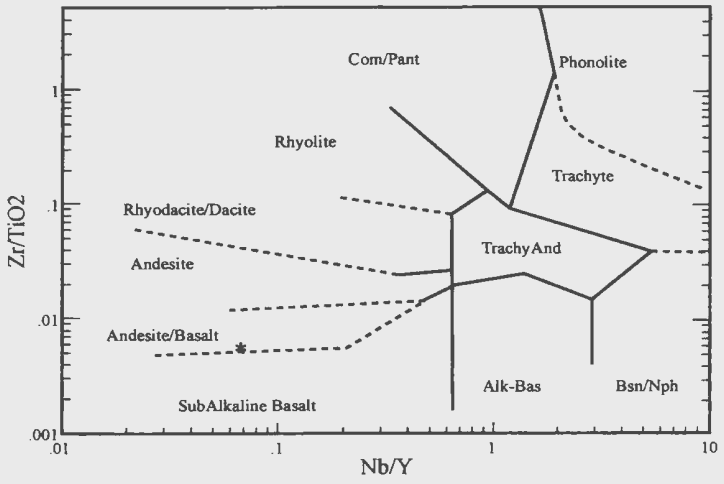

a. Geochemical discrimination chart (Winchester and Floyd, 1977) using Nb, Y, Zr, and TiO_2. (*) Sample from Wood's Island Volcanics (stn S0306, Section N-N', Insert III).

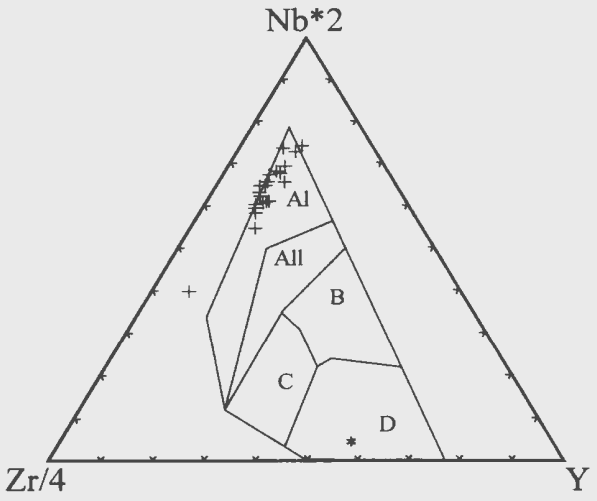

b. Tectonic discrimination plot (Meschede, 1986) using trace elements Zr, Nb, and Y. (+) alkali basalt samples from the Skinner Cove Formation, analysed by Baker (1979), (*) basalt sample from Wood's Island Volcanics. (Al) within-plate alkali basalt, (All, C) within plate tholeiite, (B,D) mid-oceanridge basalt, (C,D) volcanic arc basalt (after McCausland and Hodych, 1998).

Figure 3.6 Rock type and tectonic setting discrimination plots using trace elements.

sedimentary strata of the early Paleozoic and have been widely used for regional correlation and dating. Burden (pers. Comm.) has recovered acritarchs from all the major stratigraphic intervals of the Humber Arm Supergroup. Preliminary results indicate that acritarchs will become increasingly important for dating the sedimentary successions and for providing information about the burial and thermal maturation histories of the rocks.

In structurally disrupted sedimentary terranes good age control becomes an important tool for the reconstruction of the structural architecture of a region. In shale dominated successions, like the Humber Arm Supergroup, biostratigraphic dating of the different formations may be the only technique available to distinguish between lithologically similar formations of different ages. Two fossil forms: trace fossils and acritarchs, were used during the course of this study. Their application is discussed in the following sections.

3.2.1 *Oldhamia* Occurrences

Oldhamia Forbes, 1848, is a trace fossil occurring on bedding planes of fine grained sedimentary rocks. It is a member of the Nereites ichnofacies (Seilacher, 1967), typical of deep-sea pelagic and turbiditic deposition. Although the organism which forms *Oldhamia* is unknown, the distinctive grazing and feeding trails are considered to be created by an organism similar to worms (Seilacher, 1967). *Oldhamia* localities described from Europe, South America, and North America establish *Oldhamia* as an important index fossil for Early to Middle Cambrian strata (Lindholm and Casey, 1989).

Five *Oldhamia* sp. localities were identified and examined during the course of this field program (Insert I). Two of the *Oldhamia* sp. localities are within domains One

and Two (Insert I), which are composed of the Blow Me Down Brook formation. The other three *Oldhamia* sp. localities are located in thin imbricate slices of the Blow Me Down Brook formation in Domain Five on the eastern end of Wood's Island (Insert I and III). The identification of *Oldhamia* in these imbricates establishes sandstone-shale successions as early Cambrian and distinguishes them from the lithologically similar, but substantially younger (Arenig to Llanvirn) strata of the Eagle Island formation.

Thin bedded sandstones and black or rusty-black shale are typical lithologies of the *Oldhamia* sp. localities in the Blow Me Down Brook formation (Figure 3b, section N-N', Insert III). This is not unique, as *Oldhamia* sp. has also been found in red shale on the central portion of Governor's Island (Insert I). Although shale intervals are infrequently preserved in Blow Me Down Brook formation deposits, *Oldhamia* traces can be abundant on the bedding surfaces of the shaly intervals, typically forming in small clusters. Individual traces are 0.5 to 1 centimetre in diametre and defined by thin, straight or gently curved burrows, which meet at a common point. *Oldhamia* species are identified by habit of their traces. The traces examined from the five localities in this study display various habits: circular radial (*Oldhamia radiata* Forbes, 1848), semi-circular radial (*Oldhamia antiqua* Forbes, 1848), and dendritic (*Oldhamia flabellata* Aceñolaza and Durand 1973).

3.2.2 Palynology of strata of the Humber Arm Allochthon

Forty-two palynology samples were processed from the eastern portion of the study area (Figure 3.7). Dr. Elliott Burden at Memorial University of Newfoundland provided processing facilities and the initial, tentative identification of recovered fossils.

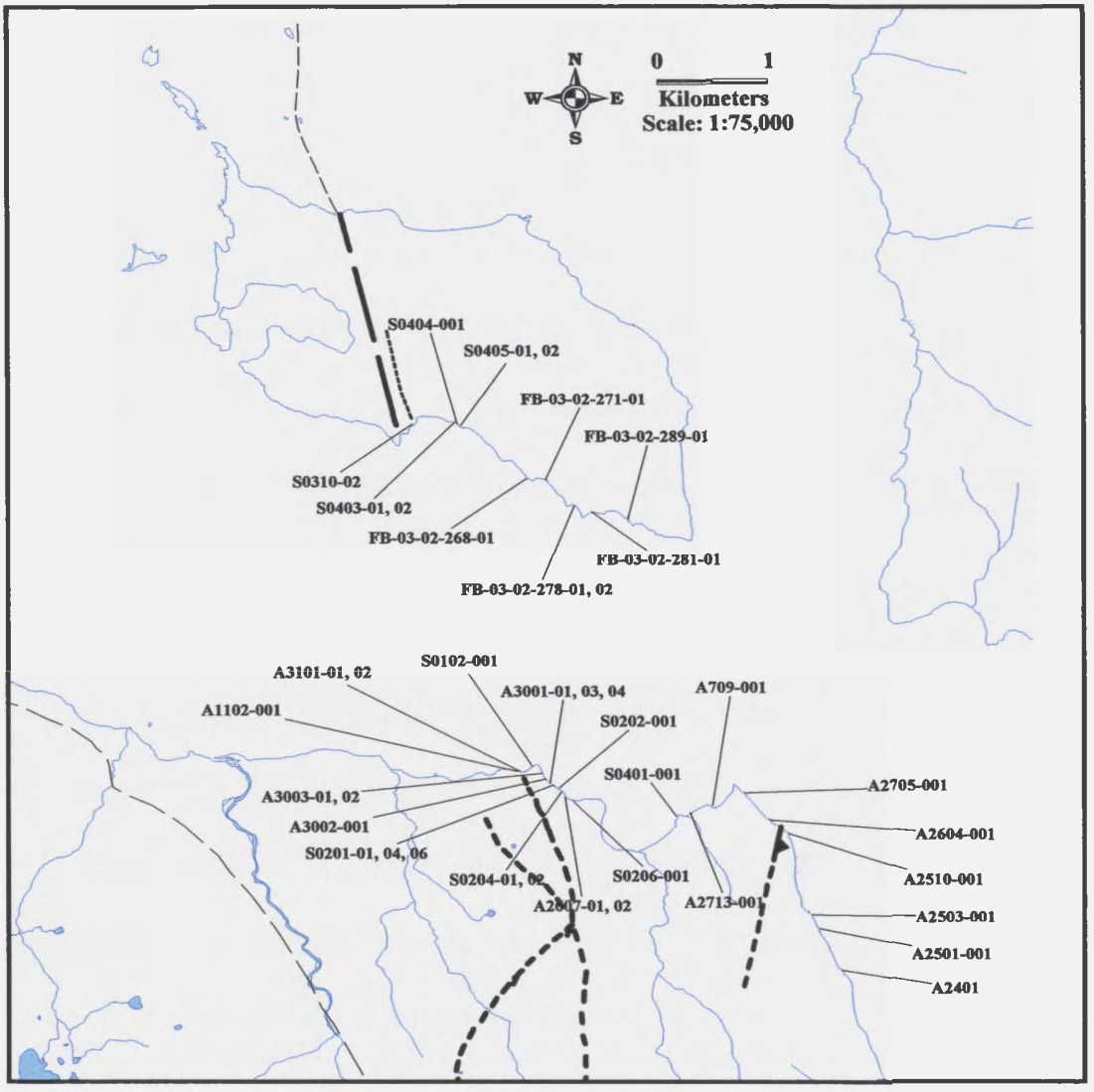

Figure 3.7 Location of samples processed for palynology in study area.

These samples are part of a regional mapping project and will be integrated into an on-going research project by Dr. Burden (pers. Comm.).

The results from this sample set are summarized in Table 3.1. Twenty-nine of the samples are carbonized and barren; non-diagnostic acritarch assemblages are present in nine samples. Four samples yielded acritarch assemblages containing the diagnostic species *Lunulidia lunula* Eisenack, 1958 and *Baltisphaeridium* sp. cf. *Baltisphaeridium crinitum* Martin, 1978. These samples were taken from sections of the Cook's Brook and Eagle Island formations on Wood's Island (sections R-R'-R" and S-S', inserts II and III).

Samples 271-01 and 281-01 contained *Lunulidia* a Tremadoc indicator fossil (Burden et al, 2001). The samples were recovered from imbricate slices, on Wood's Island and mapped as Cook's Brook formation (sections R-R'-R" and S-S' (Insert I and III). The slices lie structurally below (271-01) and above (281-01) an imbricate slice correlated with siliciclastic successions of the Eagle Island formation. The occurrences of *Lunulidia* at these two locations are associated with common lithologies in the Cook's Brook formation. This lithology\fossil relationship supports the separation of Cook's Brook and Middle Arm Point strata in otherwise barren outcrops with similar lithology.

Another acritarch assemblage, containing cf. *B. crinitum* has been recovered in samples 278-01 and 278-02, collected within an imbricate slice mapped as strata of the Eagle Island formation (section R-R'-R", Insert II). Cf. *B. crinitum* ranges from late Cambrian to early Ordovician and is not be limited to the Eagle Island formation. However, late Cambrian siliciclastic strata are not currently identified in the Humber Arm Supergroup and the presence of cf. *B. crinitum* eliminates the possibility of

Stratigraphic Unit	# of samples	Results	Age	Diagnostic Fossil	Relative Thermal Alteration
Blow Me Down Brook formatio	1	Barren	NA	NA	High
	7	Non-diagnostic	NA	NA	Low - Medium
Total	**8**				
Irishtown formation	4	Barren	NA	NA	High
Total	**4**				
Cook's Brook formation	5	Barren	NA	NA	High
	2	Diagnostic	Tremadoc	*Lunulidia*	Medium - High
Total	**7**				
Middle Arm Point formation	11	Barren	NA	NA	High
Total	**11**				
Eagle Island formation	8	Barren	NA	NA	Medium
	2	Non-Diagnostic	NA	NA	Medium
	2	Diagnostic	Tremadoc-Arenig	cf. *Baltisphaeridium crinitum*	Medium
Total	**12**				
Total Number of Samples	42				

Table 3.1 Summary of palynology results correlated to each formation of the Humber Arm Supergroup in the study area.

correlating the sandstone-shale successions with the Blow Me Down Brook formation. Lithologically, the ribbon to thick-bedded, bioturbated, coarse-grained sandstone resembles the Eagle Island formation at other localities in the region. The presence of *B. crinitum* in the distinctive strata of the Eagle Island formation on Wood's Island distinguishes these sections from otherwise similar imbricate slices containing sandstone of the older Blow Me Down Brook formation.

Palmer et al. (2001) published the occurrence of an acritarch assemblage in a sample of the Blow Me Down Brook formation on Wood's Island. Several acritarch species from the genus *Skiagia* Downie, 1981 were present in this sample. *Skiagia* is diagnostic of the Early Cambrian and is considered to be a good index fossil of this period (Burden, p. com.). Palynology samples collected from the Blow Me Down Brook formation during this study yielded assemblages of acritarchs, but none of the samples contained a diagnostic fossil. However, the recovery of even non-diagnostic acritarch assemblages allows the degree of thermal alteration within a stratigraphic succession to be assessed (see section 3.2.3).

3.2.3 Thermal alteration patterns from processed palynology samples

The thermal alteration of acritarchs is assessed on a scale established by Batten (1982). The colour of acritarchs ranges from pale yellow to black and are correlated to burial temperatures in a range of 0°C to 180°C. Thermal alteration increases with burial, from ongoing deposition or tectonic loading of a sedimentary basin and it is expected that the oldest strata should be the most altered. Discrepancies in the thermal alteration of fossil assemblages may reveal important information about the tectonic history of a

sedimentary succession.

Table 3.1 summarizes the degree thermal alteration for palynology samples processed from each formation in the study area. Black, carbonized palynodebris and unidentifiable palynomorphs are common in the Northern Head Group and the Irishtown formation. This indicates that these sedimentary successions have been exposed to temperatures in excess of 180°C (Batten, 1996). Contrasting with these highly altered fossil fragments, the acritarch assemblages recovered from the Blow Me Down Brook formation are dark shades of brown, indicating a burial temperature between 120°C and 180°C. An exception to this pattern in the Blow Me Down Brook formation is sample 289-01 (Figure 3.7). The palynological residue recovered from this sample is high in organic content, but is strongly carbonized and thermally altered to black. Sample 289-01 is located in close proximity to the floor thrust of an imbricate slice of Blow Me Down Brook formation. It is possible that higher fluid flows may have altered the hanging wall rock. Sample 289-01 is located much further east than most samples from the Blow Me Down Brook formation, which are clustered along the western boundary of the east verging thrust system and are proximal to the large, western domain of Blow Me Down Brook formation. Samples recovered in the Eagle Island formation consist of brown to dark brown palynomorphs. This range represents an intermediate level of thermal alteration for the Humber Arm Supergroup stratigraphy and suggests burial temperatures of 120°C to 180°C.

The observed thermal alteration patterns in the stratigraphy of the Humber Arm Supergroup do not match the expected pattern of increasing alteration during increased

burial and older rocks. The stratigraphically intermediate, middle Cambrian to early Ordovician, Northern Head Group has the highest thermal alteration of sedimentary rocks in the Bay of Islands. The least altered formation, the early Cambrian Blow Me Down Brook formation, is the oldest stratigraphic unit in the area. This unique pattern of the distribution of thermally altered rocks reflects the complex tectonic history of the allochthon.

Chapter four:

Tectono-stratigraphic domains

The geology of the Frenchman's Cove-York Harbour area is complex and highly variable from one location to another. The coastal section at Frenchman's Cove can be divided into five tectono-stratigraphic domains based on distinct lithostratigraphy and structure (Insert I). Structural criteria used to identify the five domains include: fold geometries considering, in particular, aspects of style, fold vergence, facing, associated fabrics, generations of structures based on overprinting criteria, orientation patterns of fold and fault systems, and other minor structures. This chapter outlines the criteria used to delineate each of the tectono-stratigraphic domains in the Frenchman's Cove-York Harbour area. Successive generations of structures as indicated by their labels (e.g., F_1, F_2, etc.) do not correlate in a simple manner between the structural domains and the sequences of generations are defined in each domain based on the observed criteria in that domain (see Chapter eight).

4.1 Domain 1

Domain 1 is the eastern most structural domain mapped in the area (Insert I and Insert II, sections A to E). It is located on the western limb of the Cook's Brook Syncline, a regional structure (Williams, 1975; Waldron, 2002). The well exposed sections of thin to thick limestone beds display the relationships between successive generations of structures and offer the best opportunity to analyse the structural architecture and evolution in this portion of the allochthon.

The structure of this domain is defined by a thinly imbricated break-thrust\fold system that is interpreted as a set of second generation (F_2) structures. The F_2 fold system is a series of northwest-verging, close to tight fault propagation folds developed on both meso- and macroscopic scales. An older generation of northwest-verging folds (F_1) is preserved as isolated, rootless fold hinges and causes several short downward facing backlimb panels within the north-west verging F_2 fold system. The distribution of broken F_1 fold elements suggests that originally macro-scale F_1 fold structures were present. Axial planar cleavage (S_1) is associated with the F_1 folds and is folded by the F_2 fold system. Progressive transposition of the S_1 fabric by the second generation (crenulation) cleavage (S_2) results in the formation of the intense scaly fabric observed in Domains 1, 2, and 5. Distinguishing the two generations of folds is locally difficult in the more dismembered sections of the domain. A detailed analysis of fold overprinting relations, fold style, and orientation patterns is presented in sections 5.2.1 and 5.4.

The F_2 fold\thrust system has a significant effect on the distribution of lithologies within the domain (Inserts I and II). The stratigraphy of Domain 1 comprises successions

of the Northern Head Group. Limestone-shale successions of the Cook's Brook formation form the main stratigraphic component and a small imbricate slice of the Middle Arm Point formation is preserved at the western end of Domain 1 (Insert II, Section E-E').

Only the western boundary of Domain 1 was mapped during this project. It is a structural contact defined by a prominent, easterly-dipping break-thrust fault through the forelimb of a northwest-verging macro-scale F_2 anticline. The fault creates two sub-domains, emplacing rocks of the older Cook's Brook formation over rocks of the Middle Arm Point formation. The hanging wall domain (1a) contains a large, meso-scale F_2 anticline formed in sedimentary rocks of the Cook's Brook formation. Domain 1b, in the footwall, is a displaced portion of the Middle Arm Point formation. The geometry of structures in Domain 1b is consistent with formation in the steep limb of the macro-scale F_2 anticline. By breaching the forelimb of the F_2 fold, the break-thrust preserves structures and sedimentary rocks from the core of the F_2 anticline (Insert II, Section E-E').

4.2 Domain 2

Domain 2 is located in Frenchman's Cove and comprises the most strongly and complexly deformed rocks in the Frenchman's Cove - York Harbour area (Insert I and Insert II, sections E to H).

The structural architecture of Domain 2 is defined by a southeast-verging F_2 fold\fault system and a significant, late oblique-slip fault system, which overprints the central portion of the domain. The F_2 fold system overprints an older northwest-verging

F_1 fold system with features similar to those seen in Domain 1. The switch in vergence direction of the F_2 fold-thrust system, from northwest to southeast, occurs in at the contact of Domains 1b and 2a (Insert II, Section E-E'). Domain 2 is divided into two sub-domains based on the late fault system and the orientation and style of F_2 folds (Insert II, Section G-G'-G"). Domain 2a is a distinctive belt of steep bedding and strong S_1 fabric development in lithologies of the Middle Arm Point and Eagle Island formations (Insert II, section E-E' to G-G'-G"). Domain 2a represents the internally broken, steep limb of a gently south plunging, easterly-verging macro-scale F_2 fold. Elements of the F_2 fold system have been rotated by the northeast-southwest striking, late fault system. The alignment of structures in Domain 2b with the trend of the fault system is demonstrated on Insert I. Domain 2b consists of highly imbricated successions of Blow Me Down Brook, Irishtown, Cook's Brook, and Eagle Island formations with gentle to moderate westerly-dips (Insert II, Section H-H'). Northwest-dipping thrust faults create thin imbricate slices, which display out-of-sequence stratigraphic-structural relationships. The geometry and style of the imbricate stack developed in Domain 2b is consistent with formation in the upward facing back limb domain of a larger macro-scale F_2 fold, but break-thrusts have caused considerable stratigraphic excision.

Both the east and west boundaries of Domain 2 are complex structural zones. The east boundary is coincident with the switch in vergence of the F_2 fold system west of a truncated duplex structure at the boundary of Domains 1b and 2a (Insert II, Section E-E', 1245 m). A broad belt of Middle Arm Point formation lies in the steep limb of a macroscopic F_2 fold is thrust eastwards over the duplex structure. The west boundary of

Domain 2 is located in the footwall of a late, west-dipping thrust fault, which emplaces the extensive successions of Blow Me Down Brook formation in Domain 3 over the mainly younger sedimentary rocks in Domain 2 (Insert II, Section I-I').

4.3 Domain 3

Domain 3 is the most extensive of all the structural domains within the map area. It extends along the shoreline from Shoal Point, west of Frenchman's Cove, to Brooms Bottom Lowlands in York Harbour (Insert I). The domain consists entirely of thick sandstone packages interbedded with thin shale intervals of the Blow Me Down Brook formation.

There are three generations of folds associated with thrust faults in this domain. The macroscopic, open, north- to northwest-verging F_2 fold-thrust system defines the structural architecture of the domain. The older (F_1) fold system is only sporadically exposed as highly broken, anomalously facing panels in the F_2 fold system and its significance in the domain is difficult to determine (Insert II, Section K-K'). The youngest fold system (F_3) is confined to a narrow belt along the east boundary of the domain (Insert I). The F_3 folds are close to tight, east-verging fault propagation folds, which are broken by thrust faults (Insert I and Section II' and JJ' on Insert II). A weak axial planar cleavage developed in the shale is associated with the F_2 fold system, but is not extensively developed in the thick sandstone beds of the Blow Me Down Brook formation.

Three sub-domains are distinguished by variations in orientation of the F_2 and F_3 fold-thrust systems. Sub-domain 3a is located on the east side of the domain and is a

narrow belt with architecture controlled by east-verging F_3 fault propagation folds (Insert I and Insert II, sections I-I' and J-J'). Sub-domain 3b is located in the central portion of the map area, northeast of the Blow Me Down Massif (Insert I). In this sub-domain the north-verging F_2 fold-thrust system is extensively developed and both forelimb and backlimb domains of this fold system can be mapped over large areas; inland and along the coast. The F_2 folds form meso- to large macroscopic folds associated with south-dipping thrust faults. Sub-domain 3c is similar to Sub-domain 3b, but here the F_2 folds and related thrust faults verge more to the northwest. The change in orientation from Domain 3b to Domain 3c is subtle and a lack of outcrop along the trend of the fold-thrust systems in the central part of the coastal section precludes a detailed analysis of the transition between sub-domains.

The west boundary of Domain 3 lies in the Brooms Bottom Lowlands, but is not exposed in the extensive bog (Insert I). The east boundary, west of Frenchman's Cove, is well exposed along the shoreline. The F_3 fold-thrust system emplaces Domain 3 over Domain 2, forming a regionally significant structural contact (Insert II, Section I-I').

4.4 Domain 4

Domain 4 encompasses outcrop of the Blow Me Down Brook formation on the west portion of Wood's Island, Governor's Island, and Seal Island. The architecture of the domain is defined by a macroscopic, northwest-verging fold\fault system (Insert III, Sections M-M' and N-N'). A prominent anticline on Wood's Island indicates the fold system in the domain consists of large, open to close polyclinal kink-style folds, which strongly resemble the geometry of fault propagation folds. Thick sandstone packages

with minor, thin shale intervals dominate the lithology of the domain.

The east boundary is well exposed along the shoreline of Wood's Island (Insert I). Previous workers (Waldron, 1985; Williams and Cawood, 1989) have mapped this boundary as a normal stratigraphic contact between the Blow Me Down Brook formation and the Wood's Island Volcanics. However, a profile construction of the large fault propagation fold on the west end of Wood's Island demonstrates that a fault contact exists between the sandstone and mafic volcanics (Insert III, Section N-N'). The mafic volcanics form an imbricate sheet within an east-verging thrust system that is incorporated in Domain 5. Therefore, the east boundary of Domain 4 is delineated by the roof fault of the Wood's Island Volcanic imbricate slice and is an important structural boundary in the region.

The west boundary of Domain 4 lies under Bay of Islands, which obscures the transition with Domain 3. The style of folds and lithologies in the two domains are similar, but the orientation of the fold system in Domain 4 is more to the northwest. Governor's Island appears to straddle the boundary between the domains, however, only a short length of its shoreline provides outcrop exposure. The orientation of bedding on the island is most compatible with Domain 4, but may also reflect changing patterns in Domain 3c. The transition between Domains 4 and 3c will never be resolved by outcrop mapping and remains enigmatic in this thesis.

4.5 Domain 5

Domain 5 encompasses the southern shoreline of Wood's Island east of the Wood's Island Volcanics. Fine-scale imbricate fault panels within Domain 5 contain

lithologies of the Blow Me Down Brook, Cook's Brook, and Eagle Island formations. Volcanic, igneous, and sedimentary rocks are also incorporated into a narrow belt of mélange at the east end of the island (Insert I). The overall structural styles and panels of shale-dominated Blow Me Down Brook formation distinguish Domain 5, setting it apart from Domains 3 and 4.

The western portion of the domain is characterized by an east-verging F_2 fold system and associated thrust faults (Insert III, section O to R). A switch in F_2 fold vergence, from east to west, occurs in the central portion of the domain (Insert III, Section R'-R"). Reclined, tight folds characterize both the east- and west-verging F_2 fold systems. A short panel within the west-verging F_2 fold system contains recumbent, west-facing, east-verging F_2 folds (Insert III, Section S-S'). An older (F_1) generation of overturned folds cause the development of locally downward facing F_2 folds and are preserved as rootless fold hinges in the more strongly dismembered stratigraphic successions. Fabric development in Domain 5 is primarily associated with the F_1 fold system. The S_1 cleavage is axial planar to F_1 folds and defines the second generation fold system. The F_2 fold-thrust system in Domain 5 is overprinted by late, sub-vertical faults with significant strike-slip displacement. These faults obscure the contact relationships between structural panels in Domain 5 and create a problem with correlation of fold generations across the domain.

A belt of mélange is present on the south-eastern end of Wood's Island (Insert I and Insert III, Section T'-T"). The mélange consists of strongly sheared shale with a steep, close-spaced, scaly cleavage. Blocks of gabbro, mafic volcanics, listwanite,

limestone, and sandstone are entrained within the scaly fabric of this mélange. The west boundary of the mélange is a sub-vertical reverse shear zone and the east boundary is a east-dipping thrust fault, which emplaces sandstone and shale of the Blow Me Down Brook formation structurally over the mélange (Insert III, Section T'-T").

Chapter five:

Fold systems

5.1 F_1 fold system

An important aspect of the structural geology in the structural domains is the effect of early meso- to macro-scale folds (F_1) on later fold generations. The F_1 fold systems are responsible for: sections of overturned bedding, downward facing meso- to macro-scale F_2 folds, and anomalous sections of F_1 steep limbs transposed in the steep limbs of younger, macro-scale folds. In addition, the original orientation patterns of the bedded successions within the F_1 fold systems have a strong effect on the orientation and style of the F_2 fold systems. F_1 folds are present throughout the Frenchman's Cove-York Harbour area, but they are rarely preserved as complete and coherent structures. Therefore, it is difficult to present a comprehensive analysis of the F_1 fold systems as developed prior to superposition of younger structures. Mechanical stratigraphy is defined by distinct rheological contrasts between lithological units and is an important control on the style of the F_1 fold systems. The frequency of F_1 folds is greater in the

shale dominated sections of Domains 1, 2, and 5. In the thick-bedded sandstone packages of Domains 3 and 4 the F_1 fold systems are weakly developed.

In Domains 1, 2, and 5 the F_1 folds are observed as small, meso-scale parasitic folds located on the limbs of macro-scale F_2 folds. The small F_1 folds can be directly distinguished from F_2 parasitic folds in cases where superposed fold geometries are observed on the outcrop. In the absence of interference patterns F_1 folds are positively distinguished from F_2 folds, when the F_1 folds show the opposite sense of asymmetry compared to that of the parasitic F_2 folds, given their positions in larger F_2 fold systems. Figure 5.1a is an example of this particular relationship; the west-verging F_1 fold preserved on a F_2 steep limb should have s-type asymmetry, not z-type, if it were to be a parasitic F_2 fold (Insert II, Section A-A', Detail A). Rootless F_1 folds in the form of isolated hinge sections are another common expression of the F_1 fold system, particularly in Domain 1. These 'cannons' are the remnants of dismembered F_1 folds, which have experienced an unknown amount of rotation during subsequent deformation events (Figure 5.1b). Isoclinal, interfolial F_1 folds are relatively abundant in shale intervals and occasionally are also observed in the bedded successions. The preservation of F_1 wave trains is rare in any of the domains and particularly in the shale dominated sections of Domains 1, 2, and 5. Upward facing F_1 folds predominate despite extensive refolding of the F_1 fold system in most sections. The refolding of bedded sections in overturned F_1 fold limbs has locally created downward facing F_2 fold trains, which typically occur in narrow imbricate panels (Insert II, Section E-E'). This spatial distribution of upward and downward facing F_2 fold trains indicates that the macroscopic F_1 fold system was

a. Downward facing, asymmetric isoclinal F_1 fold (yellow) on overturned limb of upward facing and west-verging F_2 fold (red). The F_1 fold remnant represents an orginally west-verging and upward facing parasitic fold in the restored F_1 fold geometry (Insert II, Section AA', Detail A).

b. A rootless F_1 fold hinge. These 'cannons' are a common expression of the dismembered F_1 fold system.

Figure 5.1 Common morphological expressions of F_1 folds in Domains 1 and 2.

markedly asymmetric. The F_1 folds consisted of long, gently dipping backlimb panels predominating over more steeply dipping and downward facing, short forelimb panels. In all of the domains the F_1 fold systems are consistently upward facing and west-verging.

The geometry of the F_1 fold system has a significant effect on the development of younger fold generations. The orientations of F_1 limb domains and the asymmetry of the F_1 fold systems exerts a primary control on the orientation patterns and variation in cylindricity of the F_2 fold systems. In Domains 1, 2, and 5 the presence of both hook- and mushroom-type fold structures, corresponding to Ramsay's (1967) Type 2 and Type 3 interference patterns, are present in thinly bedded successions of the Northern Head Group (e.g., Insert III, Section R-R', Detail A). The development of these interference patterns and their significance for the geometric and kinematic relationships between the F_1 and F_2 fold systems are discussed in detail in section 5.4.

Only a few examples of F_1 folds have been observed in the thick-bedded sandstone successions and subordinate shale intervals that define Domain 3. Section K-K' (Insert II) depicts an out-of-sequence thrust truncating an F_2 duplex in Domain 3b. In the footwall of the roof thrust an isoclinal F_1 fold hinge is refolded by an F_2 synclinal antiform (Figure 5.2a). The geometry and orientation of this fold and its relationship to a folded F_1 thrust indicates the F_1 fold system in Domain 3 is also verging to the northwest. Downwards facing F_2 folds are also present in shale intervals of the Blow Me Down Brook formation in Domain 3, demonstrating that F_1 folds formed in these intervals too (Figure 5.2b). Slickensided bedding surfaces are very common in the sandstone

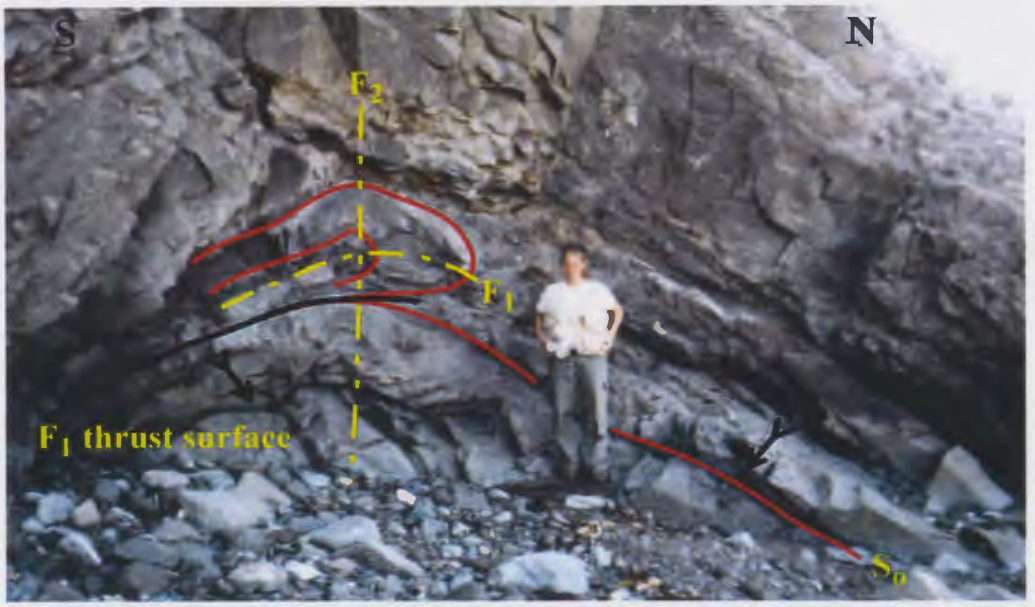

a. Broken F_1 fold, refolded by an F_2 synformal antiform (Insert II, Section KK').

b. Detachment zone in a shale bed with downwards facing F_2 fold in Domain 3c. See insert IV, station J1801 for location of outcrop.

Figure 5.2 Morphological expressions of F_1 folds in Domain 3.

succession and indicate that bedding parallel slip is an important feature of the developing flexural slip folds in Domain 3. The shale intervals are incompetent compared to the thick sandstone beds and act as detachment zones, partitioning the strain developed during the deformation events.

In Domain 4, F_1 folds have not been directly observed due to limited outcrop exposure and could not be accurately reconstructed in cross-section based on available field data. However, variations in the orientations and facing directions of bedding, particularly on Wood's Island and Governor's Island, strongly suggests that macro-scale F_1 folds must be present in this domain (Insert I). The geometry of the superposed F_2 fold system is strongly affected by the presence of the cryptic F_1 fold system in Domain 4. The relationship between the two fold systems is discussed in section 5.2.4.

5.2 F_2 fold systems

The orientation and style of F2 folds varies considerably across the map area. The style and vergence directions of asymmetric F_2 fold systems are important criteria for distinguishing the five tectono-stratigraphic domains. Furthermore, a thorough analysis of the F_2 fold systems is critical to fully understand and determine the sequence of deformation events in the Frenchman's Cove-York Harbour area.

5.2.1 Domain 1

Domain 1 is characterized by the formation of overturned, gently southwest plunging, moderately inclined F_2 folds with close to tight interlimb angles (Insert II, sections A to E). The presence of a number of easterly-dipping, overturned forelimbs

give the F_2 fold system in Domain 1 an overall westerly vergence (Figure 5.3a). This relationship is consistent with the presence of a regional scale antiform, seen on Section E-E' (Insert II). Measured fold axes (1-209) and the calculated beta-axis (5-209) for this fold system are compatible, plunging gently southwest and indicate that the fold system verges towards 300° (Figure 5.4). Figure 5.3b is an example of a large, northwest-verging meso-scale F_2 anticline.

Lower hemisphere, equal area projections of the orientation data collected in Domain 1 highlight the salient features of the F_2 fold system (Figure 5.4). Pi-plots of bedding and cleavage (S_1) form reasonable, but diffuse, girdles. The calculated pi-girdle for Domain 1 has an orientation of 299\85 RH. The broad spread of poles to bedding across the pi-girdle indicates a fair degree of non-cylindricity of the F_2 fold system. The population of fold axes shows minor scatter and bi-polar trends, indicating that the fold axes curve through the hinge zones, defining weakly doubly plunging folds (Figure 5.4). Axial surfaces measured in Domain 1 show minor variation, contributing to the non-cylindricity of the F_2 fold system, but in general strike northeast and dip moderately to steeply southeast (Figure 5.4).

The orientation of F_2 folds is strongly affected by the pre-existing orientation of the F_1 folds in Domain 1. Overturned bedding measurements form a cluster of steep, southeast dipping planes which are coincident with the forelimb domain of the asymmetric F_2 folds and represent the refolded backlimb of the F_1 fold system. However, a few overturned beds are distributed through the pi-girdle (Figure 5.4). These anomalous bed orientations are the result of F_2 folds forming on the overturned forelimbs

a. A typical close F_2 fold with z-type asymmetry, looking down plunge to the southwest (Insert II, Section A-A').

b. Oblique section of a northwest-verging parasitic F_2 antiform (Insert II, Section E-E'). Note the rapid transition between overturned and steep normal beds on the short forelimb at right-hand side.

Figure 5.3 Morphological expressions of F_2 folds in Domain 1.

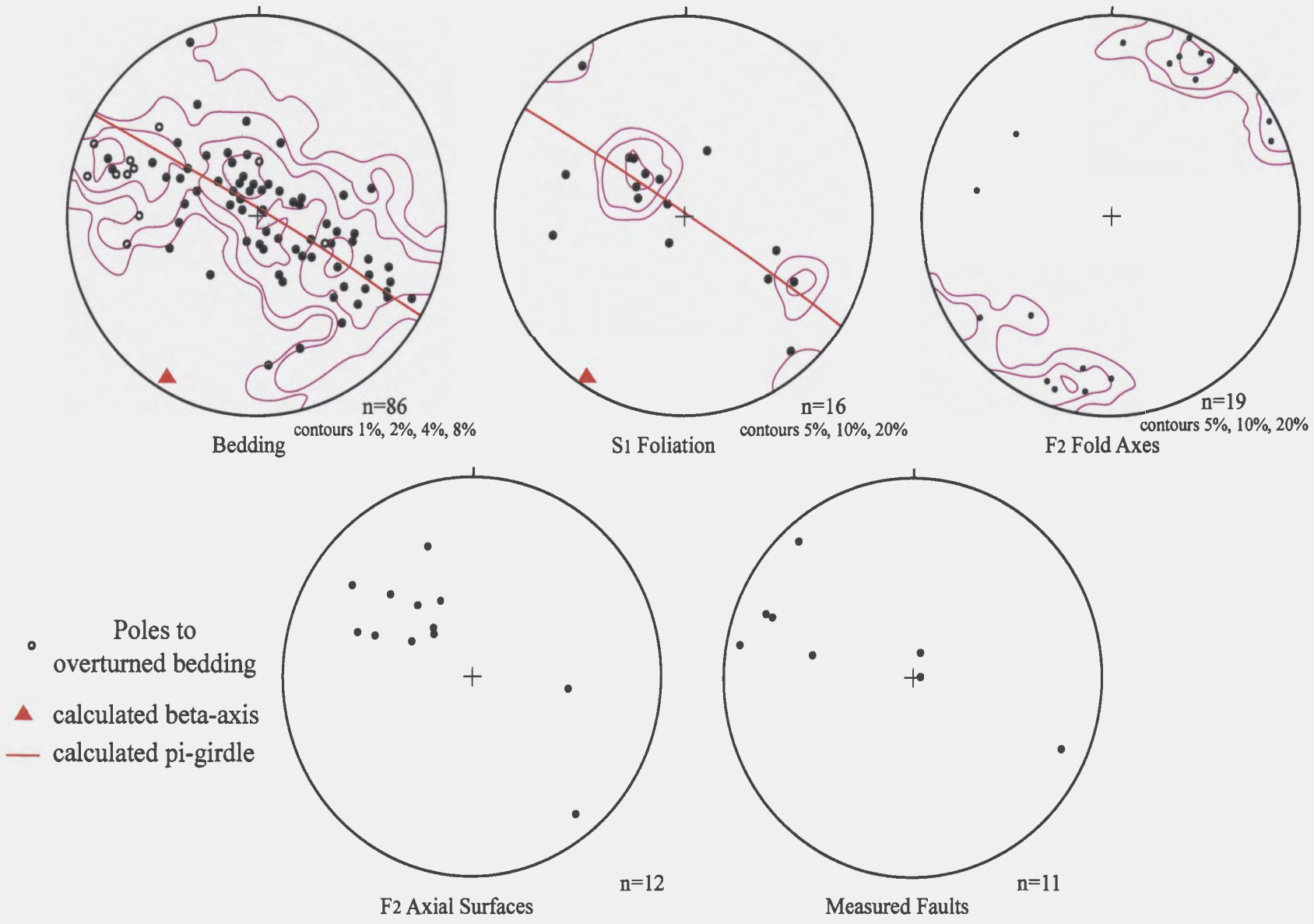

Figure 5.4 Lower hemisphere, equal area projections for orientation data defining the F_2 fold-thrust system in Domain 1.

of F_1 folds; generating downwards facing F_2 folds (Insert II, Section B-B'). The effect of F_1 orientations is probably one of the most important causes of the F_2 fold systems deviating from cylindricity. The implications of the F_2 fold geometries for the reconstruction of the F_1 fold orientation patter are further treated in section 5.2.4.

5.2.2 Domain 2

Domain 2 is characterized by moderately inclined, southeast-verging asymmetric F_2 folds. The folds have close to tight interlimb angles and are gently to moderately southwest plunging with westerly-dipping axial surfaces (Figure 5.5a). Two sub-domains are sub-domains are recognized in Domain 2 and the style of the F_2 fold system differs between Domains 2a and 2b. Analysis demonstrates the presence of a broken, macro-scale southeast-verging fold wave train with steep forelimb panels predominating in the Domain 2a. The west dipping, overturned forelimb of the F_2 folds define an s-type asymmetry (looking down-plunge), indicating that the presence of a regional scale antiformal culmination may be expected to the southeast (Insert II, sections E to G). In Domain 2b, gently dipping backlimb panels of the broken, macros-scale, southeast-verging F_2 fold system are more common (Figure 5.5b and Insert II, Section H-H').

Lower hemisphere, equal area projections of orientation data collected in Domain 2 show that the distribution patterns of poles to bedding is similar in the two sub-domains (figures 5.6 and 5.7). The diffuse spread of poles to bedding across the pi-girdles indicates a strong degree of non-cylindricity of the F_2 fold systems in Domains 2a and 2b. In both plots the steep-dipping beds form broader clusters of poles that tail off from the pi-girdle, while the more gently-dipping beds cluster tight to the pi-girdle. This pattern of

a. A southeast verging F_2 fold formed in dismembered Middle Arm Point formation, Domain 2a (Insert II, Section F-F').

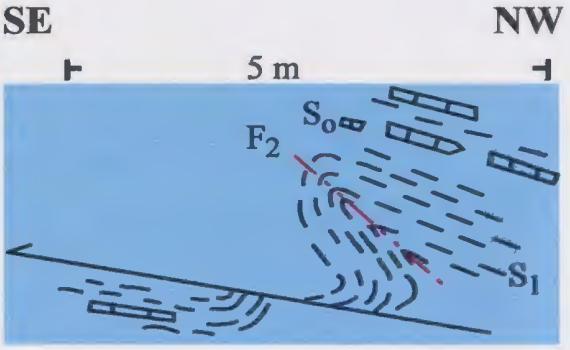

b. Break thrust through a non-cylindrical, southeast verging F_2 fold in a section of Cooks Brook formation near the west side of Domain 2b (Insert IV, station FB-03-02-207).

Figure 5.5 Morphological expressions of F_2 folds in Domain 2.

pole distribution is typical of mushroom-type interference patterns created during the superposition of F_2 folds on F_1 folds. Downward facing F_2 folds are common in Domain 2a and are the result of F_2 folds refolding overturned F_1 fold limbs (Insert II, Section E-E'). The interaction of the F_1 and F_2 fold systems in the sub-domains and development of the resultant interference patterns is discussed in detail in section 5.4.

Pi-girdles calculated from the bedding plots for have an orientation of 275\56 RH in Domain 2a and 312\52 RH in Domain 2b (figures 5.6 and 5.7). Measured fold axes and axial surfaces from each of the sub-domains display a diverse range of values. In Domain 2a the fold axes orientations show considerable variation, with a concentration around 25-167 (Figure 5.6). In Domain 2b the fold axes appear more clustered and are oriented 43-200 (Figure 5.7). A difference of 37° exists between the strikes of the pi-girdles calculated for Domains 2a and 2b (figures 5.6 and 5.7). Applying a clockwise rigid body rotation of 37° to the bedding plot for Domain 2a demonstrates that the Domain 2a pi-girdle becomes coplanar with the Domain 2b pi-girdle (figure 5.6 and 5.7). Furthermore, the spatial distribution patterns of poles to bedding are almost identical in Domains 2a and 2b. This similarity in style, geometry, and kinematics of the F_2 fold systems in the domains indicates that the fold systems could be correlative with a post-F_2 folding rigid body rotation. A number of steeply-dipping to sub-vertical oblique-slip faults cut the F_2 fold system in Domain 2. These faults may be part of a strike-slip fault system responsible for this late, rigid body rotation of elements of the F_2 fold system in Domain 2a (Insert II, sections E to F). The geometry of the late fault system and its

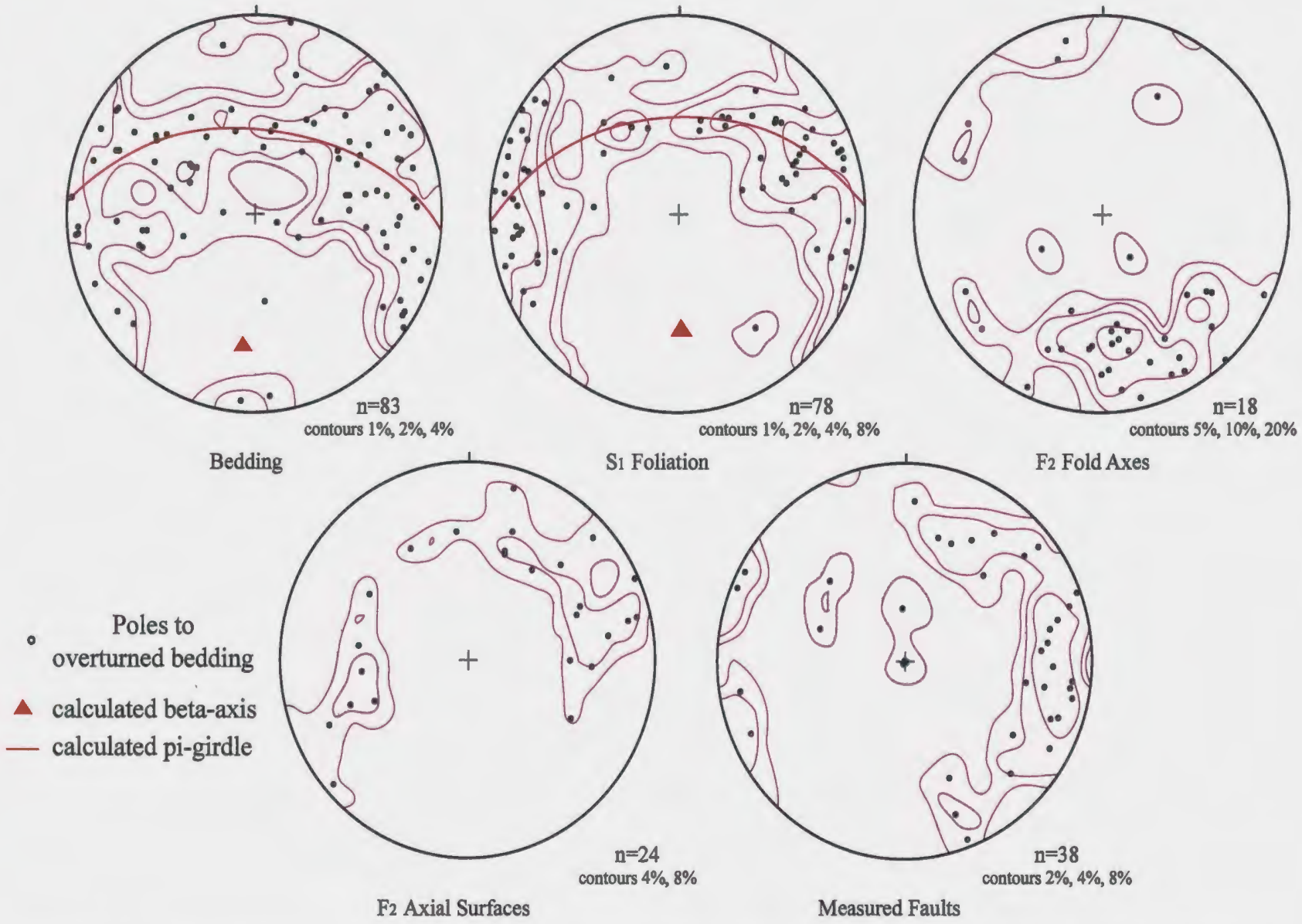

Figure 5.6 Lower hemisphere, equal area projections for orientation data defining the F_2 fold-thrust system in Domain 2a (Insert II, sections E-E', F-F', and G-G'-G").

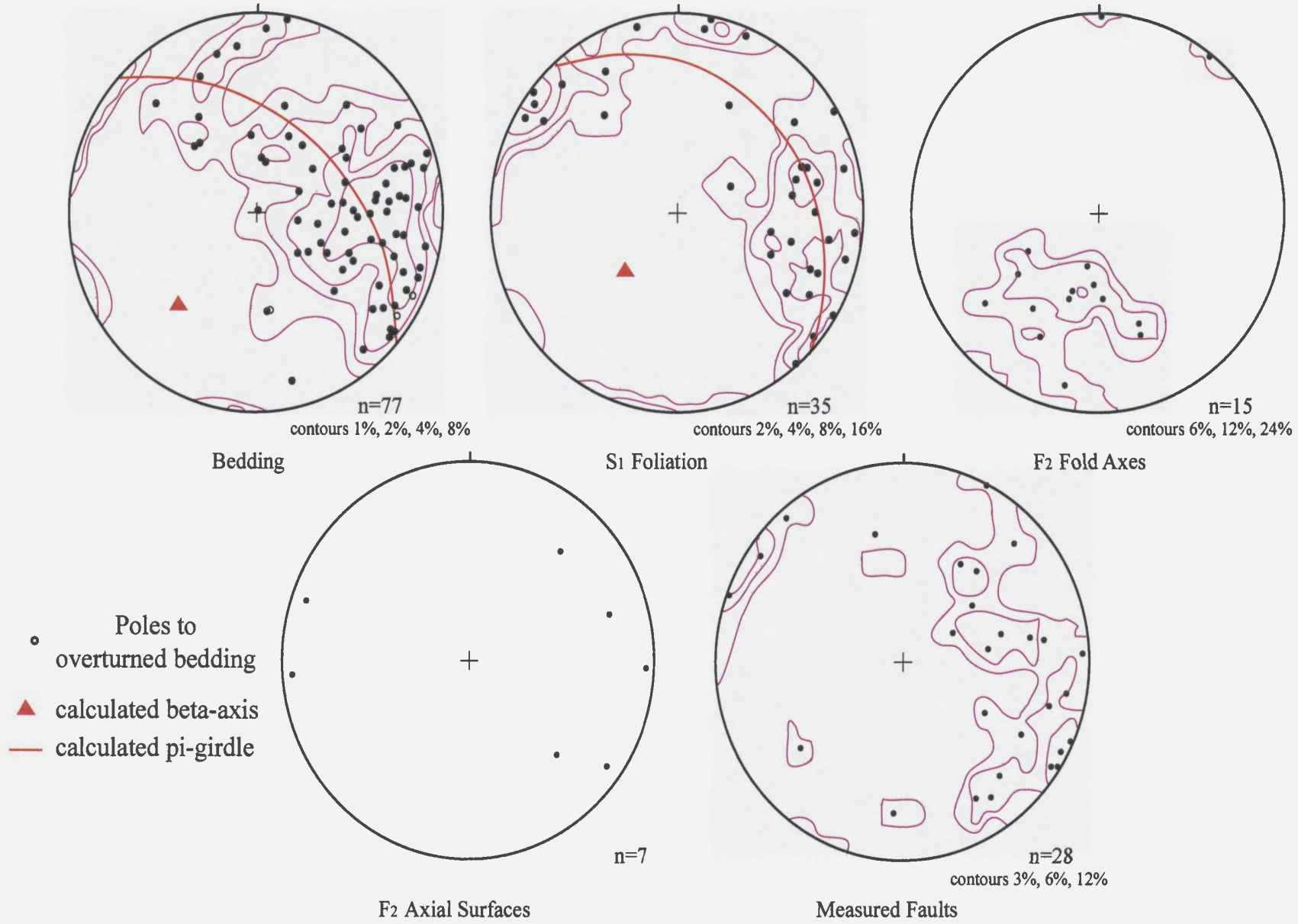

Figure 5.7 Lower hemisphere, equal area projections for orientation data defining the F_2 fold-thrust system in Domain 2b (Insert II, Section H-H')

implications to the structural architecture and evolution of the Frenchman's Cove - York Harbour area is discussed in greater detail in Chapter 7.4.

5.2.3 Domain 3

Domain 3 is divided into three sub-domains (see Chapter four). Domain 3a is primarily defined by the F_3 fold system and the F_2 fold system is poorly exposed. The architecture of Domains 3b and 3c is primarily defined by the geometry of F_2 folds. These folds form large, macro- to regional scale structures (Figure 5.8). The folds are large, sub-horizontal, open to close, north- to northwest-verging asymmetric folds. Thrust faults associated with the F_2 folds have broken the folds and locally form duplex structures (Insert II, Section K-K'). These regional scale folds create large dip domains with consistent bedding orientations, consisting of long limb domains with gently south-dipping beds and short limb domains with vertical to slightly overturned beds (Insert I). An extensive steep forelimb domain of the regional fold system is located along the shoreline and the large, gentle backlimb domain is located in the southern portions of the map area (Insert I).

Lower hemisphere, equal area projections of poles to bedding in Domain 3b show a well populated great circle girdle distribution pattern. The calculated pi-girdle is orientated 177\89 RH (Figure 5.9). The pole distribution across the pi-girdle is somewhat broad and diffuse, this relates to the presence of an F_1 fold system. The orientation of the calculated beta-point (01-087) is consistent with the concentration of measured, gently plunging fold axes. A bipolar distribution of fold axes forms two populations on the plot representing a composite of F_1 and F_2 fold axes (Figure 5.9). This distribution arises

Figure 5.8 Gently east-plunging F_2 fold in thick-bedded sandstones within Domain 3b (Insert IV, station J1001)

from miss-identifying F_1 folds due to the difficulty of distinguishing fold generations in the thick-bedded sandstone packages, especially in isolated outcrops. The pi-plot for the S_1 cleavage demonstrates the F_2 folding of this F_1 axial planar fabric element. The orientation of the pi-girdle for the poles to S_1 cleavage is 350\89 RH, a subtle difference in orientation, compared to the pi-girdle for bedding. The shift in the orientation of F_2 folds formed by folding S_1 cleavage demonstrates that the F_1\F_2 fold systems were not strictly coaxial during superposition (see also section 5.4). Younging directions are difficult to obtain in the thick, massive sandstone beds of the Blow Me Down Brook formation. Measurements on overturned beds cluster in the northern portions of the plot and are consistent with the presence of F_2 forelimbs (Figure 5.9). Overturned bedding measurements scattered along the great circle of the pi-girdle correlate with downward facing F_2 folds. These folds have formed in stratigraphic successions overturned during the F_1 folding event, particularly within shale intervals of the Blow Me Down Brook formation (Figure 5.2b).

Domain 3c is located on a narrow strip of coastal exposures comprising steep-dipping, thick-bedded sandstone packages of the Blow Me Down Brook formation located in the immediate footwall of the ophiolite massif. The structural geometry of this sub-domain is anomalous in comparison to Domain 3b to the east. Lower hemisphere, equal area plots of poles to bedding in Domain 3c comprise almost solely steep, southerly-dipping beds with peculiar variations in younging directions (Figure 5.10). Wojtal (2001) presented a plot of poles to bedding along this coastal section that displays a similar distribution pattern, but Wojtal's (2001) plot does not display the facing

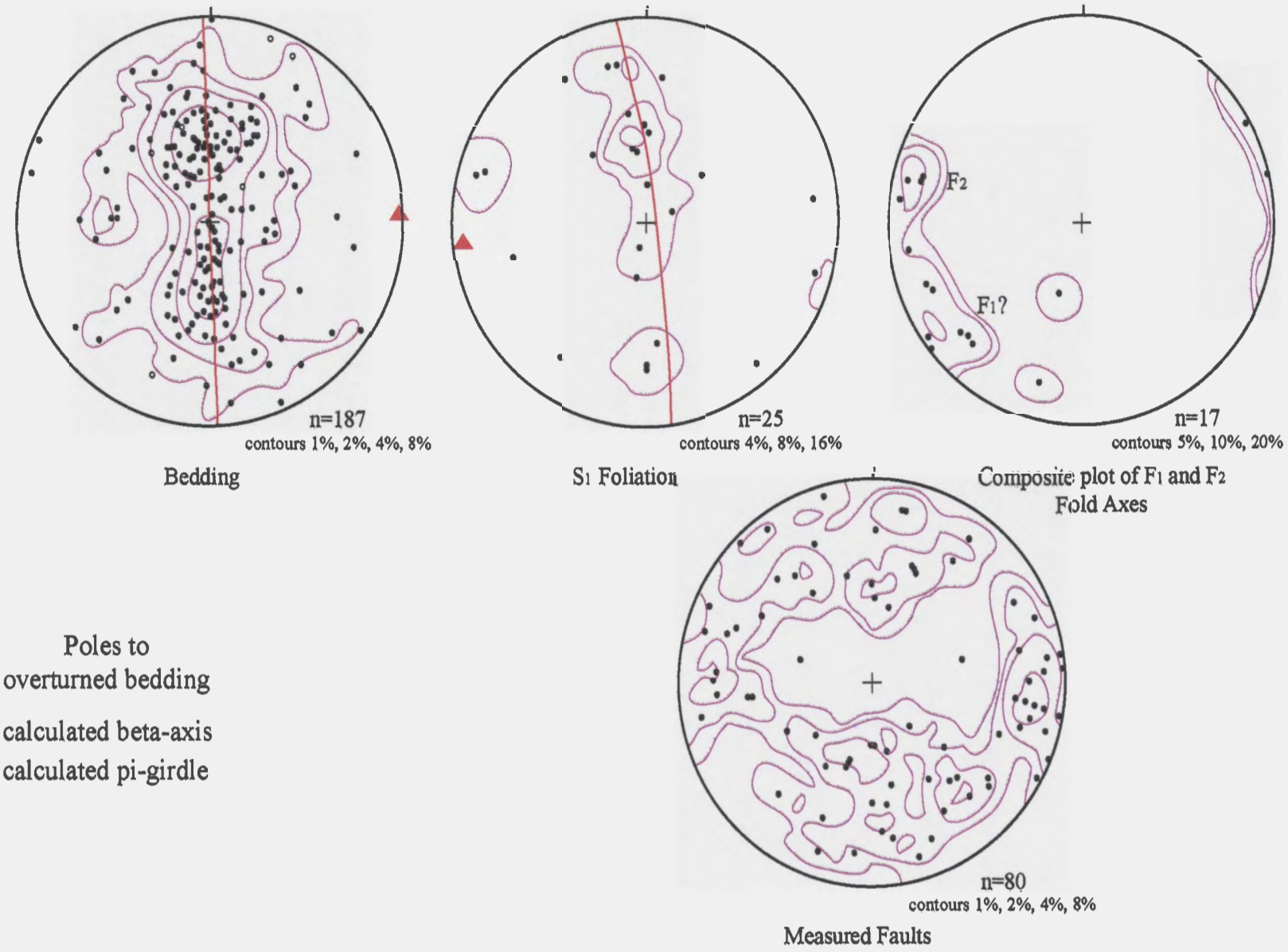

Figure 5.9 Lower hemisphere, equal area projections for orientation data defining the F_2 fold-thrust system in Domain 3b (Insert II, Section K-K').

direction. The pi-plot, in Figure 5.10, demonstrates that the measured bedding planes in Domain 3c form two populations of bedding orientations: a steep northeast-southwest striking population and a population of steep-dipping west-east to northwest-southeast striking beds. The tailing of the main population of poles in the northern hemisphere of the plot suggest the presence of a mushroom-style interference structure caused by $F_1 \backslash F_2$ fold superposition (see section 5.4). Insert I shows that the spatial distribution the two bedding populations forms small-scale structural domains within Domain 3c. The plot of measured faults in this domain indicates an increasing degree of structural complexity is introduced by the proximity of the sub-domain to the ophiolite complex (Figure 5.10). A population of late, steep, approximately north-south striking oblique slip faults are present in the domain and demarcate the boundaries of the smaller scale domains and possibly caused rigid body rotation of blocks within Domain 3c (Insert I). The significance of the geometry and kinematics of this late fault population is presented in more detail in Chapter seven, section 7.4.

5.2.4 Domain 4

Domain 4 is dominated by the presence of macro- to regional scale folds with thick limbs and wavelengths greater than 1.5 km. The folds are gently plunging, open, northwest-verging, asymmetric structures (Insert III, sections M-M" and N-N'). Thick sandstone packages of the Blow Me Down Brook formation on Wood's Island and Seal Island define distinct dip-domains, suggesting the development of polyclinal kink-style fault-propagation folds. On the western shore of Wood's Island the broad crestal region of an anticline is partially exposed and displays angular, open, kink-style hinges between

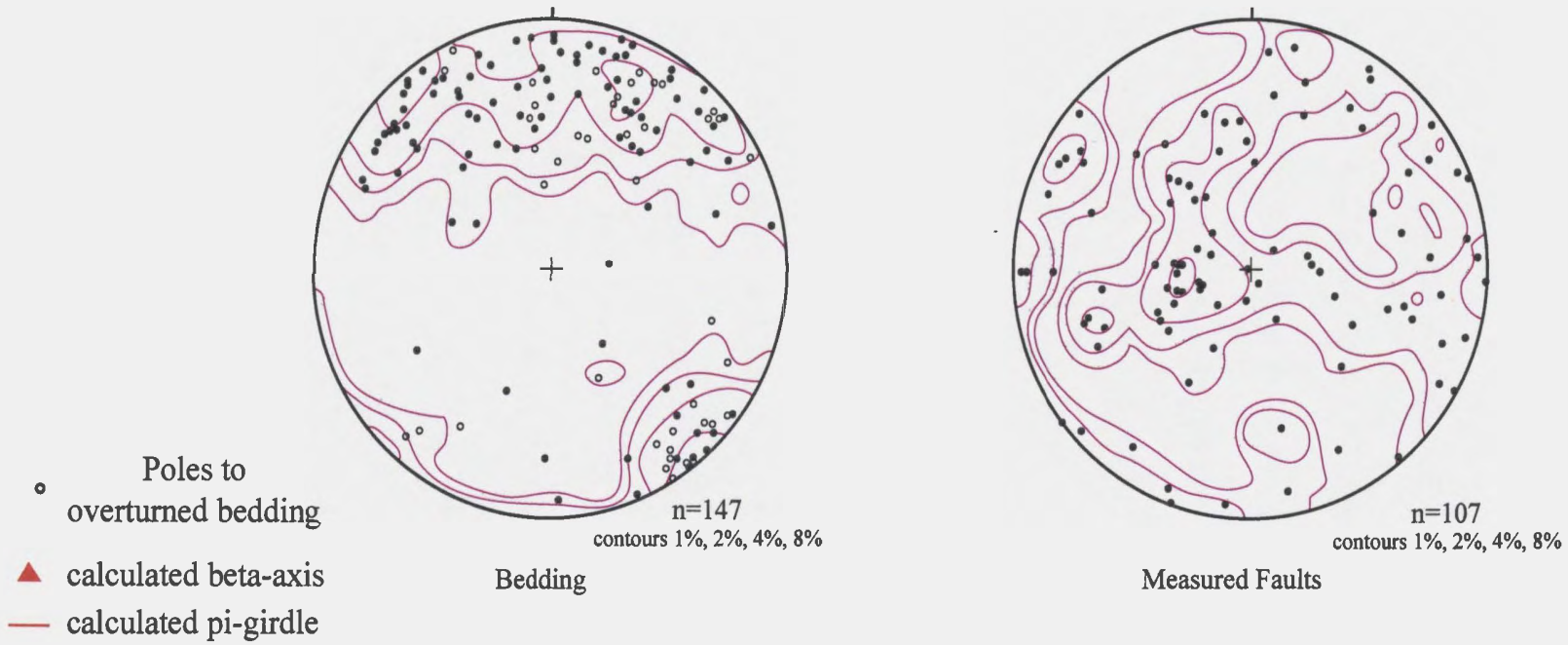

Figure 5.10 Lower hemisphere, equal area projections for orientation data defining the F2 fold-thrust system in Domain 3c (Insert II, Section L-L').

adjacent dip-domains (Insert III, Section N-N'). Assuming stratigraphic thickness is preserved in the fold limbs, the fold profiles may be constructed using kink method techniques. A profile of the Wood's Island fold presented in Section N-N' (Insert III). Section N-N' contains the most complete section of the Blow Me Down Brook formation in the area, but does not expose either the base or top the Blow Me Down Brook formation. However, the profile constrains the stratigraphic thickness of the formation to a minimum of 636 m measured perpendicular to bedding in the backlimb of the fold.

Pi-plots created for Domain 4 include orientation data measured on Wood's Island, Seal Island, and Governor's Island (Figure 5.11). The bedding data show a girdle distribution oriented 287\77 RH, which is consistent with the observed northwest-vergence of the fold system. The calculated beta-axis of the fold system plunges gently to the southwest (13-197), sub-parallel to the strike of the steep limb exposed on small islands at the western end of Wood's Island (Insert I). The normal, west-facing steep forelimb of the F_2 fold system is locally southeast-dipping and overturned (Figure 5.11). There is no observed evidence for two generations of folds in Domain 4. Based on orientation and style of the macro-scale folds the Domain 4 fold system is correlated with the F_2 fold system documented in Domain 3. Indirect evidence for the correlation with F_2 folds is provided by the diffuse distribution of poles to bedding (Figure 5.11) and an anomalous, steeply-plunging F_2 fold axis measured on Governor's Island. A broad distribution of poles around the pi-girdle is mainly generated by the presence of a panel of moderately southeast-dipping, normal bedding planes along the northwestern shore of Wood's Island (Figure 5.11, cluster A). The tails on the distribution pattern of poles to

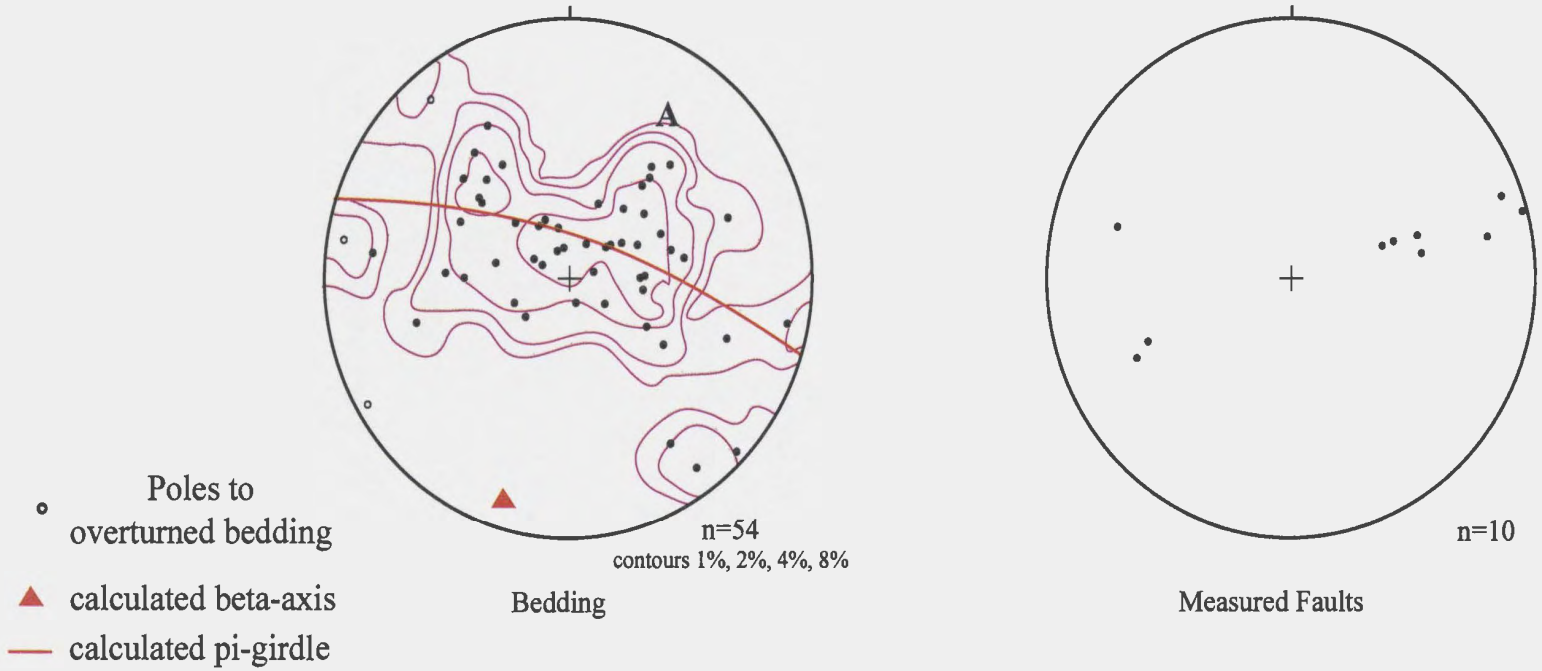

Figure 5.11 Lower hemisphere, equal area projections of orientation data defining the F_2 fold-thrust system in Domain 4, on Wood's Island and Seal Island (Insert III, sections M-M' and N-N').

bedding indicates the presence of unmapped mushroom-type structures formed as the result $F_1\backslash F_2$ superposition. A second aspect of the F_2 fold geometry is the contrast between gently plunging fold axes on Wood's Island and a moderately plunging fold axis measured on Governor's Island (53-240). Moderate to steep plunging and gentle fold axes are a geometric component of mushroom-type fold superposition structures. The range in measured F_2 fold axes suggests that an earlier fold generation (F_1) has been refolded by the F_2 fold system in Domain 4. The development and implications of fold superposition is treated in detail by section 5.4.

A prominent seven metre thick shale layer on the west end of Wood's Island shows evidence of detachment during bedding-parallel shear. Thin sandstone beds have formed metre scale break-thrust folds and create shale duplex structures with bed-parallel floor and roof thrusts (Insert III, Section N-N', Detail A). The geometry and orientation of these small-scale folds is identical to the macroscopic fold on Wood's Island and are considered to be a model of the F_2 fold system in Domain 4.

5.2.5 Domain 5

The eastern portion of the southern shore of Wood's Island consists of a large number of discreet, thin imbricate slices composed of different formations of the Humber Arm Supergroup (Insert I). F_2 fold systems control the structural architecture within the imbricate slices and are similar in style and orientation to the F_2 fold systems in Domains 1 and 2. The style and orientation of these folds varies considerably between the various fault panels and is strongly dependent on the lithology. Overall the F_2 fold systems in Domain 5 are gently to moderately southwest plunging. The vergence of the fold

systems switches from southeast-verging in the western portion of the domain to northwest-verging in the eastern portion (Insert III, sections R-R'-R"). The F_2 fold system becomes more upright and symmetrical, towards the eastern end of the island (Insert III, Section T-T'-T").

Sections O to Q (Insert III) consist of southeast-verging F_2 folds in imbricate sheets of the Blow Me Down Brook and Cook's Brook formations. The west end of Section O-O' lies under a series of southeast-verging thrust faults which imbricate gently, west-dipping sandstone beds of the Blow Me Down Brook formation. As the shale content of this formation increases eastwards, the competent bedding becomes disrupted and the fault panels appear as sections of broken formation. In the shale dominated sections the S_1 cleavage delineates the geometry of the F_2 folds. The rheological contrast between sections of coherent bedding and broken formation cause the fold system to form highly non-cylindrical folds. Fold axes of the F_2 fold system in sections O to Q plunge gently to moderately southwest (03-202 to 52-232) and the pi-girdle orientation varies between 328\38 RH and 292\87 RH (figures 5.12 (bedding) and 5.13 (foliation)). The arrangement of bedding poles fore sections P-P' and Q-Q' in a diffuse partial girdle oblique to the main concentration of F_2 fold axes indicates the presence of superposed fold geometries in Domain 5 (see section 5.4). The folds in these sections form moderately to steeply inclined, asymmetric, close folds which are part of a southeast-verging F_2 fold-thrust system.

On Section R-R'-R" (Insert III) a significant fault break occurs at 390 m. The large stratigraphic separation between the Cook's Brook and Eagle Island formations, and

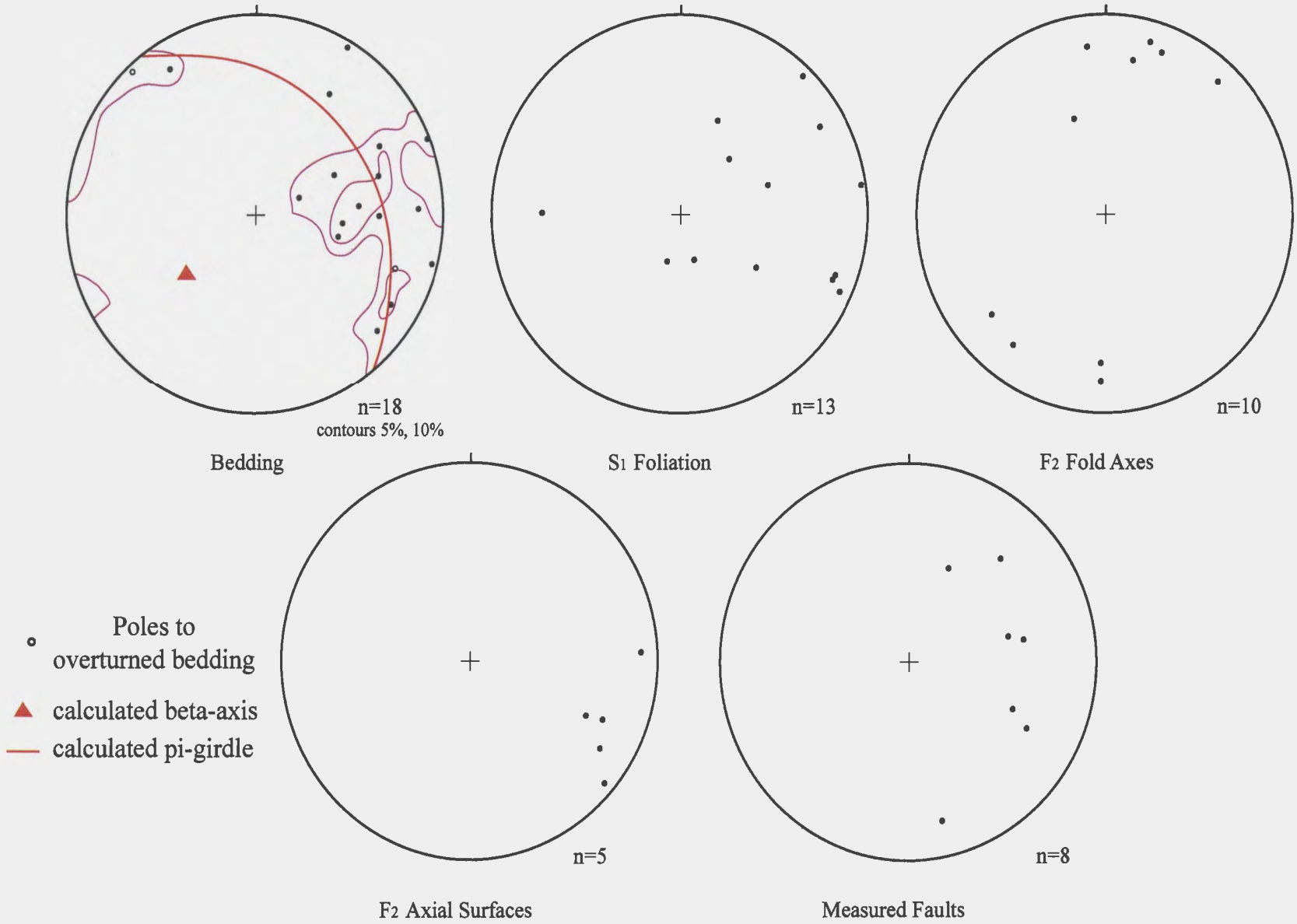

Figure 5.12 Lower hemisphere, equal area projections for orientation data defining the F_2 fold-thrust system in Domain 5 (Insert III, Section O-O').

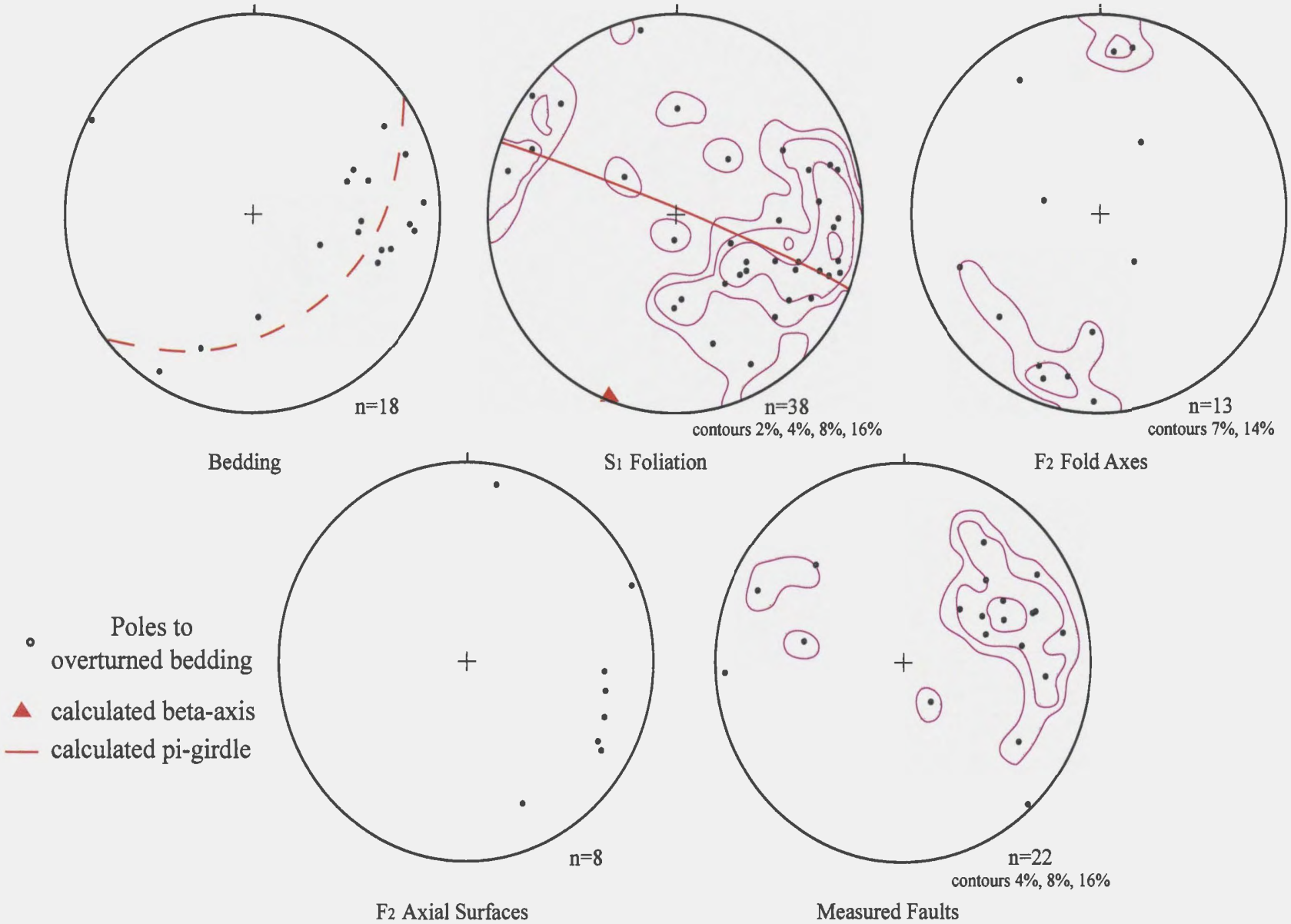

Figure 5.13 Lower hemisphere, equal area projections for orientation data defining the F_2 fold-thrust system in Domain 5 (Insert III, sections P-P' and Q-Q').

contrasting structural styles across the fault indicates that the fault has a large strike-slip component. East of the fault the asymmetry of the regional scale F_2 fold system switches and the fold system becomes northwest-verging. The F_2 folds plunge moderately to the southwest (42-211) and their axial surfaces are moderately inclined (Figure 5.14); in section R to S the F_2 fold system displays a reclined orientation pattern. Overall, the orientation of the northwest-verging folds F_2 folds is the same as the southeast-verging folds to the west. Imbricate panels shown on sections R'-R" and S-S' contain components of the hinge zone and steep forelimb of a broken, regional scale F_2 folds. Macro-scale parasitic folds in sandstone beds of the Eagle Island formation dominate the initial 200 m of Section R'-R". The gently-dipping beds form a wave train of open, gently inclined folds that indicates this structural panel is located in the synformal hinge domain of a regional scale F_2 fold. At 590 m a critical break in the section occurs at an unseen fault in the section. The east-side of the fault is a structural panel comprising a succession of vertical, west-facing sandstone beds of the Eagle Island formation. Although, it is unknown if the fault is an F_2 break-thrust, or younger strike-slip fault; the contrast in structural architecture across it indicates the excision of a regional scale synform. East of the fault is a series of structural panels which contain a wave train of broken, macro-scale, east-verging parasitic folds (Insert III, sections R'-R" and S-S'). The steep-dip of bedding in the panels indicates the folds are located on the steep limb of a regional scale F_2 fold, and the asymmetry of the parasitic F_2 folds suggest a regional antiformal culmination may lie to the east of the section. A narrow structural panel containing a west-facing, southeast-verging recumbent F_2 fold train is located on the east end of

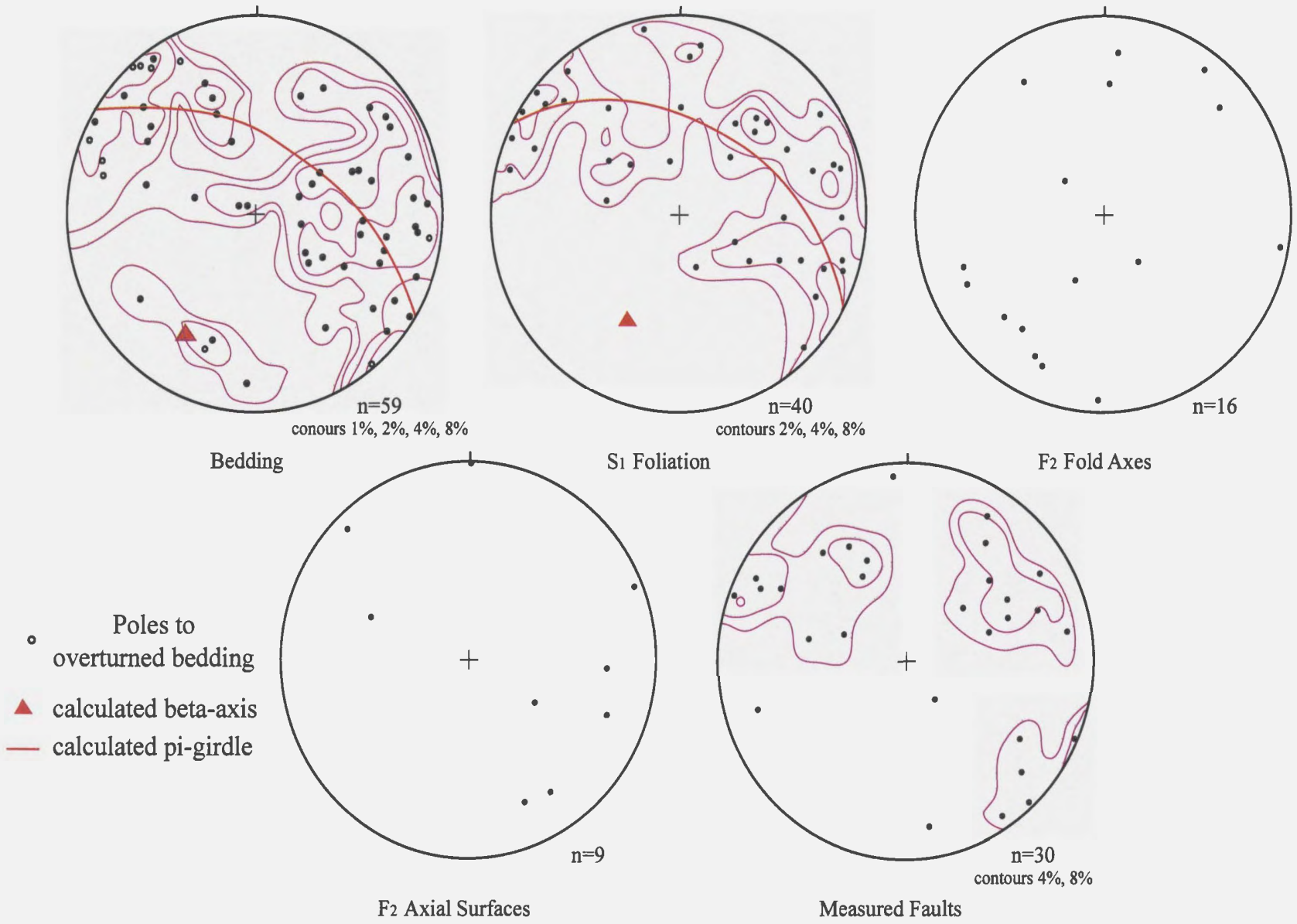

Figure 5.14 Lower hemisphere, equal area projections for orientation data defining the F_2 fold-thrust system in Domain 5 (Insert III, sections R-R'-R" and S-S').

Section S-S' (Figure 5.15). This imbricate panel of small, macro-scale F_2 folds formed in response to a back-thrust developed on the gentle limb of a macro-scale parasitic F_2 fold; located on the steep, forelimb of a regional scale, northwest-verging F_2 fold.

In Domain 5 the generations of folds are assigned on the basis of observed overprinting criteria. The reconstruction of regional scale, northwest-verging folds, described on sections R to S (Insert III); indicate that an F_2 backlimb panel with northwest-verging, parasitic F_2 folds should be located in the western-portions of Domain 5. However, the F_2 fold-thrust system identified on sections O to Q (Insert III) is southeast-verging. The incompatibility of the F_2 vergence directions raises significant questions about the labelling of fold generations in the western portion of Domain 5. The late faults which overprint the area have a large component of strike-slip displacement; stratigraphic separations created by these faults are large, and they strongly disrupt continuity of macro- to regional scale structures. Although, no evidence for three generations of folds was observed during this project, the southeast-verging fold system may correlate with the easterly-verging F_3 thrust system developed at the contact between Domains 4 and 5. The geometry and orientation patterns of the southeast-verging fold system on Wood's Island are compatible with the easterly-verging F_3 fold-thrust system in Domain 3a (see section 5.3). Further mapping of Wood's Island, with particular emphasis on overprinting criteria for the fold systems, is required to properly resolve this problem of correlating the F_2 fold systems on Wood's Island.

Folds documented in Section T-T'-T" (Insert III) differ in style from F_2 folds elsewhere in Domain 5, but share similar orientations. The fold system consists of

Figure 5.15 Recumbent F_2 fold related to a southeast-verging backthrust in the F_2 fold-thrust system in Domain 5 (Insert III, Section S-S').

reasonably symmetric, gently southwest plunging to sub-horizontal, moderately inclined, close to tight folds. The folds are highly broken by west-verging thrust faults, forming an imbricate stack of Blow Me Down Brook and Eagle Island formations. Several well-preserved macro-scale antiformal and synformal hinge domains are present in the section, but many of the imbricate slices in this section preferentially preserve the steeper limb domains of the folds. Only rare, meso- to macro-scale parasitic folds are present in these sections. An equal area plot of bedding and S_1 cleavage indicates that the geometry of the folds is compatible with the overall southwesterly plunging F_2 fold system in Domain 5 (Figure 5.16). The dispersion of bedding and cleavage poles across the pi-girdle on the lower hemisphere, equal area projections forms a distinctive tailing of the steep-dipping elements. This pattern, as mentioned elsewhere, suggests the development of mushroom-type structures developed during $F_1\backslash F_2$ superposition. Fold superposition and the effects of earlier fold generations on the younger generation is discussed in detail in section 5.4.

On the eastern tip of Wood's Island the F_2 fold system is cut by a narrow, steep belt of mélange, containing knockers of mafic igneous rocks. The strong cleavage fabric in the matrix of the mélange zone does not display any evidence of the F_2 fold system. The structural style and contact relationships of the mélange with imbricate slices containing the Humber Arm Supergroup suggest the mélange is younger than the F_2 fold system (see Section 7.5).

5.3 F_3 fold systems

The macro-scale F_3 fold system exposed along the shore west of Shoal Point is a uniquely oriented fold system which overprints early fold generations in Domain 3 (see

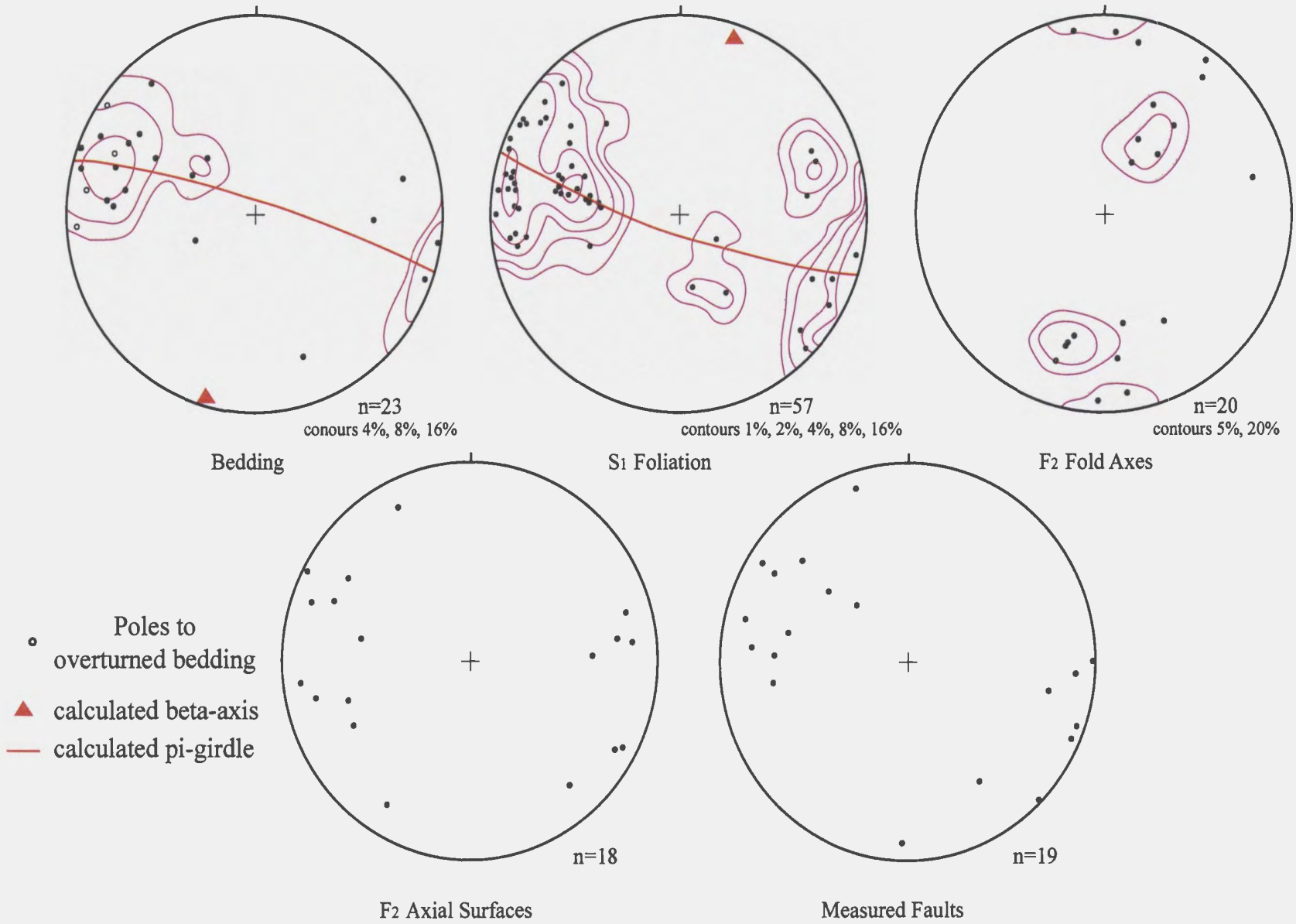

Figure 5.16 Lower hemisphere, equal area projections for orientation data defining the F_2 fold-thrust system in Domain 5 (Insert III, Section T-T'-T'').

Chapter four, section 4.3). A train of east-verging asymmetric, gently plunging, open folds is observed in Domain 3a at the contact between domains 2 and 3 (Figure 5.17). The folds form as fault-propagation folds, broken by east-verging thrust faults (Insert II, sections I-I' and J-J'). The younging direction of the sandstone beds can be determined at several locations in the fold system and consistently indicate that bedding is normal way-up and the structural facing of the fold system is upright. The steep limb domain of the F_3 folds is only overturned in one, broken parasitic fold (Insert II, Section I-I'). On the western side of Domain 3a the F_3 folds form asymmetric folds with long, gently west-dipping normal limbs and a steeply east-dipping short limb domain (Insert II, Section J-J'). The presence of distinct dip domains in the Blow Me Down Brook formation is consistent with the development of F_3 folds with angular, kinked hinge zones; the section was therefore constructed using kink-style methods and illustrates the regularity of the geometry in this late fold-thrust system.

Figure 5.18 presents lower hemisphere, equal area plots of structural data measured on the fold system. The pi-plot for bedding has a well delineated, but broad distribution about a girdle, oriented 259\80 RH. The calculated beta-intersection plunges gently to the southeast (10-169) and is compatible with measured F_3 fold axes. The S_1 pi-plot is a girdle oriented 41\262 RH, a minor orientation difference from the bedding plot. S_1 and bedding are initially non-parallel planes and during the development of younger fold generations will form folds with different geometries (Ramsay and Huber, 1987). The degree of variation in the folds depends on the bedding\cleavage angle, which is small in this fold system. The girdle for bedding demonstrates a dispersion of poles

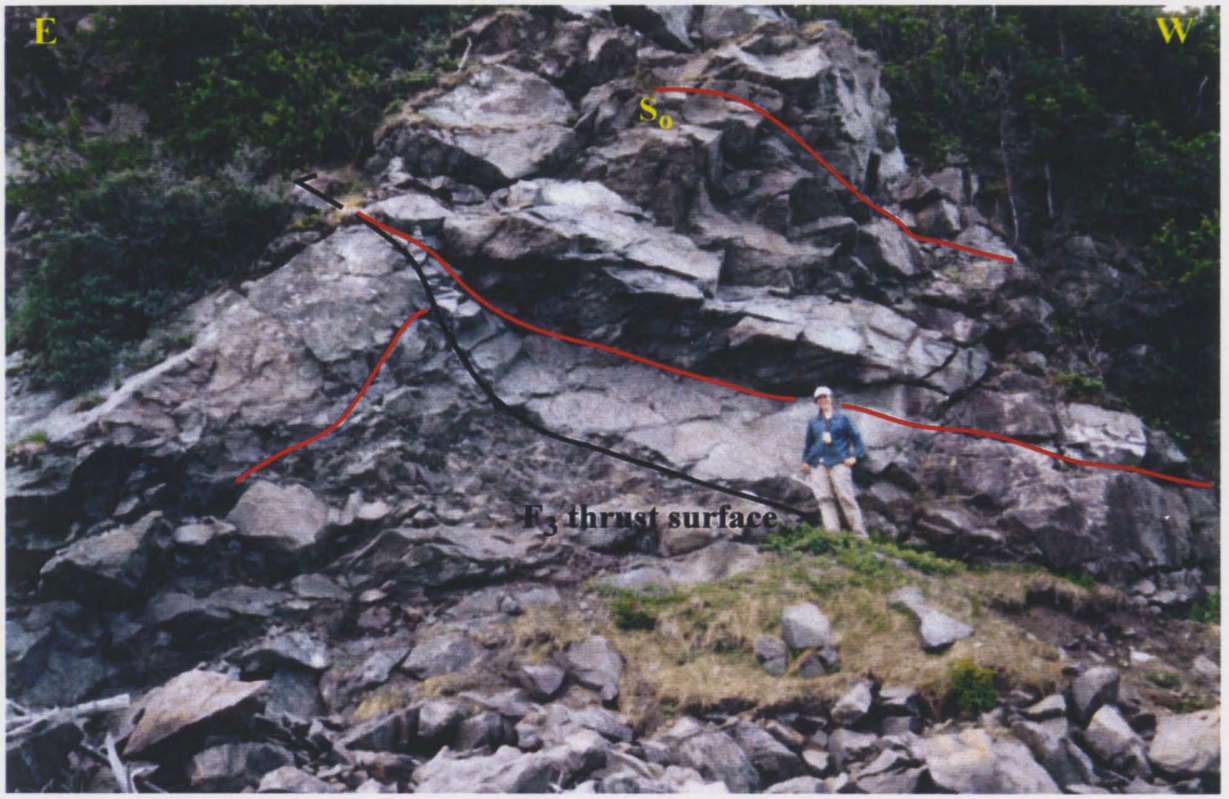

Figure 5.17 A broken F_3 fault propagation fold in sandstone succession of the Blow Me Down Brook formation (Insert II, Section I-I').

across the pi-girdle, suggesting some deviation from cylindricity of the folds. The non-cylindricity of the folds is also supported by variation in the orientation of the fold axes (Figure 5.18). Distinct tailing of dispersion patterns of bedding poles suggests the presence of interference patterns with earlier fold generations (see section 5.4).

The criteria for labelling this fold system as F_3 includes: overprinting, orientation patterns, and kinematic compatibility with the F_3 fault system that thrusts over Domain 2b (see Chapter 7, section 7.31). Although, Domains 3b and 3c contain regional scale F_2 folds no direct evidence of this fold system is observed in Domain 3a. However, the presence of earlier fold systems is indicated by the dispersion patterns of bedding poles, which suggest the formation of fold interference patterns (Figure 5.18). The vergence direction of the F_3 fold system has an easterly trend; this orientation of the fold system is almost perpendicular to the F_2 fold system in Domain 3, and strongly oblique to the F_2 fold system in Domain 2b. However, the easterly-vergence and style of the F_3 folds is consistent with formation as fault-propagation folds related to the east-verging F_3 fault system that defines the east boundary of Domain 3.

5.4 Interference patterns formed by superposition of fold generations

In fold belts with multiple folding events the superposition of successive fold generations creates complex fold interference patterns which exert a significant control on elements of the regional geology. The orientation and style of younger fold generations is strongly affected by the pre-existing geometry of the earlier fold generation. Ramsay (1967) related the formation of interference patterns to two primary factors: the angle between the F_1 axial plane and the F_2 displacement direction and the

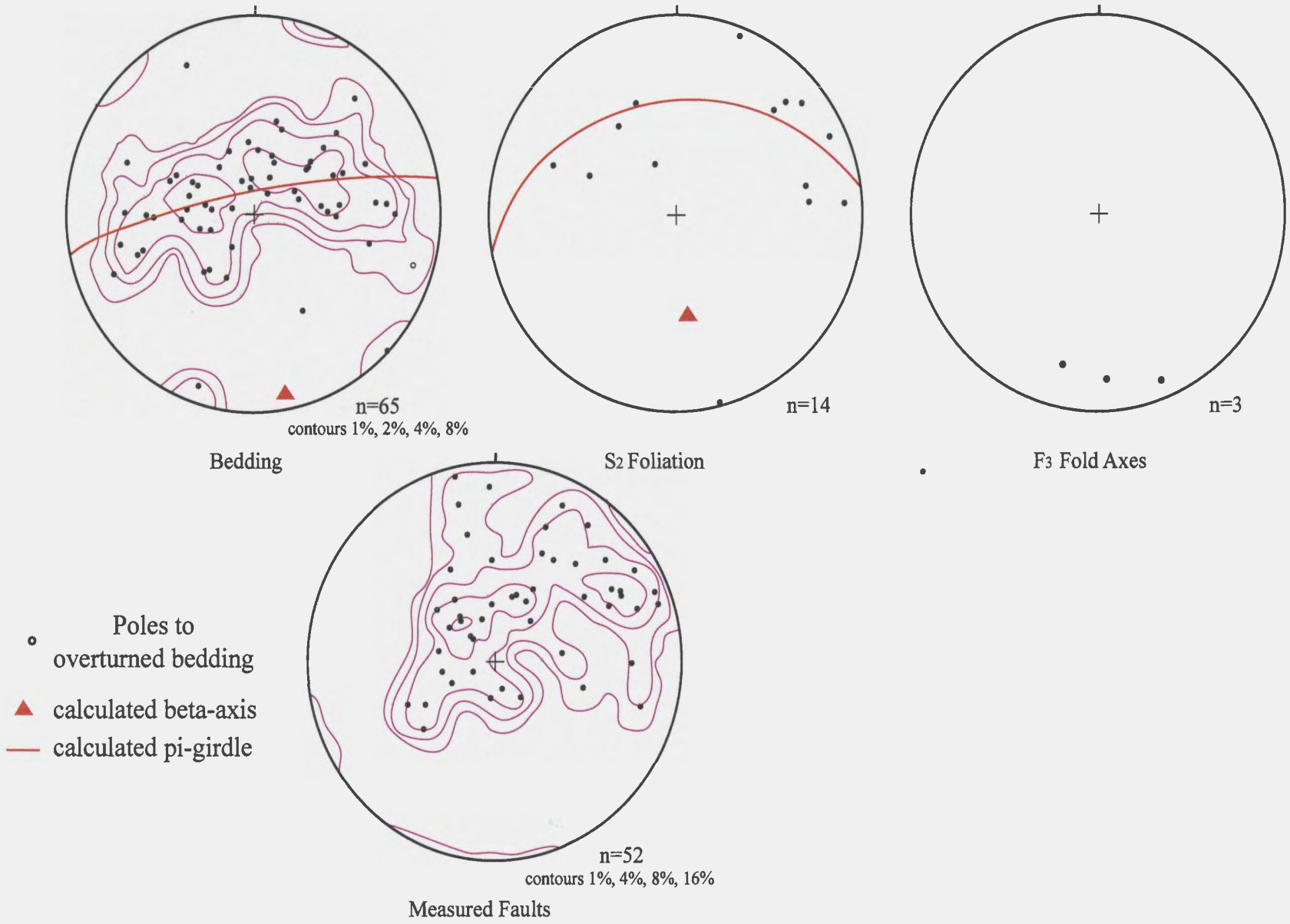

Figure 5.18 Lower hemisphere, equal area projections for orientation data defining the F_3 fold-thrust system in Domain 3c (Insert II, sections I-I' and J-J').

angle between the F_1 and F_2 fold axes (Figure 5.19a). The result of the interaction between the components of superposed fold systems is a spectrum of interference patterns (Figure 5.19b). The four end members of the interference pattern spectrum are: Type 0 - redundant superposition, Type 1 - Dome and basin interference, Type 2 - mushroom interference, and Type 3 - convergent-divergent (hook) interference (see also Ramsay and Huber, 1987). The recognition of fold interference patterns in polyphase fold belts aids in the identification of individual fold generations and constrains the orientation of the regional strain field and kinematic features of each successive deformation event (Ramsay and Huber, 1987).

In the Frenchman's Cove-York Harbour area superposition of the F_1 and F_2 fold systems has formed interference patterns which lie on the continuum between Type 2 and 3 of Ramsay's (1967) classification scheme (Figure 5.19b). Exposures of the interference patterns are found in lithologies of the Northern Head Group within Domains 1, 2, and 5. Figure 5.20a shows a hook interferences pattern (Type 3) formed in lithologies of the Cook's Brook formation on Wood's Island. This interference pattern represents an end member of the spectrum, but is not common in the Frenchman's Cove York Harbour area. The most commonly observed interference pattern in the area generates closed bedding trace forms with strongly asymmetric hooks, similar to Ramsay's (1967) Type 2H interference pattern (Figure 5.19b), or so-called oblique mushroom interference patterns (Figure 5.20). Sea cliffs form oblique sections through the three-dimensional superposed fold geometries, creating spectacular outcrop patterns (Insert III, Section R-R', Detail A).

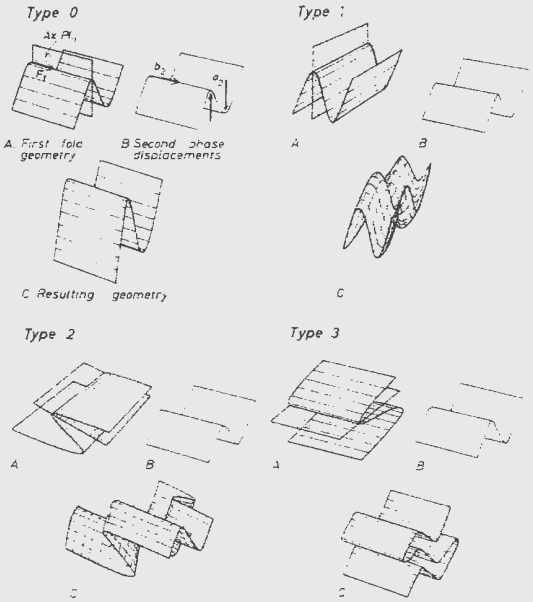

a. The geometric components controlling the development of fold interference patterns (b2 - orientation of second fold axis; a2 - direction of transport in the second deformation.

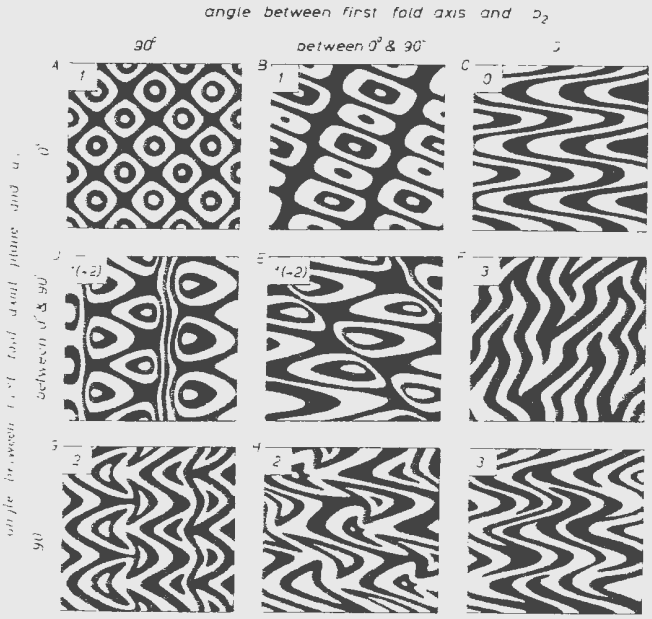

b. Horizontal sections of fold interference patterns generated during fold superposition.

Figure 5.19 Spectrum of interference patterns developed by the superposition of fold systems with different orientations (from Ramsay and Huber, 1987).

Figure 5.20b displays a large oblique mushroom structure on Wood's Island. The oblique mushroom interference pattern is distinguished from hook interference patterns by the short, steep F_1 limb, located in the along the bottom of the cliff in Figure 5.20b.

Recognition of the interference patterns places constraints on the geometry and style of the F_1 fold system developed in the area. F_1 folds are highly dismembered and poorly preserved; however, observations of rare F_1 folds indicate the system is overall asymmetric, west-verging, and west-facing on a macroscopic scale. Rootless F_1 fold hinges are common, but have been rotated during F_2 folding and the small orientation dataset collected from these fold remnants does not reflect the original geometry of the F_1 fold system. The presence of almost ideal Type 3 hook structures (Figure 5.20a) and oblique Type 2 mushroom patterns (Figure 5.20b), as well as the absence of ideal Type 2 mushroom structures and Type 1 dome and basin structures indicates several geometric relations of the superposed fold systems. The observed refolded fold geometries regionally constrain the angle between the trends of F_1 and F_2 fold axes and the angle between the axial surfaces. Figure 5.21 shows the asymmetry of mushroom-type structures caused by the original orientation of the F_1 axial surface at the time of F_2 superposition. In Domains 1, 2, and 5 observed oblique mushroom structures constrain the overall asymmetry of the interference pattern to that shown in Figure 5.21a; indicating that in general the F_1 axial surfaces were northeast-trending and easterly-dipping.

The interference patterns observed in Domains 1, 2, and 5 vary in style and geometry. In Domain 1 the interference pattern is more of a hook pattern (Type 3) than a

a. A 1 m wide Type 3 fold interference pattern (hook) within complexely refolded limestone-shale lithologies of the Cook's Brook formation (Insert III, Section R-R').

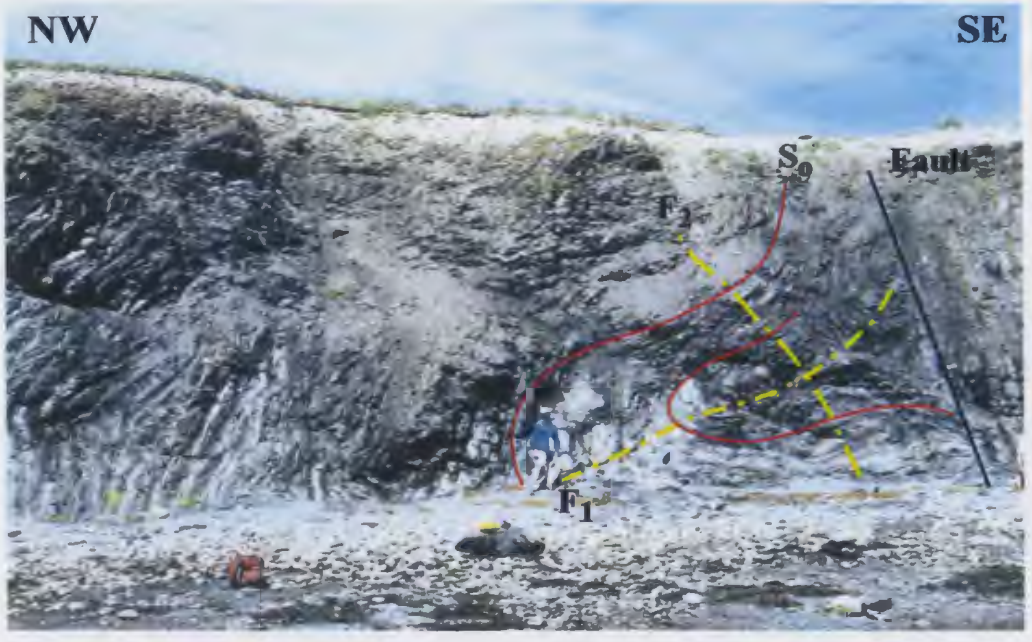

b. Fold interference pattern intermediate between types 2 and 3 developed in limestone-shale successions of the Cook's Brook formation (Insert III, Section R-R', Detail A).

Figure 5.20 Examples of the dominant fold interference patterns developed by the superposition of F_1 and F_2 fold systems in the map area.

mushroom pattern (Type 2). This indicates that F_1 and F_2 fold axes were almost coaxial and both trending north-northeast. If the axes were close to being coaxial than the angle between the F_1 axial surface and the F_2 transport direction must have been small, and the axial surfaces of both superposed fold generations were almost co-planer. Therefore, in Domain 1 the F_1 fold system was originally a close to tight, asymmetric, north-northeast trending, gently inclined fold system with a high degree of cylindricity. The vergence of the F_1 fold system is constrained by the superpose fold geometry to have been similar to the vergence of the F_2 fold system, approximately west-northwest (310^o).

In Domains 2 and 5 the interference patterns observed in outcrop are distinctly more mushroom-like than in Domain 1. The asymmetry of the oblique mushrooms suggests the F_1 axial surface was northeast trending and easterly-dipping (Figure 5.21a). The morphology of the mushroom-type interference pattern indicates the original orientation of the F_1 fold system has changed from Domain 1. The interference pattern demonstrates that the angle between the F_1 and F_2 fold axes has increased and the axes are no longer coaxial, and the axial surfaces are not coplanar. This indicates that the F_1 fold system had a higher degree of non-cylindricity in Domains 2 and 5. Therefore, in Domains 2 and 5 the F_1 fold system is a close to tight, asymmetric, northeast trending, gently inclined fold system. The geometric relationships of the interference patterns in Domains 2 and 5 suggest that the vergence direction of the F_1 fold system has increased toward the northwest (approximately 330^o).

The cylindricity of the F_1 fold system systematically decreases from east to west across the map area. This suggests that on a regional scale the F_1 fold system was both

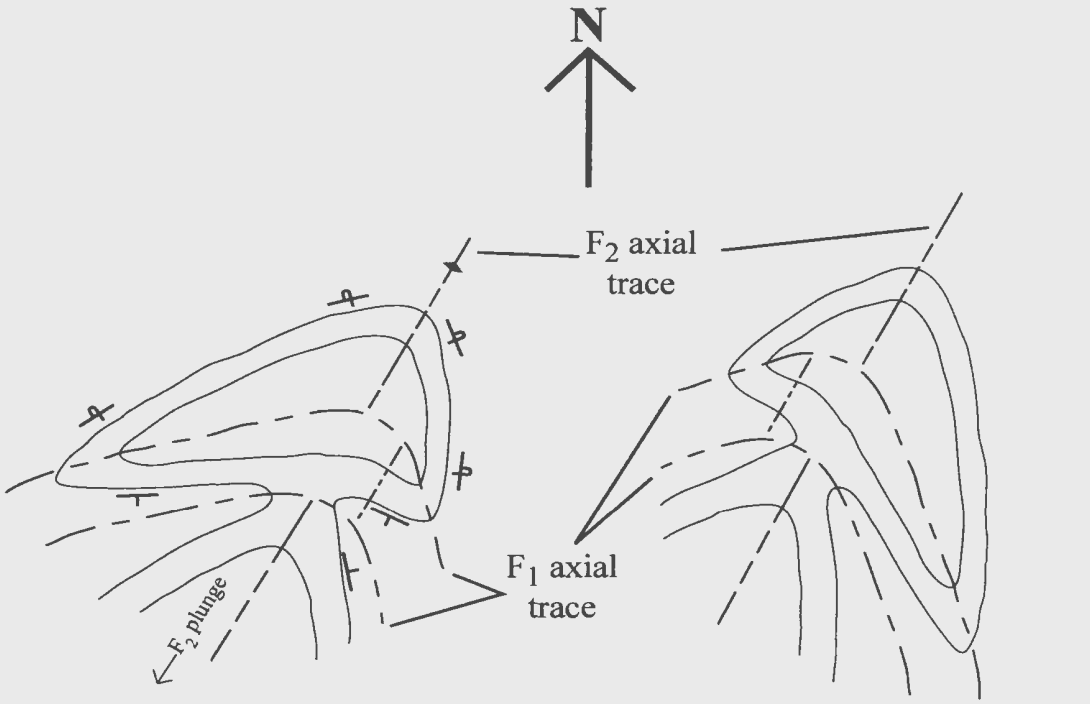

Figure 5.21 Possible asymmetries of mushroom-type structures, depending on the trend of the F_1 fold system at the time of F_2 superposition.

non-cylindrical with curved hinges and non-planar with curved axial surfaces. However, the central portions of a F_1 fold may be locally cylindrical and planar forming Type 3 interference patterns, and along the trend of the curving hinges oblique-mushroom patterns (Type 2H) with opposing asymmetries would form, depending on the direction of curvature (Figure 5.21). The pattern of decreasing cylindricity between Domain 1 and Domains 2 and 5 is the result of imbrication during the F_2 thrust system juxtaposing domains of contrasting cylindricity from different portions of the regional curvature of F_1 hinges.

Chapter six:

Cleavage development

Two tectonic cleavages are prominent features of the sedimentary rocks in the study area. The morphology, geometry, and cross-cutting relationships of these fabrics provide important constraints on the local strain fields, the rheological behaviour of the rocks, and the relative timing of deformation events. The various cleavage fabrics observed in the area and their relationships to the deformation events are described in this chapter.

6.1 S_1 cleavage

The S_1 cleavage is the salient component of the fabric in domains 1, 2, and 5. S_1 is a very strong, penetrative, domainal slaty (Hobbs et. al., 1976) or scaly cleavage that is most intensely developed in shale beds of the Northern Head Group. In carbonate beds of the group the S_1 cleavage is refracted and is manifested as a poorly developed spaced cleavage (Borradaile, et. al., 1982), or fracture cleavage (Hobbs et. al., 1976). The development of a pervasive, slaty cleavage in low grade sedimentary rocks is uncommon

relative to higher grade metamorphic rocks (Hobbs et al., 1976). The mechanisms which generate axial planar cleavage are not well-understood, but have a fundamental relationship with the quantity of strain and the orientation of the XY-plane of the finite strain ellipsoid (e.g., Hobbs et al., 1976; P.F. Williams, 1977). Three mechanisms are considered to be important in the development of axial planar cleavage: rigid body rotation of existing mineral grains, grain shape modification by crystal slip or diffusion, and growth of new mineral grains with a preferred orientation (Hobbs et al., 1976). Each of these mechanisms produces a preferred orientation of mineral grains and depending on local metamorphic conditions all three mechanism may, to varying degrees, operate simultaneously during cleavage development (Hobbs et al., 1976). The sub-greenschist metamorphic grade of the Northern Head Group in Domains 1, 2, and 5 suggests that rotation of pre-existing detrital mica is the primary mechanism of cleavage development in this area. Locally, a weak mineral lineation is developed on the S_1 cleavage surface in high strain zones. The growth of new minerals preferentially aligned with the XY-plane and the X-axis of the finite strain ellipsoid is a secondary mechanism of axial planar cleavage development in the area. The style and morphology of the S_1 fabrics supports development of during tectonic deformation of the Northern Head Group at shallow burial depths and in low temperature brittle to plastic deformation regimes. Together with bedding the S_1 cleavage is the principle surface folded by the F_2 fold system and it defines the dominant structural fabric in the shale-dominated successions of domains 1, 2 and 5, where it may be present to the exclusion of bedding (Figure 5.3b).

Local perturbations of the fabric are common in the S_1 cleavage. Divergent cleavage fans form in the shale layers around the hinge zones of many F_1 meso-scale folds. This special relationship provides insight into both the mechanical properties of the rock and the strain history of the S_1 cleavage. Figure 6.1 illustrates an example of the S_1 cleavage in shales fanning around the hinges of F_1 folds delineated by thin limestone beds of the Cook's Brook formation (Insert III, Section R-R'). This type of cleavage fan is formed in response to the competency contrast between the shale and limestone beds during the initial buckling of the competent carbonate beds. Tangential longitudinal strain fields are developed along the outer-arcs of folds in the competent beds, causing the S_1 cleavage in less competent layers to deflect around the hinge (Ramsay and Huber, 1987). The triangular trace of the S_1 cleavage around the extensional outer-arc of the hinge area is a common expression of these strain trajectories (Figure 6.1b). The inside arc of the fold is a compressional zone where the cleavage develops in an axial planar orientation (e.g., Ramsay, 1967; Ramsay and Huber, 1987). In the more competent layers these strain fields generate extensional fissures on the outer-arcs, and contractional faults on the inner-arcs of the fold hinges. The more ductile shale frequently flows into the extensional fractures and is dragged along the contractional faults into the carbonate layer. These features are commonly considered to be shale injection by previous workers (Stevens, 1970; Waldron, 1985). Notably, however, these features are mainly observed in hinge zones of F_1 folds, and are considered to be the product of local strain histories related to the evolution of the fold system.

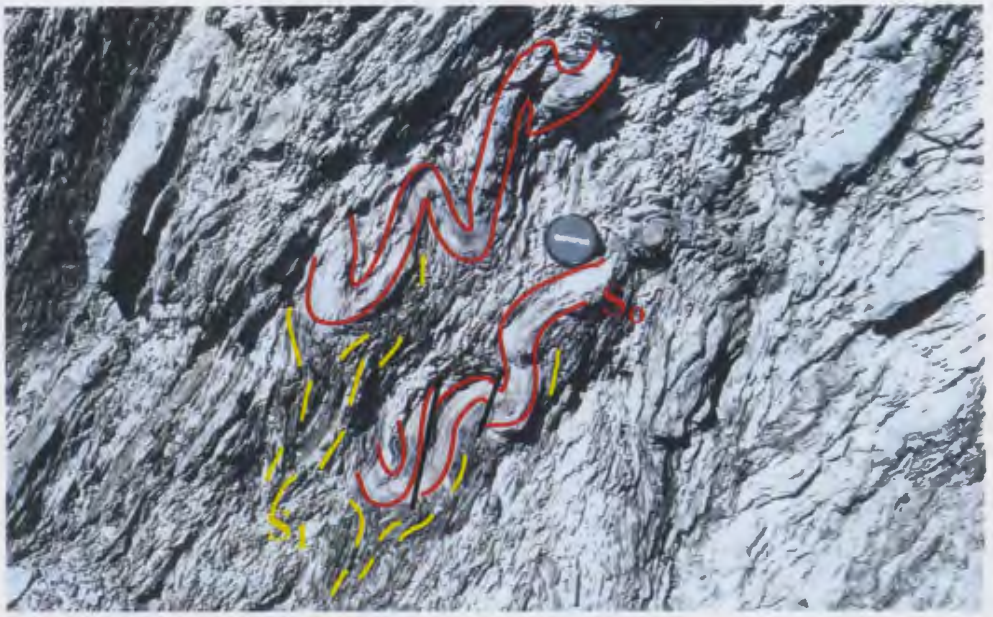

a. Photograph of F_1 folds in thin limestone beds which display axial planar S_1 cleavage fanning around the hinge zone.

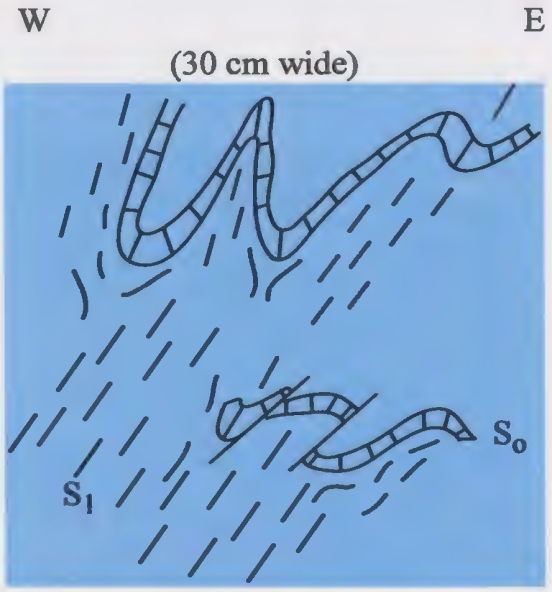

b. Field sketch of photograph in Figure 6.1a.

Figure 6.1 F_1 folds demonstrating cleavage fanning around the hinge due to the development of longitudinal strain fields in the competent limestone beds (Insert III, Section R-R').

During progressive F_1 fold development bedding in the fold limbs rotates with the evolving S_1 cleavage fabric, which will track the position of the XY plane of the finite strain ellipsoid (e.g., P.F. Williams, 1977; Hobbs et. al., 1976). This progressive limb rotation causes the beds to rotate out of the field of incremental and finite shortening, and ultimately into the field of incremental and finite extension and flattening (e.g., Ramsay, 1967). This new relationship with the evolving strain field has a significant effect on the geometry and style of the fold system. The flattening strain creates additional shortening perpendicular to the axial plane of the fold system, resulting in tightening of fold hinges, limb thinning, and hinge thickening (e.g., Hobbs et al, 1976). A secondary result is the development of boudinage of the beds, and the development of bedding-perpendicular tension veins on the limbs of the folds, which are now oriented sub-parallel to the plane of the S_1 cleavage. Progressive F_1 deformation of the shale and ribbon limestone successions of the Northern Head Group, therefore, generated a complicated fold system with a strong axial planar cleavage fabric. The strain paths of bedding accounts for the formation of many meso-scale structural features observed in domains 1, 2, and 5, particularly the stratigraphic dismemberment, the formation of bedding-perpendicular quartz-carbonate veins, and the strong (sub-)parallelism of bedding and cleavage, particularly on the overturned limb of the folds.

In the eastern portion of the area scaly cleavage is developed in high strain zones associated with the occurrence of cataclasite formed in F_1 faults. S_1 microlithons are poorly preserved within the S_1 cleavage and pervasively cut by anastamosing cleavage domains. The development of the S_1 cleavage is the result of progressive deformation of

the F_1 fold system and the cleavage becomes more intense as strain increases within the fold system. If the incipient S_1 cleavage planes are not strictly parallel to the XY-plane of the finite strain ellipsoid they will experience some degree of rigid body rotation into this preferred orientation (P.F. Williams, 1977). The cleavage planes will also be subjected to a component of shear strain during this rigid body rotation (Hobbs, et al., 1976). Slickenlines and polished fault mirrors, common features on the scaly S_1 cleavage planes, are the result the shear strain and support an initial cleavage orientation that is oblique to the XY-plane of the finite strain ellipsoid. As the axial planar cleavage continues to develop in the fold-thrust system later S_1 cleavage planes will overprint the earlier, rotated S_1 cleavage planes within a single generation of cleavage. The resulting cleavage fabric is a highly anastamosing network of sub-parallel cleavage planes, and highly dismembered microlithons formed during the earliest phases of cleavage development.

6.2 S_2 Cleavage

The S_2 cleavage is not pervasively developed in the Frenchman's Cove-York Harbour area. A non-penetrative, axial planar, closely spaced, slaty (Borradaile, et. al., 1982) S_2 cleavage is associated with the F_2 fold systems in Domains 1, 2, and 5. The S_2 cleavage is primarily developed in shale beds of the Northern Head Group, although it may also occur as a weak, refracted fracture cleavage (Hobbs et al., 1976) in the carbonate beds too. The S_2 cleavage was observed at a number of localities in the hinge regions of F_2 fold trains in ribbon-bedded limestone of the Cook's Brook formation (Insert II, Section B-B'). At locations where the S_2 cleavage is observed, it is primarily

developed as either a strong, axial planar, spaced cleavage or a crenulation cleavage (e.g., Hobbs et al., 1976). This spatial relationship of the S_2 cleavage being predominant in the fold hinge regions suggests that the strongest S_2 cleavages formed in response to localized compressional strain fields generated by development of the F_2 fold system in areas where the pre-existing planar fabrics (i.e. bedding and S_1) are at a high angle to the axial surfaces of the evolving F_2 folds. This spatial relationship of the S_2 cleavage being predominate in the fold hinge regions suggests that the strongest S_2 cleavages formed in response to localized compressional strain fields generated by development of the F_2 fold system in areas where the pre-existing planar fabrics (i.e. bedding and S_1) are at a high angle to the axial surfaces of the evolving F_2 folds.

The poor S_2 cleavage development is somewhat inconsistent with the pervasiveness of the F_2 fold system in Domains 1, 2, and 5. F_2 folds are observed from micro- to macro-scale, and the S_1 cleavage is often visibly crenulated by the smaller-scale, parasitic F_2 fold trains. Insert III, Section O - O', Detail A illustrates a unique case of crenulated S_1 cleavage in a situation where the steep limb of a F_2 fold overprints the steep limb of a F_1 fold. The steep, west-dipping bedding planes were already oriented sub-parallel to the XY-plane of the finite strain ellipsoid for the F_2 fold system and were therefore not folded by the F_2 fold system. However, the moderately to steeply east-dipping S_1 cleavage formed a small bedding\ S_1 cleavage angle, and was oriented such that it was crenulated by the F_2 fold system. The result is the formation of centimetre-scale F_2 fold trains formed between thin sandstone beds, which are not folded by the F_2 fold system.

An absence of low-temperature pressure solution features in outcrop and hand samples, differentiated layering, and a lack of new growth metamorphic minerals aligned with the S_2 cleavage fabric indicates that the ambient pressure and temperature conditions were low during the F_2 deformation event. The development of a composite $S_1\backslash S_2$ cleavage related to transposition of S_1 during intense F_2 folding occurs at some locations, and it may be difficult to distinguish S_2 and S_1. This process involves the progressive rotation of the pre-existing S_1 cleavage into near parallelism with the orientation of the F_2 axial surfaces, and the resultant re-working of the old fabric. Intense transposition the F_2 fold event makes the identification of individual early fabric generations difficult. A composite cleavage could form in any tight F_2 folds where bedding parallel S_1 cleavage fabrics are rotated to be near parallel with the F_2 axial surface (Insert II, Section F-F'). In the steep forelimb of the F_2 fold system, bedding and the S_1 cleavage are sub-parallel to the XY-plane of the strain fields which generate the F_2 folds and associated S_2 cleavage fabric. In this orientation the strain field will thin and extend the bedding and S_1 cleavage planes during progressive deformation and the S_1 cleavage will be overprinted by S_2. The evidence for this intense transposition includes rotated, rootless F_1 hinges, strongly dismembered (boudinaged) bedding, and discrete, fabric parallel cataclasite zones. The cataclasite zones occur as thin, discontinuous bands of strongly brecciated shale at the west end of Section F-F' (Insert II). These are interpreted to be dismembered brittle-shear zones formed during the F_1 folding event and subsequently have been transposed into the S_2 cleavage. Transposition of S_1 generates strong strain patterns and it becomes difficult to distinguish bedding and successive tectonic fabrics. The development of a composite

$S_1 \backslash S_2$ cleavage suggests that the S_2 cleavage may in fact be more common in the area than documented by this study. However, the overall conditions of deformation indicate that although S_2 may be more common, it will still be a poorly developed, non-penetrative cleavage fabric.

6.3 Cleavage development in the Blow Me Down Brook formation

In Domains 3 and 4 a cleavage is poorly developed within the shale intervals of the Blow Me Down Brook formation. It is a closely spaced, slaty cleavage and is typically oriented sub-parallel to bedding. Bedding-parallel shear is commonly observed in the shale beds of the Blow Me Down Brook formation and is considered to reflect flexural slip along bedding planes during the amplification of the F_2 fold system. The development of cleavage in these intervals is considered to have formed as part of the bedding-parallel shear zones during the F_2 fold-thrust event. Section L-L' (Insert II) presents a north-verging thrust fault developed parallel to bedding. In this fault zone the cleavage is observed as a well developed S-fabric, which supports the northerly displacement of the hanging wall. The shale intervals are a minor component of the stratigraphic succession in the Blow Me Down Brook formation and are not common, or extensively exposed. Therefore, a detailed analysis of the mechanical processes involved in cleavage development and the timing of the observed cleavage fabrics is not possible in Domains 3 and 4.

Chapter seven:

Fault systems

Polyphase faulting in the Frenchman's Cove-York Harbour area has strongly disrupted the stratigraphy. The segmentation makes correlation of generations of structures difficult, especially between domains where macro-structures also show variations in orientation. Furthermore, difficulties in structural reconstructions arise within domains where faults show anomalous stratigraphic separation, requiring omission of stratigraphic units of considerable thickness.

Four significant generations of faults are identified in the area. The earlier fault generations are break-thrust systems related to the F_1 and F_2 fold systems in each of the structural domains. The later fault generations are out-of-sequence thrust faults that truncate early fault systems in each of the domains and cause mixing of a variety of Humber Arm Allochthon rock units in a belt of mélange. The youngest generation of faults is a set of sub-vertical, north-south striking faults that cut across the older structures in each domain. The geometry, fault mechanisms, and relative timing relationships of these fault systems are described in this chapter.

7.1 F_1 thrust faults

7.1.1 Domains 1, 2, and 5

The identification of faults associated with the first generation of folds is difficult in the broken and dismembered shale-dominated stratigraphic successions of Domains 1, 2, and 5. However, remnants of these faults are subtly preserved at several locations. Sudden changes in facing direction of F_2 fold limbs, transposed cataclasite, folded fault surfaces, and broken F_1 folds features attesting to the development of a fault system associated with the development of F_1 folds.

In section E-E' (Insert II) at 1270m a F_1 thrust surface causes an abrupt reversal in the facing direction within the eastern limb of a synform causing this F_2 fold to change its facing direction from upwards (syncline) to downwards (anticlinal synform) across the folded, pre-existing fault. In this situation the normal, upright backlimb of an F_1 fold was juxtaposed against the overturned F_1 forelimb prior to refolding in the F_2 folding event. Details A and B of Section F-F' (Insert II) illustrate F_1 folds which are broken by thrust faults in Domain 2. Detail B demonstrates that the F_1 folding is associated with the formation of thrust faults that break through the forelimb of the folds. This geometric relationship is consistent with the F_1 folds and thrusts forming contemporaneously as part of a west-verging fold-thrust system.

At station A2711 two F_1 faults in a sandstone-shale succession of the Eagle Island formation have been folded by F_2 (Insert II, Section G-G', station A2711). An upwards facing, truncated F_1 synform is contained in the imbricate slice formed by the two fault surfaces. Based on the asymmetry of the F_1 fold and the east-dipping attitude of the fault

planes, the vergence of the F_1 faults is inferred to be to the west. The attitude of the two faults and geometry of the broken F_1 fold hinge are consistent with the development of F_1 folding related imbricate slices. Subsequent deformation of the F_1 slices and their bounding faults formed a west-verging macro-scale F_2 fold. The z-type asymmetry of this F_2 fold indicates it formed as a parasitic structure on the steep forelimb of the overall east-verging F_2 fold system in Domain 2a.

The style of the F_1 fold trains in Domains 1, 2, and 5 are consistent with fold-thrust system developed under conditions of relatively high, non-coaxial strain (Ramsay et al., 1983). An advanced, highly amplified, and overturned asymmetric fold system is associated with a penetrative, axial planar cleavage (S_1) reflecting the more ductile deformation conditions as tectonic loading increases in the hinterland of the fold-thrust belt. The S_1 cleavage is defined by the alignment and weak growth of mica minerals; but very little pressure solution driven remobilization of quartz and carbonate indicating that the deformation event occurred in the lowest temperature ranges required to develop a slaty cleavage. During the later stages of the deformation and the development of the F_1 fold trains, the imbricate thrust system parcelled geometrically variable sections of the fold trains, including complete hinge domains. This early imbrication of the high strain F_1 fold system suggests that initial dismemberment and thrust-stacking of stratigraphic successions in the Humber Arm Supergroup was related to the development of regional scale nappe type-structure during the earliest phase of deformation in this area.

7.1.2 Shear zone at boundary of Domains 4 and 5

A regionally significant brittle-ductile shear zone is preserved at the structural base of the Wood's Island Volcanics (Insert I). The shear zone is a dark red, strongly foliated cataclasite (Figure 7.1a). The fabric of the shear zone is primarily formed from sheared and altered Wood's Island Volcanics. Clasts in the shear zone are composed of volcanic fragments, fragmented syn-deformational quartz veins, and fragments of limestone. The formation of a C-S fabric, shear bands, and rotated clasts indicates the shear zone formed in a brittle-ductile environment of deformation (Figure 7.1b). Folded tension veins and antithetic shear fractures in elongate limestone clasts and quartz veins are also common kinematic indicators in the shear zone (Insert III, Section N-N', Detail B).

C-S fabrics are well developed within portions of the shear zone characterized by fine grained matrix in the shear zone. Both planes are west-dipping and form a 25° acute angle which opens to the east. The geometry of the C-S fabric demonstrates that the hanging wall moved down to the west relative to the footwall, implying an apparent normal sense of displacement of the shear zone in its current orientation (Insert III, Section N-N', Detail B). All of the other kinematic indicators developed in the shear zone are consistent with development in a west-verging shear zone with this inferred sense of displacement. Notable features are the elongation of the clasts parallel to the S-plane and oblique to the shear zone boundary, and the sense of asymmetry of the folded quartz veins.

a. An oblique view of the F_1 shear zone showing the angular relationship between the S-fabric and the shear zone boundary (SZB), which indicates the hanging wall moved down to the west.

b. Kinematic indicators in the F_1 shear zone. (C) c-plane, (S) s-plane, (SB) shear band, (AT) antithetic shear fractures, and (TV) quartz tension vein. Note the rootless, west-verging, asymmetric meso-fold in the lower-right portion of the shear zone.

Figure 7.1 F_1 shear zone at the base of the Wood's Island Volcanics and the associated kinematic indicators. (Insert III, Section N-N', Detail B).

Previous workers considered the west-dipping fault zone to be a part of the east-verging regional fold-thrust system observed along the coastline east of Frenchman's Cove (e.g., Williams and Cawood, 1989; Waldron et. al., 2003). However, the kinematic analysis of the shear zone fabrics clearly demonstrates that the postulated sense of displacement for the fault is incompatible with the formation of the late, east-verging regional fold-thrust system.

East-verging thrust faults are present in the Blow Me Down Brook formation east of the shear zone and at the structural top of the Wood's Island Volcanics to the west. Section N-N', Detail C, on Insert III, is constructed perpendicular to the strike of the shear zone and the east-verging thrust faults, but demonstrates the angular relationships between the fault systems and the Wood's Island Volcanics. The volcanics form a thin imbricate sheet in an east-verging thrust system which marks the boundary between Domains 4 and 5. The shear zone at the base of the volcanic slice is truncated by the younger east-verging thrust system and is a demonstrably older structure.

The shear zone is markedly different in structural style than the F_2 and F_3 fold-thrust systems mapped elsewhere in Domain 5. The development of a foliated cataclasite, penetrative C-S fabrics, and other brittle-ductile fabrics in the matrix of the shear zone indicates it formed in a higher temperature and strain environment is a marked contrast with the more brittle F_2 and F_3 structural systems which truncate the shear zone. The S-fabric developed in the shear zone has similar characteristics to the style of the axial planar, slaty S_1 cleavage associated with the F_1 fold system. The slaty, penetrative nature of the S_1 cleavage indicates it formed in higher temperature, more ductile strain

environments, which would be consistent with the shear fabrics within the shear zone. Based on overprinting criteria and the similarity of deformational environments, this shear zone is, therefore, tentatively interpreted to be a major, west-verging F_1 thrust fault that has been folded and imbricated by the F_2 fold-thrust belt and younger deformation events (see Chapter eight).

7.2 F_2 thrust faults

7.2.1 Domains 1 and 5

The F_2 thrust system in Domain 1 forms a stack of thin imbricate slices bound by northwest-verging thrust faults. The faults predominately dip to the southeast and dismember the F_2 fold system. The fact that complete F_2 fold hinges lie isolated within the imbricate slices indicates that the thrust faults break through the steep fore limb of the already amplified fold system juxtaposing forelimb and back limb domains (Section A-A', Insert II). The development of the F_2 thrust system is penetrative, occurring on several scales of observation.

A large meso-scale fold-fault structure is developed at the southeast end of Section E-E' (Insert II) and demonstrates the relationship between fold and thrust fault development. The fold limbs are tens of meters thick at this location, forming large cliff faces of well-bedded ribbon limestone successions of the Cook's Brook formation. A major, northwest-verging F_2 thrust fault breaks through the steep forelimb of the fold emplacing Domain 1a over 1b. Sub-vertical accommodation faults are developed in the hinge and steep limb domains of the F_2 fold (Insert II, Section E-E'). The

accommodation faults splay upwards in a triangular fashion, forming small pop-up structures within the F_2 anticline. A lower hemisphere, equal area plot of the faults measured in Domain 1 shows the main cluster of poles on this plot correlates to the southeast-dipping thrust faults (Figure 5.4). The distribution of poles along a girdle parallel to the pi-girdle of the F_2 fold system demonstrates the faults are generally parallel to the trend of the F_2 folds. This relationship indicates that the faults are syn-genetic with the F_2 fold system. The steeply-dipping faults and the westerly-dipping faults may represent sub-vertical pop-up structures and backthrusts in the F_2 thrust system, respectively.

Locally, duplex structures are present at the meso- and macro-scales within the F_2 thrust fault system. A complicated duplex structure in the footwall of the main thrust in Section E-E' is formed in the steep limb of the northwest-verging fold at the switch in structural vergence between domains 1 and 2. At this location it is difficult to accurately resolve the fault overprinting relationships, but it appears that the structure is a duplex formed within the north-west verging F_2 thrust system of Domain 1 at the time that Domain 1 was thrust over Domain 2.

7.2.2 Domain 2

The F_2 thrust system in Domain 2 consists of southeast-verging thrust faults, forming the mirror image of the thrust system developed in Domain 1. The F_2 thrust system in Domain 2 mainly imbricates slices of the Irishtown, Cook's Brook, Middle Arm Point, and Eagle Island formations. The imbricate slices are thin and on a macro-scale form an imbricate fan, but are also internally imbricated, forming small scale

duplex structures (Insert II, Section F-F'). A lower hemisphere, equal area plot of faults in Domain 2 shows the largest population of measured faults are moderately westerly- to northwesterly-dipping faults, and strike sub-parallel to the trend of the F_2 fold system, suggesting the fault system is syn-genetic with the fold system (Figures 5.6 and 5.7). The F_2 thrust system formed after the amplification of F_2 fold trains and imbricate slices formed in the F_2 fault system contain complete F_2 antiforms and synforms parcelled by the faults. The close relationship between F_2 faults and dismembered F_2 folds suggests the F_2 thrust system developed as part of a southeast-verging fold-thrust system.

In Domain 2 the F_2 thrust system forms an imbricate stack that repeats a section consisting mainly of the Middle Arm Point and Eagle Island formations (Insert I and II, sections E to G). The conformable stratigraphic contact between these two formations makes repetition of the sequence possible during the regular development of an imbricate stack. However, the presence of small scale duplex structures throughout Domain 2 suggests that the F_2 thrust system in Domain 2 forms may also comprise regional scale duplex structures. The first 160 m of Section H-H' (Insert II) displays a duplex structure in a well-bedded sandstone-shale succession of the Eagle Island formation. The internal architecture of this imbricate slice is representative of the structural style of larger scale second generation fault systems in Domain 2 and the development of an east-verging duplex structure.

The fine-scale imbrication with the F_2 fault system created an anomalous distribution of stratigraphic panels in Domain 2 (Insert II, sections G-G' and H-H'). Distinctive, although, limited stratigraphic successions are often contained within an

imbricate slice, but typically the successions do not cross formational boundaries within slice. The consistent repetition of these imbricate slices with "singled-out" lithologies creates anomalous stratigraphic separations within the imbricate stack (e.g., both older over younger, and younger over older). These anomalous stratigraphic separations between fault panels are particularly apparent on sections G-G' and H-H' (Insert II), where panels of the Eagle Island formation are repeated in the imbricate stack and juxtaposed with the Irishtown formation.

7.2.3 Domain 3

The structural style of domains 3b and 3c is characterized by the presence of a north- to northwest-verging, F_2 thrust system. The faults commonly lie parallel to bedding as detachment surfaces in shale beds of the Blow Me Down Brook formation (Figure 7.3a and Insert II, Section L-L'). The thrusts commonly break through the steep forelimb of F_2 folds and this demonstrably occurred late in the evolution of the F_2 fold system (Insert II, Section K-K'). Figure 7.2 displays the typical geometry of the moderately south-dipping thrust faults exposed along the shoreline in Domain 3.

Lower hemisphere, equal area plots of faults in Domain 3 show a broad distribution of orientations as a result of plotting multiple fault generations on a single plot (Figures 5.9 and 5.10). A large population of faults on both the stereonets belongs to moderately south- to southeast-dipping faults. Figure 5.9 also shows a population of moderate to steeply north-dipping faults. This particular population is interpreted to be backthrusts formed during movement of the principal, north-verging thrust system in Domain 3b. Kinematic indicators developed in the brittle thrust faults include: fracture

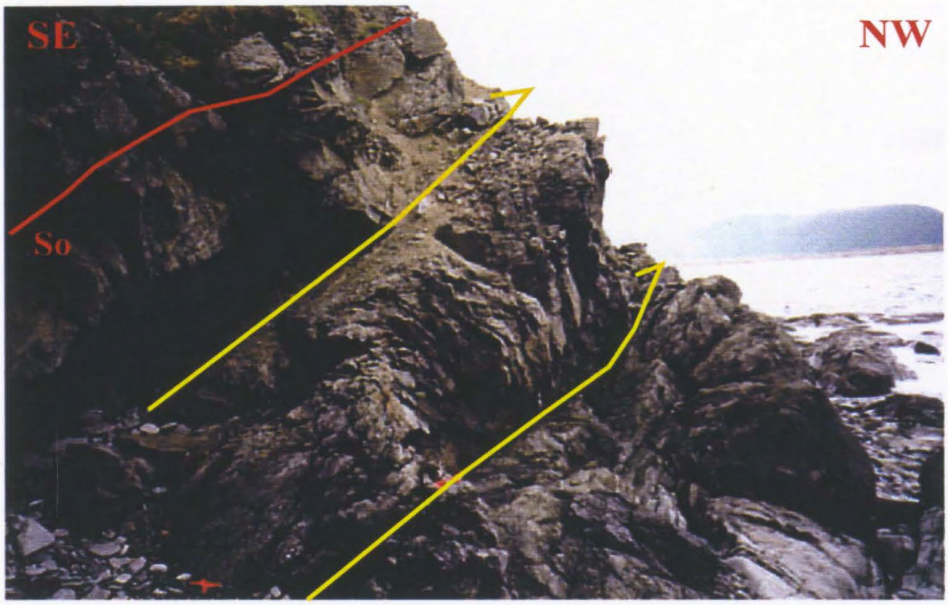

a. Northwest-verging, bedding parallel F_2 thrust surfaces in the Blow Me Down Brook formation (yellow) (Insert IV, station JN2401).

Figure 7.2 Style of F_2 thrust faults in Domain 3.

sets corresponding to the geometry of synthetic p- and r-fractures, slickensides on bedding surfaces, and rare C-S fabrics in detached shale beds. Slickensides are the most common and reliable kinematic indicator observed in Domain 3. Unfortunately their use is limited in view of the known polyphase movement history with unclear overprinting relationships and limited exposure. Thick quartz-carbonate fibre packages are most often observed on dislodged sandstone blocks. Exposures of well-developed insitu slickenlines on bedding are relatively rare in this area. The southerly- and northerly-dipping fault planes with slickenfibers in Domains 3b and 3c are plotted as slip linears in Figure 7.3. The slip linears highlight the variability in the sense of movement on faults in this area. The populations of both northerly- and southerly-dipping faults indicate predominately reverse and reverse-oblique senses of movement. This is consistent with the formation of these populations in north-verging thrust systems and syn-genetic backthrust accommodation faults. The relationship of between the southerly-dipping F_2 faults and the north-verging F_2 fold system, the few observed kinematic indicators, and the slip linear plot constrain the overall oblique, reverse sense movement on this dominant north- to northwest-verging fault system (Figure 7.2 and Insert II, Section L-L').

Duplex structures are present within the F_2 fault system. Section K-K' (Insert II) is an example of a duplex structure where a set of thrust faults truncate an early F_2 synclinal antiform. The southerly-dipping F_2 thrust faults break an already amplified F_2 fold, isolating a macro-scale synclinal antiform in the footwall of the duplex structure. In the hanging wall, the thrust faults form hanging wall flats and footwall ramps, emplacing gently-dipping, upright beds of the F_2 back limb over the macro-scale F_2 synclinal

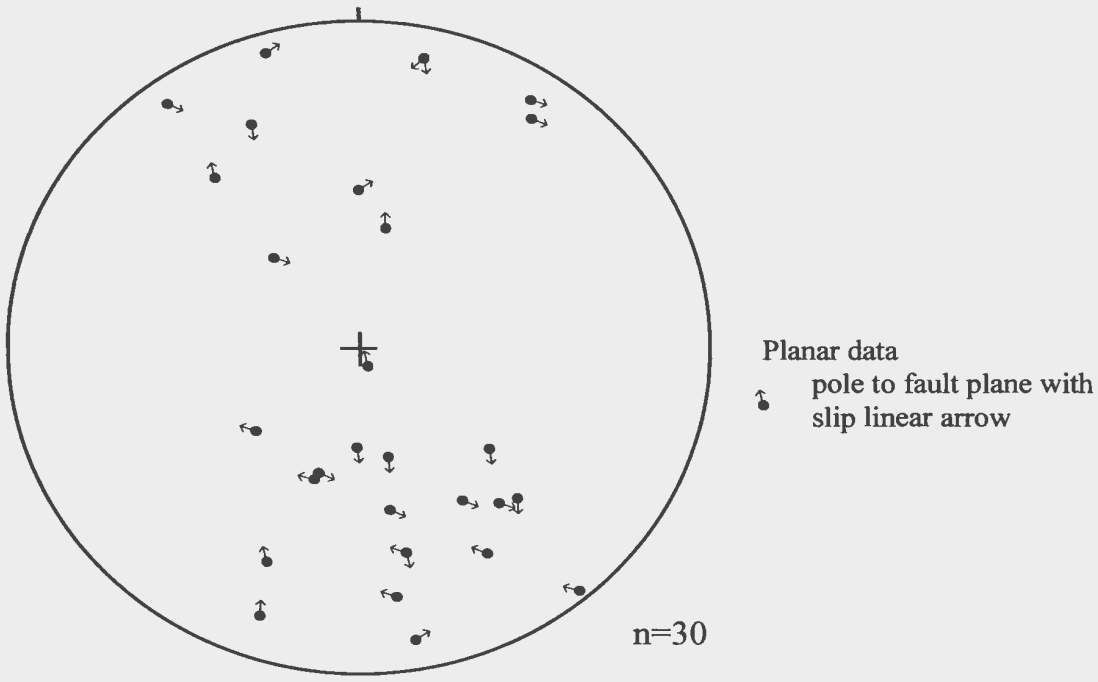

a. Lower hemisphere, equal area projection showing poles to southerly- and northerly-dipping faults in Domain 3. Slip linear arrows on each pole indicate the sense of movement. Only the measurements of faults with slickenfibres are plotted.

Figure 7.3 Stereoplots presenting fault plane and fault kinematic data for the late, northerly striking fault population, which overprints the area.

antiform in the footwall. The geometry of the duplex is complicated by a late out-of-sequence reverse fault that breaches the roof of the duplex and truncates the upper, south-dipping thrust faults. The reverse fault juxtaposes vertical beds of the F_2 steep, forelimb, from the footwall of the duplex structure, against gently-dipping beds of the F_2 back limb in the hanging wall of the duplex structure (Insert II, Section K-K'). The complex geometry presented by this duplex structure and dismembered fold are similar to out-of-sequence thrust systems described by Morley (1988) for thrust faults with complex footwall geometries at El Kansera Dam in Morocco.

The presence of out-of-sequence faulting during development of the F_2 thrusting indicates the system forms over a long period as the result of progressive deformation. The out-of-sequence faults generate thrust surfaces that locally cut down section and create complex map and section patterns (Morley, 1988). The population of steep- to moderate-dipping faults on the lower hemisphere, equal area plots in Figure 7.3 and Figure 5.9 are formed as part of the group of the out-of-sequence accommodation faults and as such must be somewhat younger than the main, southerly dipping F_2 thrusts. This relative timing relationship is also depicted by cross-cutting relationships of the vertical reverse fault shown in Section K-K' (Insert II).

7.2.4 Domain 4

Domain 4 is characterized by the presence of the large F_2 anticline located on Wood's Island (Insert III, Section N-N'). Faults in Domain 4 are primarily inferred by the abrupt juxtaposition of different bedding dip domains in the F_2 fold system. In the central portion of Seal Island a west-verging thrust fault is inferred between two easterly-dipping

and facing bedding panels (Insert III, Section M-M'). On Wood's Island small, meso-scale fault-propagation folds are developed in thin sandstone beds in a nine meter thick shale sequence (Insert III, Section N-N', Detail A). The F_2 folds are transected by moderately east-dipping thrust faults. In Detail A, two fault splays can be seen breaking through the steep forelimbs of the asymmetric folds. The geometric and timing relationships shown in Detail A are considered to represent a small scale fold-thrust system that mimics the much larger system in Domain 4. The large folds observed on Wood's Island and Seal Island are interpreted to have formed as fault-propagation folds in the thick, mechanically competent sandstone beds of the Blow Me Down Brook formation. During progressive development of the fold-thrust system the thrust faults eventually break through the steep forelimb of these folds. Outcrop of each significant dip domain that defines the polyclinal kink geometry of fault-propagation folds (e.g. Mitra, 1990) is present on the islands in Domain 4, but the master faults are not exposed at any of these localities.

Figure 5.11 contains a lower hemisphere, equal area plot of the measured faults in Domain 4. Three distinct populations of faults are present on the plot. Moderately east-dipping, west-verging thrust faults form a cluster in the western hemisphere of the stereonet and two populations are present in the eastern hemisphere. The cluster of three sub-vertical, northwest striking faults is correlated with a younger generation of faults. The central cluster of moderate to steep west-dipping faults are interpreted as out-of-sequence backthrusts related to the main westerly-verging F_2 fold-thrust system in Domain 4. This group of faults is exposed on Seal Island, but no kinematic indicators

were present in the fault zones. However, their orientation and spatial association is consistent with development as part of the fold-thrust system in Domain 4. The structure in the central portion of Seal Island resembles a pop-up structure developed across a fault-propagation fold (Mitra, 2002) (Insert III, Section M-M').

No early generation of structures have been measured in Domain 4. The backlimb of the anticline on Wood's Island is truncated by third generation thrust faults (Insert III, Section N-N' and Detail C). This important hanging wall cut-off is the only direct evidence for the relative timing of formation of the fold-thrust system. The style and geometry of structures observed in Domain 4 are similar to the F_2 fold-thrust system measured in Domain 3. Because of this geometry the fault-propagation folds and associated thrust faults in Domain 4 are considered to be second generation structures.

7.2.5 Domain 5

The second generation thrust systems developed in Domain 5 imbricate lithologies of the Blow Me Down Brook, Cook's Brook, and Eagle Island formations. Inside the panels the style and geometry of the F_2 fold thrust system is similar to the second generation structures mapped in Domain 2 at Frenchman's Cove. A switch from east- to west-vergence occurs in the thrust system in the middle of Domain 5, this change is co-incident with the change in vergence of the F_2 fold system (see section 5.2.5).

East-verging thrust system

The thrust system in sections O-O', P-P', Q-Q', and the initial 550 m of R-R'-R" forms an east-verging imbricate fan. Each imbricate slice in the fan is defined by a single

lithology of the Humber Arm Supergroup. Internally each slice is strongly imbricated by smaller scale faults. The F_2 fold system is dismembered by the F_2 fault system (Insert I and III). The coincidence of major thrust faults with steep bedding domains and the presence of isolated synforms entrained within fault panels indicates that the faults mainly broke through already well-amplified fold structures. The F_2 thrust faults do not necessarily demarcate the boundaries of lithological panels in Domain 5. At several locations late, sub-vertical faults truncate the F_2 fold-thrust panels juxtaposing different lithological successions (Section R-R', Insert III). Notably, the stratigraphic excision created by these fault contacts cannot be accounted for by simple fold-thrust related separations.

Lower hemisphere, equal area plots in figures 5.12 and 5.13 show the faults measured in Domain 5. On each plot there is a dominant population of moderately to steeply, west-dipping fault planes, which are associated with this thrust system. The small population of steeper faults with northerly strikes represent the late fault structures that form the boundaries of some structural panels (Figure 5.13).

West-verging thrust system

The F_2 structural system in Domain 5 switches vergence at 550 m on Section R'-R" (Insert III). The imbricate fan formed by the thrust system is similar in style and geometry to the thrust system in the western part of Domain 5. The imbricate sheets are thin and occur on several scales, forming multiple imbricate sheets within larger panels. The larger imbricate sheets are defined by the lithology within the structural panel. The panel boundaries are complex fault zones that have been modified by later fault

generations. The vergence of the thrust faults is defined by the dismembered F_2 folds preserved in the imbricate slices. The F_2 fold trains were well-amplified when the F_2 thrust system breached the folds and parcelled meso- to regional scale antiforms and synforms within fault panels (Insert III, R'-R").

Lower hemisphere, equal area plots for the faults measured in the eastern portion of domain 5 are presented in figures 5.14 and 5.16. The orientation patterns of the faults on these plots are similar. The moderate, southeast dipping fault planes correspond to the thrust faults which define the west-verging imbricate fan (Insert III, sections R' to T). The population of sub-vertical, northeast striking faults are related to the set of later faults which cut across the older generations of structures in the Frenchman's Cove-York Harbour area.

Section S-S' (Insert III) contains two structural features that highlight the progressive nature of the F_2 deformation event and the repetition of structural style in small scale features within the imbricate slices. Detail C (Section S-S') is a map of a small scale duplex developed on the limb of a fairly large scale downwards facing F_2 fold. The duplex is approximately eight meters wide, measured perpendicular to the strike of its bounding faults. Internally the horses of this small duplex contain small, tight to isoclinal F_2 folds with orientations that demonstrate the genetic relationship between folding and thrusting. The duplex formed on an overturned stratigraphic panel causing downwards facing folds within the horses. The presence of a complex structure like this emphasizes the increase in structural complexity caused by overprinting of younger structures.

Ten meters west of the F_2 duplex structure is a 65 m wide panel of recumbent, downwards facing, east-verging folds. The vergence of the folds is anomalous for their position in Domain 5, but they are demonstrably second generation structures. This panel of east-verging folds can be traced into a small bay where it becomes covered by glacial tills. The next exposure to the west is a west-verging thrust fault which emplaces sandstone and shale units of the Blow Me Down Brook formation over the panel of Cook's Brook formation. The east-verging fold-thrust system in Section S-S' is interpreted to be an out-of-sequence backthrust structure formed as part of the main west-verging fold-thrust system. The backthrust formed in the same downwards facing fold limb as the duplex in Detail A.

7.3 F_3 thrust system

The F_3 thrust system is a significant component of the structural geology in the Frenchman's Cove-York Harbour area. This late, east-verging fault system overprints the fold-thrust systems developed during the earlier deformation events, causing re-imbrication of earlier imbricate fans. The F_3 fault system forms an important structural boundary emplacing predominately sandstone successions of the Blow Me Down Brook formation eastwards over the carbonate dominated successions of the Northern Head Group. This section discusses the three localities that provide the most extensive exposure of the F_3 thrust system on Wood's Island, west of Frenchman's Cove, and scattered outcrops south of Frenchman's Cove.

7.3.1 West of Frenchman's Cove

A distinctive, east-verging F_3 fold system which is exposed west of Shoal Point, in Domain 3a, is associated with geometrically related F_3 thrust faults (Insert II, sections I-I' and J-J'). The thrust system consists of moderate to steep, west dipping faults that break through the steep forelimbs of F_3 folds (Figure 5.17). The faults are generated on several orders of scale. The faults of the east-verging imbricate fan depicted on Section I-I' are second order faults which rise to the east and are rooted on a blind, deeper, and higher order fault in the system. The vergence of the thrust faults is determined by the asymmetry of the associated folds. A lower hemisphere, equal area plot for the faults measured in Domain 3a indicates that many of the faults are southwesterly- to westerly-dipping (Figure 5.18). A population of east-dipping faults is also present in the domain. These faults constitute a broad group and are interpreted to comprise of small scale backthrusts and other faults which formed to accommodate movements on the main east-verging F_3 fault system.

Two important first-order thrust faults are identified Domain 3a. The most significant of these two faults occurs at the structural base of the Blow Me Down Brook formation (Insert II, Section J-J', 85 m). The fault zone is approximately two meters thick and developed along a shale bed of the Blow Me Down Brook formation. Shear bands and rotated S_1 cleavage in the shear zone indicate a reverse-sinistral sense of displacement, consistent with the asymmetry of the F_3 fold system. This is a master fault that emplaces the Blow Me Down Brook formation in Domain 3 over the early formed

structures present in Domain 2, truncating the western extent of the imbricate fan developed in lithologies of the Northern Head Group and Eagle Island formation.

The second first-order fault in Domain 3a is not directly observed but a construction of F_3 folds on (Insert II, Section J-J', 85 m) implies the presence of a significant thrust at the west end of the section. The fault forms as a footwall ramp in the long, gently dipping back limb of a large F_3 fold. Its position is identified by the juxtaposition of two distinct dip domains, with the steeper-dipping domain defining a hanging wall flat. In the hanging wall a small exposure of red shale is present stratigraphically and structurally below sandstone beds of the Blow Me Down Brook formation. This indicates that the fault initially detached along a shale bed within the Blow Me Down Brook formation before it propagated up-section to form the footwall ramp. The geometry and style of this fault is consistent with faults of the F_3 fold-thrust system observed elsewhere in Domain 3a.

A large F_3 kink fold is present east of the first-order fault, in the central portion of the Section J-J' (Insert II). The geometry and angular relationships of the kinked hinges of the fold is similar to the geometry of polyclinal kink-style fault-propagation folds (Mitra, 1990). The east-verging fold is formed as a ramp anticline due to the presence of a blind-thrust. The fault must have a hanging wall ramp geometry in order to cut up-section to the east and form the F_3 fold (Mitra, 1990). The displacement direction and orientation of this fault is compatible with the first-order thrust fault mapped further west on Section J-J' (Insert II), suggesting the blind-thrust fault is a footwall splay of the

higher order fault, or a there is a deeper detachment zone which propagates the faults as an imbricate fan.

7.3.2 Wood's Island

On Wood's Island the F_3 fault system defines the boundary between domains 4 and 5. The fault system forms an east-verging imbricate fan on the west side of Domain 5 (Insert I). The structurally lower imbricates to the east contain thick sandstone beds of the Blow Me Down Brook formation. The Wood's Island Volcanics lie in the highest imbricate slice of the fan. Section N-N', Detail C (Insert III) shows the upper slices of the imbricate fan and their relationship to the contact between Domains 4 and 5. The upper contact is the best exposed portion of the F_3 thrust system on Wood's Island, whereas the remainder of the fault system is mostly covered by glacial deposits.

The fault at the top of the Wood's Island Volcanics is a first-order fault in the F_3 thrust system (Insert III, Section N-N', Detail C). An angular cut-off between thick sandstone beds of the Blow Me Down Brook formation and the Wood's Island Volcanics defines the position of the fault and marks the western extent of the late east-verging fault system. Deformation related to the fault affects both the hanging wall and footwall of the fault.

In the hanging wall, bedding in the thick-bedded sandstone of the Blow Me Down Brook formation has experienced fault drag and is dipping steeper than the back limb of the large F_2 anticline in Domain 4 (Insert III, Section N-N'). The rotated beds are upright and dip 55° to the east. The orientation of the beds is consistent with normal drag associated with the easterly thrust sense and displacement of the hanging wall.

The footwall of the fault displays strong cataclasis and brittle-ductile shear fabrics in the Wood's Island Volcanics. Figure 7.4a shows a microphotograph of shear fabrics formed in a 15 cm thick band of red indurated, foliated cataclasite. C-S fabrics, shear bands, and quartz veins are developed in the cataclasite. The shear zone is approximately two meters thick in the footwall. Below the cataclasite zone, shear fabrics are strongly developed in the deformed volcanics and have a more ductile appearance. The matrix of the fault zone in the volcanics is strongly clay altered and the most intense fabrics are developed in this portion of the fault zone. Microscopic to centimetre scale C-S fabrics are observed in the strong fabric of the sheared volcanic rocks (Figure 7.4b). The C-S fabrics in both the cataclasite and the sheared volcanics indicate reverse shear sense for this significant F_3 fault. Normal, upright pillow basalts of the Wood's Island Volcanics are present in the immediate footwall of the sheared volcanics at this locality.

7.3.3 South of Frenchman's Cove

The F_3 fault system is difficult to trace in the heavily forested hills south of Frenchman's Cove. Two important, isolated outcrops help to constrain the position of the main F_3 fault system along strike to the south. Unfortunately the poor exposure and difficulty traversing the area south of Frenchman's Cove hinders the detailed mapping and analysis in this portion of the F_3 fold system.

The first outcrop is located 25 m south of the highway near the top of the hill on the west-side of the townsite (station 486, Insert IV). A west-dipping thrust fault is exposed in a small cliff face along a small ridge. The fault emplaces listwanite and serpentinite over dismembered sandstone and shale in the footwall (Figure 7.5). The

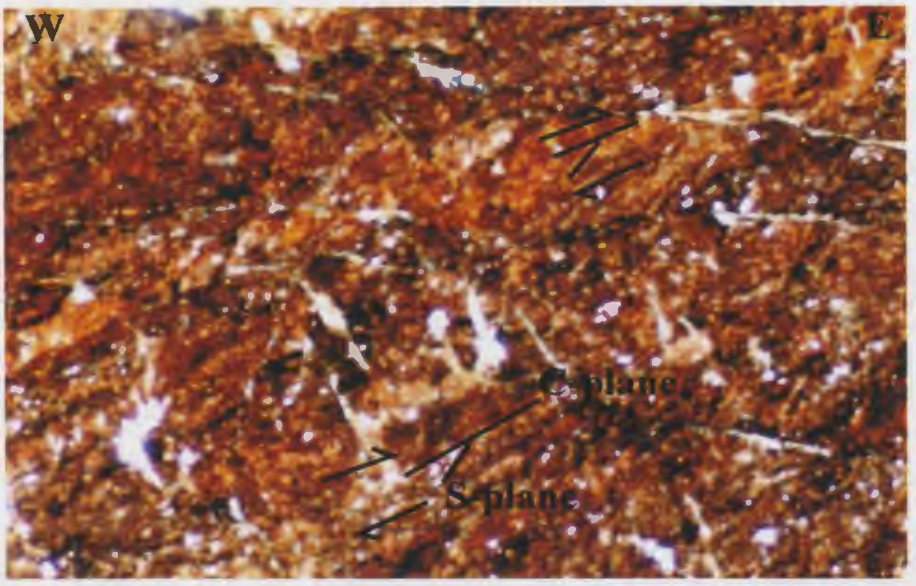

a. A microphotograph (10x) of C-S fabrics in the thin cataclasite developed in the F3 fault zone (Insert III, Section N-N', station 245, sample 01).

b. C-S fabric developed in sheared volcanics near the base of the fault zone (Insert III, Section N-N', station 245).

Figure 7.4 Kinematic indicaters developed in brittle-ductile fault zone a the top of the Wood's Island Volcanics. Arrows depict the shear sense.

Figure 7.5 An east-verging F3 thrust fault separating listwanite in the hanging wall from dismembered shale and sandstone in the footwall (station 486, Insert I).

reverse shear sense of the fault is constrained by the presence of coarse C-S fabrics developed in the fault gouge and grooves on the fault surface oriented sub-parallel to the dip. This is the only locality in Frenchman's Cove where igneous rocks are present in the section. The dismembered shale and sandstone in the footwall of the thrust is interpreted to be part of an imbricate slice in Domain 2 consisting of the Eagle Island formation (see Insert I).

The second outcrop that displays an F_3 fault is located at the base of a volcanic imbricate slice. The fault is poorly exposed in a small cliff on the hillside (station 300602-02, Insert IV). The fault dips 45° to the west, but no kinematic indicators were observed in the fault zone. The hanging wall is composed of vesicular pillow basalts and brecciated limestone of the Frenchman's Cove Volcanics (see section 3.1.6). The pillow basalts are part of an imbricate stack that forms a series of distinctive ridges and hills south of Frenchman's Cove (Insert I). In the footwall of the fault is black shale of unknown stratigraphic affinity. This fault is interpreted to be the basal fault of the F_3 thrust system, overriding the shale dominated lithologies of the Northern Head Group in Domain 2. The volcanic ridges west of the basal thrust are interpreted to be part of a westerly-dipping duplex structure formed F_3 thrust event (Insert I). An alternative interpretation of the Frenchman's Cove Volcanics is that the duplex structure was formed during the F_1 fold-thrust event. This interpretation requires the thrust faults bounding each volcanic horse to be folded, west-verging F_1 thrust faults, similar to the shear zone at the base of the Wood's Island Volcanics (see section 7.1.2). This implies that the Frenchman's Cove Volcanics were incorporated into folded F_1 duplex structures, which

were subsequently truncated by the F_3 thrust faults. The current structural position of the volcanic duplex structure is the result of foot-wall plucking and exhumation in the out-of-sequence, easterly-verging F_3 fold-thrust system.

7.5 Post F_3 faults

A prominent set of regularly spaced, northerly-striking faults cut the coastal sections across the entire Frenchman's Cove-York Harbour area. The Blow Me Down Brook formation in Domain 3 contains the highest proportion of recognized faults in this late array (Insert I). Poor inland exposure makes it difficult to delineate the large scale geometry of the fault system. However, offsets along these faults have a significant impact on the regional distribution of the Humber Arm Supergroup components.

The faults are steeply-dipping and strike north-northeast to north-northwest (Figure 7.6a). Grooves and quartz-carbonate slickenfibers packages are common kinematic indicators observed on the fault surfaces. They show that the faults experienced complex polyphase movement. Individual faults typically display multiple generations of slickenfibers showing normal, reverse, dextral, sinistral, and oblique fault displacement. The nature of the outcrop exposure generally makes it difficult to determine overprinting relationships of the fibre packages and the movement history seems different for almost every fault. Figure 7.6a presents a slip linear plot on a lower hemisphere, equal area projection accompanied by the distribution of the polar slickenlines. The plot presents fault and fault lineation data measured from each of the structural domains and highlights the complex movement histories of these faults. The fault movements range from pure dip-slip to pure strike-slip and as described above all

senses of fault displacements are represented within the population. The most visually striking feature of these faults is the juxtaposition of dip domains in the footwall and hanging wall of the faults. An excellent example of this relationship is shown at 675 m on Section J-J' (Insert II). The hanging wall of this fault contains vertical beds of Blow Me Down Brook formation and the footwall consists of moderately dipping beds.

A lack of extensive marker units in the formation, poor exposure, and multiple displacement events limit the kinematic analysis of this fault set. The structural architecture of Domain 2a appears to be strongly controlled by the trend of these late faults (Insert I and Insert II, Section G-G'-G"). The elongate distribution of lithological panels in this sub-domain is sub-parallel to the strike of the late faults. Section G-G'-G" (Insert II) displays several thin structural panels, containing stratigraphic successions of the Middle Arm Point and Eagle Island formations, which are bound by sub-vertical faults, with sinistral-reverse oblique-slip displacement (Insert II, Section G-G', station A2712). The development of numerous, thin fault panels such as these indicates the intensity of the late fault system and suggests it is more penetrative than previously recognized. Figure 7.6b presents three, lower hemisphere, equal area plots for bedding data measured in both Domains 2a and 2b. As discussed in section 5.2.2 the distribution of poles on the two plots is very similar, but there is a 37° difference in the trend of the pi-girdles calculated for the F_2 fold systems. A 37°, clockwise rigid body rotation about a vertical axis was applied to the data in Domain 2a. The right hand plot (Figure 7.6b) shows the results of the rigid body rotation and demonstrates that the pi-girdles for Domains 2a and 2b become coaxial and coplanar, and is taken to suggest that the F_2 fold

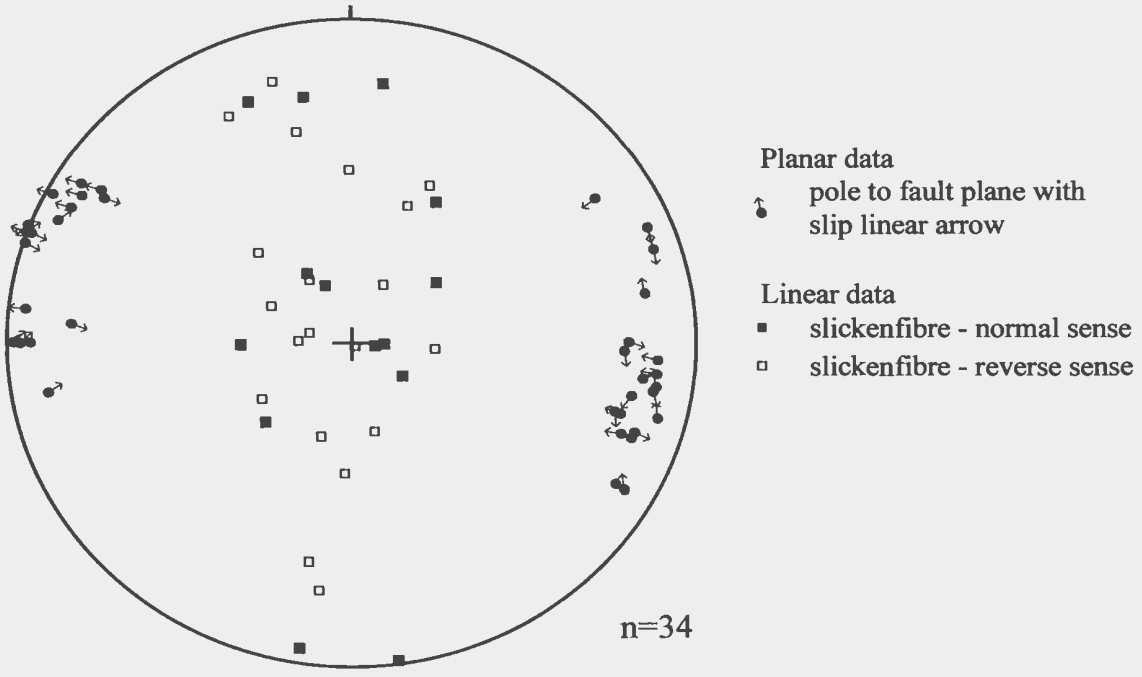

a. Lower hemisphere, equal area projection showing poles to the northerly striking young fault population (circles) and lineations on the surfaces of the faults (squares). Slip linear arrows on each pole indicate the sense of movement. Only the measurements of faults with slickenfibres are plotted. Data is presented from faults measured in all of the structural domains.

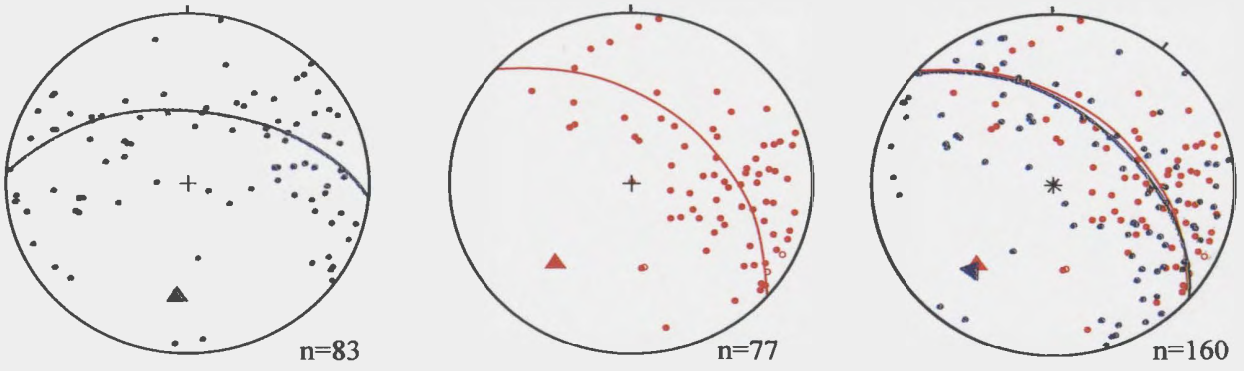

Domain 2a | Domain 2b | Domains 2a and 2b

b. Lower hemisphere, equal area projections for bedding in Domains 2a and 2b. The third plot, on the right, shows the combined datasets after the data from Domain 2b was rotated 37° in a clockwise direction, about a vertical axis. The co-incidence of the pole distribution patterns and pi-girdle orientation suggests that Domain 2a experienced post-F_2 block rotation in a fault system with a sinistral sense of movement relative to Domain 2b.

Figure 7.6 Stereoplots presenting fault plane and fault kinematic data for the late, northerly striking fault population, which overprints the area.

systems are correlative. The northeast-trend of the F_2 fold system in Domain 2b is similar to the northeast-trends of the F_2 fold systems observed in Domains 1 and 5; the northerly-trend of the F_2 fold system in Domain 2a appears anomalous in comparison. Therefore, based on the trend of the F_2 fold systems and the preponderance of late, northerly-striking faults in Domain 2a, the rigid body rotation is considered to have been applied to Domain 2a. In order to generate the current orientation of the F_2 fold system in Domain 2a the original rigid body rotation would have been counter-clockwise (sinistral), relative to Domain 2b. This indicates that the population of steep, northerly-striking faults in Domain 2a belong to a late, sinistral strike-slip fault system, which overprints the domain.

7.6 Mélange in the Frenchman's Cove-York Harbour area

Mélange containing exotic blocks of igneous rocks in a chaotic shale or serpentinite matrix is limited to a 140 m section along the shoreline at the east end of Wood's Island (Section T-T'-T", Insert III). The Wood's Island mélange zone is 123 m thick and strikes northeast across the eastern tip of the island. Igneous blocks are exposed along strike and in sea cliffs on the shoreline of the island (Insert I).

The western boundary of the mélange zone is marked by a steeply east-dipping, five to six meter thick brittle-ductile shear zone. A panel of Eagle Island formation sandstone and shale lies in the footwall of the shear zone and the shear zone is primarily developed in this panel. Internally the shear zone has an intensely developed scaly cleavage relative to the S_1 cleavage exhibited by shale in the Eagle Island formation in the fault panels situated further east. This contrast in strain patterns indicates that a high

strain gradient occurs across the boundaries of the shear zone. Kinematic indicators are poorly developed in the basal shear zone, but the angle of the internal scaly cleavage with the shear zone boundary and the presence synthetic shear fractures forming a small angle to the shear zone boundary indicate the shear zone is reverse and the hanging wall moves up, relative to the footwall (Insert III, Section T-T', station 295). A narrow high strain zone parallel to the basal shear zone is present in the immediate hanging wall. This shear zone lies within the strongly cleaved black shale that makes up the matrix of the mélange. Small scale, upright chevron folds locally overprint the scaly cleavage of the mélange at this location. These small scale folds are interpreted to have formed late in the development of the mélange. The eastern boundary of the mélange zone is not as distinct as the western boundary. The contact is not exposed, but it is interpreted to be a fault based on lithological contrasts. The footwall of this contact is cleaved black shale with broken clasts of igneous blocks and the hanging wall is black shale containing dismembered, green sandstone beds. The hanging wall is interpreted to be part of the Blow Me Down Brook formation. The difference in orientation of cleavage in the footwall and hanging wall indicates the presence of the fault, but does not help to constrain the nature of its displacement.

The contrasting lithologies of blocks in the mélange are one of the most distinctive features of this section. Gabbro, pillow basalt, amygdular basalt, listwanite, sandstone, limestone, and dolostone are all represented as blocks in the matrix (Figure 7.7a). Significantly, these are all rock types which can be found within the known tectono-stratigraphic units of the Humber Arm Allochthon. The exotic blocks range from

cobble size fragments to large boulders. A large block of fine-grained gabbro measuring seven metres by five meters and extends at least fifteen metres along strike is partially exposed fifty metres inland from the shoreline. This is the largest exotic block observed in the mélange zone on Wood's Island. The long axis of the average block in the mélange measures two to three metres. The reduction in fragment size is the result of transposition into the sub-vertical scaly cleavage and continued extensions during progressive deformation of the high strain zone.

An intense, sub-vertical scaly cleavage is pervasively developed throughout matrix of the mélange, in black shale of unknown lithological affinity. Early generations of structures are poorly preserved in the matrix of the mélange, other than the scaly cleavage, and it is therefore not clear to what generation of structures the development of the cleavage fabric is related. Ghosts of highly dismembered folds with the cleavage being axial planar provides some evidence for the transposition of early generations of structures (Figure 7.7a). The intensity of transposition in this zone is demonstrated by the strong alignment of elongate blocks within the matrix. The presence of small fragments trailing off the blocks indicates that the strain paths during transposition passed through the zones of finite extension of the strain ellipsoid, causing boudinage in the tails of the rotating blocks (Figure 7.7a). Figure 7.7b is a close-up of a flattened and elongated block of pillow basalt. The pillow is strongly aligned with the orientation of the cleavage fabric, which fans around the upper end of the block. These features all provide qualitative evidence of the intensity of transposition during and after the initial development of cleavage fabric in the sub-vertical high strain zone.

a. Mélange on Wood's Island with blocks of pillow basalt (PB), gabbro (GB), and sandstone (ST) aligned into the sub-vertical, penetrative scaly cleavage.

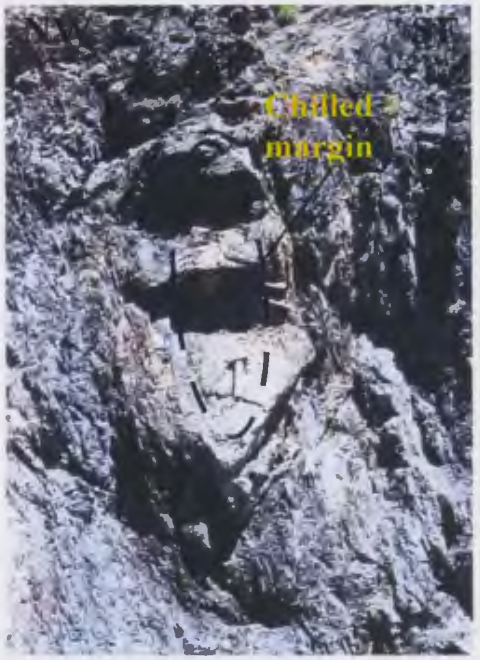

b. A close-up of a 2 m long pillow with a preserved chilled margin wrapped in the sub-vertical scaly cleavage of the shale matrix in the mélange interval.

Figure 7.7 Fabrics and exotic blocks of mixed lithologies set in a strongly cleaved shale matrix in the mélange zone on Wood's Island (Insert III, Section T'-T").

The structural style of the mélange zone on Wood's Island is unique in the Frenchman's Cove - York Harbour area and its orientation is distinct from the F_1 and F_2 structures mapped elsewhere in Domain 5. The steep brittle-ductile shear zone, which defines the western boundary, is oblique to the structural fabric of Domain 5. This cross-cutting relationship suggests that the mélange formed late in the structural history of the Humber Arm Allochthon.

The outcrop of listwanite (station 486, Insert IV) and duplex horses containing pillow basalts, south of Frenchman's Cove (Insert I and Section N-N', Insert II), are correlated with the F_3 fold-thrust system described in section 7.3.3. The occurrence of these igneous rocks within shear zones is not considered to represent mélange in this area. The duplex horses are interpreted to be part of the F_1 fold-thrust system which has been re-imbricated and uplifted by east-verging F_3 faults. This geometry of this fault system is described in detail in section 7.3.3.

Chapter eight:

Sequence and timing of structural events in the Frenchman's Cove-York Harbour area

Five tectono-stratigraphic domains have been identified in the Frenchman's Cove - York Harbour area. These domains are delineated by distinctive lithostratigraphic units, and the style and orientations of structures. The boundaries of each domain, where exposed, form important structural contacts in the area (Insert I). The structural architecture and evolution of this area is the result of polyphase deformation. The complexity of the deformation history in this area reflects the long structural history of the poly-orogenic Humber Zone.

8.1 Determination of regional deformation events

Multiple generations of structures are present in each of the domains, providing the evidence for polyphase deformation. Based on overprinting relationships successive fold-thrust systems are identified and mapped within the domains. However, correlating

the individual structural systems across domain boundaries is difficult. Domains 1, 2, 3, and 5 each have two generations of fold-thrust systems. The structural architecture of these domains is largely defined by the style and orientation of the F_2 fold-thrust systems, which is controlled by the mechanical stratigraphy in the domain. A fundamental difference in the mechanical stratigraphy occurs across the map area: competent, thick-bedded sandstone units dominate in the west (Domains 3 and 4), whereas incompetent, thin-bedded, shale units dominate in the east (Domains 1, 2, and 5). The two groupings of tectono-stratigraphic domains is the result of the changes in mechanical stratigraphy, and presents firm structural correlations within the two groups, based on fundamental similarities in the style and orientation of the fold-thrust systems, and sequences of structural generations. Domains 1, 2, and 5 each contain an early phase of westerly-verging folds, overprinted by a second phase of northwesterly-verging folds formed in lithologies of the Northern Head Group and the Eagle Island formation, allowing them to be correlated. Domains 3 and 4 consist predominately of thick-bedded sandstone successions of the Blow Me Down Brook formation which form large, regional scale fold trains with associated thrust faults. The correlation of structural systems within the two groupings of domains allows comparisons of the sequences of generations from east to west across the area. The similarities and differences between the orientations, relative timing, and the overprinting relationships of the structural systems within the two groupings of domains provides a framework to describe the sequence of deformation events that produced the current structural architecture of the area.

The sequencing and overprinting relationships of the structural generations indicates that four phases of deformation have progressively developed the complex structural architecture observed in the Frenchman's Cove - York Harbour area. The deformation events are labelled D_1 to D_4 and are represented by specific generations of fold-fault systems in the domains. D_1 is sub-divided into D_{1a} in the east and D_{1b} in the west. D_{1a} includes the development of the F_1 fold-thrust systems in Domains 1, 2, and 5 and D_{1b} represents the northerly- to northwesterly-verging F_1 folds in Domain 3. Although the F_1 fold system in Domain 3 is considered to be a D_1 structure based on the lack of evidence of any pre-existing structures, it may not have been either spatially associated with D_1 deformation in the east or have formed at the same time as the F_1 fold system in the east. D_2 is a northwesterly-verging deformation event in which F_2 fold-thrust systems overprint the earlier fold-thrust systems developed in D_1. D_2 must also be sub-divided into D_{2a} (east) and D_{2b} (west), specifically because of the differences in the orientation patterns of F_2 fold systems from east to west across the area. The D_3 deformation is defined by a spatially limited out-of-sequence, easterly-verging F_3 fold-thrust system observed west of Shoal Point and on Wood's Island (Insert 1). Firmly correlatable structural elements of this system affect portions of both Domains 3 and 5. Furthermore, near Frenchman's Cove (Wood's Island also) the F_3 system overprints the regional F_1 and F_2 fold-thrust systems, correlated with D_1 and D_2, in Domains 1, 2, and 5. Hence, the F_3 fold-thrust system must represent the effects of a third deformation event. D_4 is the latest deformation event in the area and demonstrably overprints the fold-thrust systems formed in D_1, D_2, and D_3. It is defined by the post F_3 fault system, which is

identified as an array of steep, north-striking faults with significant strike-slip displacement. The evolution of structural systems within each period of deformation is discussed in detail in section 8.2.

The overprinting relationships of the generations of structures which define D_1 to D_4 provide the relative timing of the deformation events. Determining the absolute timing and correlating the individual deformation events to regional orogenic events on the geological time-scale is more difficult. The standard techniques of dating structural events include: biostratigraphy, general stratigraphic relationships (i.e., unconformities), and radiometric dating of metamorphic minerals which define structural fabrics of known generation.

Limited paleontological analysis in the area has been useful for constraining, to some extent, the depositional ages of sedimentary rocks in the Humber Arm Supergroup and refining lithostratigraphic relationships of the Humber Arm Super Group (see section 2.1). However, the use of fossils has only been able to broadly limit the onset of Taconic deformation in this area to the late Arenig (Botsford, 1988). This is based on graptolite occurrences in the flysch units of the Arenig-aged Eagle Island formation, which demonstrably contains D_1 structures. No stratigraphic top for the Eagle Island formation or younger sedimentary rocks has been identified in Bay of Islands and the age of the termination of the Taconic Orogeny in this area cannot be constrained using the fossil record. A regional unconformity between the late Ordovician Long Point and the late Silurian Clam Bank groups suggests that Taconic deformation ended during this hiatus between the late Ordovician and early Silurian (Waldron et al., 1998)

Stratigraphic relationships in the Eagle Island formation could potentially be used to refine the age of the D_1 deformation event. Quinn (1995) suggested the Lower Head Group, which according to Quinn (1988) contains the Eagle Island formation, was deposited in satellite basins similar to the piggy back basins that develop within the evolving foreland basins of fold-thrust belts. This depositional setting for the Eagle Island formation would generate special types of so-called growth strata architectures as continued deformation and flysch deposition created progressive, syntectonic unconformities (e.g., Riba, 1976). These stratigraphic relationships are used with success in the frontal portions of young, less exhumed orogenic belts. However, the lack of identifiable and mappable unconformities within the flysch deposits of the Eagle Island formation, due to the fine-scale imbrication in D_1 and D_2, limits the use of these relationships to date the phases of deformation and they are not applicable in this area. It is not possible to demonstrate the development of satellite basins in the Frenchman's Cove - York Harbour area during the Taconic Orogeny, as hypothesized by Quinn (1995), because of a lack of primary stratigraphic relationships

Radiometric dating of metamorphic minerals which define structural fabrics of known generations is a common method of dating deformation events. Regionally, radiometric techniques have been used to identify Salinian aged and younger fabrics developed in the Internal Humber Zone (Cawood et al., 1996). Relict foliations preserved in porphyroblasts in the Internal Humber Zone indicate the existence of early, westerly-verging deformation events (Waldron et al., 1998). These timing relationships in the Internal Humber Zone suggest that early deformation in the External Humber Zone

was pre-Salinian. In the western portions of the External Humber Zone the deformation events were less ductile than to the east, and metamorphic fabrics in which minerals can be easily dated using radiometric techniques (e.g., Ar/Ar) did not form in the southwestern portion of Bay of Islands. Wojtal and Mitra (1988) suggested the Blow Me Down Ophiolite Massif was emplaced as a hot slab, overprinting the amphibolite facies metamorphic aureole with greenschist facies metamorphism during emplacement; the suite of metamorphic minerals developed in the greenschist facies overprint indicate an overburden depth of approximately fifteen kilometres and an ambient temperature of approximately 300° C within the aureole. They hypothesize that heat from the ophiolite massif was dissipated through fluid interaction with the underlying sedimentary rocks of the Humber Arm Supergroup. However, exposure of these sedimentary rocks in the footwall of the Blow Me Down Ophiolite Massif do not show the effects of hydrothermal alteration that must have accompanied the flow of hot (300° C) fluids emanating from the basal shear zone of the ophiolite massif The S_1 slaty cleavage developed in the Northern Head Group of Domains 1, 2, and 5 does not show evidence for the pressure solution fabrics typically developed in similar sedimentary rocks under higher grade metamorphic conditions; indicating that this area was not subjected to metamorphism beyond sub-greenschist facies. Acritarch assemblages recovered from the Blow Me Down Brook and Eagle Island formations in the immediate footwall of the Blow Me Down Ophiolite Massif exhibit thermal maturation indexes within the oil window, supporting an ambient temperature of deformation between 150° C and 180° C. These relatively low ambient temperatures suggest that the ophiolite massif had already cooled prior to its

emplacement in the upper structural slices of the allochthon and behaved as a rigid body during subsequent deformation events.

Therefore, although the older deformation events in this area cannot be directly dated, because the Arenig-aged Eagle Island formation is incorporated in both D_1 and D_2 structures the Taconic deformation can be no older than the late Arenig in the Frenchman's Cove - York Harbour area (Botsford, 1988). Overprinting criteria of structures in D_3 and D_4 only constrain the timing of these younger events to having occurred after the D_2 deformation event. However, the style and regional significance of the structural systems developed in these two later deformation events may be compared with, and possibly correlated to, regional structural systems developed during younger orogenic events. The possibilities of correlating the D_3 and D_4 deformation events to younger orogenic events that regionally affect the Humber Zone is discussed in more detail in sections 8.1.3 and 8.1.4, respectively.

8.2 Phases of deformation

8.2.1 D_1 deformation

D_{1a} deformation event, Domains 1, 2, and 5

The initial phase of deformation in Domains 1, 2, and 5 is represented by the F_1 fold system (Figure 8.1). The tight, asymmetric, gently inclined to recumbent folds are the earliest structural feature in this part of the Humber Arm Allochthon. This early fold-thrust system is strongly dismembered by subsequent, younger fold-thrust systems and is poorly preserved in the eastern portions of the area.

Initially the F_1 fold system formed as open to close, westerly-verging folds. The shale dominated successions of the Northern Head Group and Eagle Island formation are mechanically weak and behaved in a brittle-ductile fashion at relatively low pressures and temperatures. The initial ductility of the fold system influenced the geometry and style of the folds early in the deformation event. During the D_1 deformation event the upper slices of the allochthon, containing the Blow Me Down Brook formation and Blow Me Down Ophiolite Massif, were moving westwards from the hinterland, and progressively increased the overburden load on the underlying sedimentary rocks, increasing the pressure and temperature conditions affecting the F_1 fold system. The overall style of deformation in the F_1 fold system became more ductile in response to changing deformation conditions, resulting in amplification of the F_1 fold trains by simple shear deformation (Ramsay, 1983). As deformation continued F_1 folds became overturned, and eventually recumbent. Associated with F_1 folds is a penetrative, axial planar slaty cleavage (S_1), which also supports the development of prograde metamorphic conditions and increasing ductility during the D_1 deformation event. Thrust faults associated with the F_1 fold system are responsible for the initial forelimb detachment, and wholesale imbrication of strata in the Northern Head Group and Eagle Island formation (Figure 8.1). The thrust faults develop within the forelimb of F_1 folds, breaking the folds and forming nappe-type structures (Ramsay, 1983). As the deformation continued the F_1 thrust system formed duplex structures, which parcelled the recumbent F_1 folds, repeating the stratigraphy of the Northern Head Group and Eagle Island formation (Figure 8.1). The roof thrust of the F_1 duplex structures is interpreted to be the basal shear zone of the

uppermost slice of the allochthon, containing the Blow Me Down Brook formation and the Blow Me Down Brook Ophiolite Massif.

The orientation of the F_1 fold system can be constrained by analysis of the interference patterns formed by F_2 superposition. The presence of coaxial hook structures and oblique mushroom structures indicate that the F_1 folds were generally northeast trending and their axial surfaces dipped to the southeast. The transition from hook- to mushroom-type interference patterns occurs from east to west across Domains 1, 2, and 5. This reflects a change in the orientation and style of the F_1 fold system from west-northwest-verging, highly cylindrical folds in Domain 1 to northwest-verging, non-cylindrical folds in Domains 2 and 5. Overall, the F_1 fold system is interpreted to be non-cylindrical and strongly asymmetric. The variations in the type of interference patterns across the map area is the result of the F_1 duplex structures parcelling domains of the F_1 fold system with non-coaxial fold axes prior to the superposition of F_2.

The overturned forelimb domain of the F_1 fold system creates the initial structural complexities in the first-phase of deformation. The overturned limb rotates bedding planes into the finite extension field of the strain ellipse, causing the forelimb domains to boudinage. This process results in the initial dismemberment of the strata. The dismemberment relates to the tightening of F_1 fold hinges, where the limb domains eventually become sub-parallel, forming tight to isoclinal recumbent F_1 folds. The two fold limbs are sub-perpendicular to the z-axis of the finite strain field and bedding in the backlimb of the fold will also begin to boudinage. Tension veins will form sub-perpendicular to bedding in the limb domains due to bed-parallel extension in response to

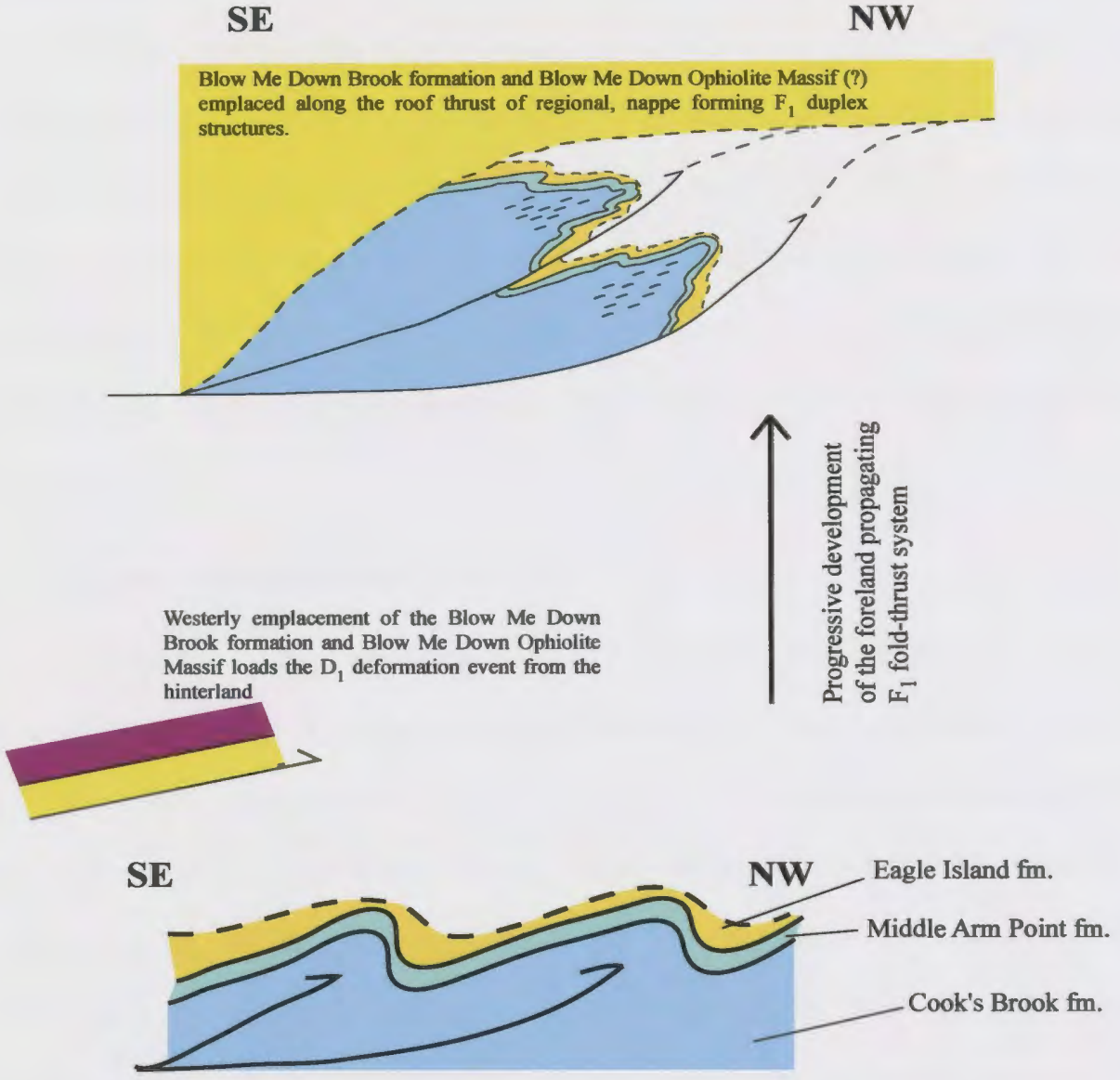

Figure 8.1 Schematic sections depicting the evolution of broken, recumbent F_1 folds, which develop nappe-type structures. The brittle-ductile style of deformation is the result of progressive loading during emplacement of the Blow Me Down Brook formation and Blow Me Down Ophiolite massif in the D_1 deformation event (not to scale).

the bulk shortening strain environment. Broken formation, axial planar scaly cleavage, and bedding-perpendicular veins are structural fabrics which previous workers have typically associated with mélange formation. However, these features may also develop in fold systems that experienced extended, progressive, heterogeneous deformation, reaching high bulk shortening strain states. The bulk ductility of the deformation event, caused by increasing pressure and temperature related to loading in the upper levels of F_1 duplex structures, may have contributed to the F_1 fold system remaining relatively coherent during the early stages of deformation. Otherwise, D_1 may have initiated the development of mélange by pervasive fracturing, assisted by high, ambient pore fluid pressure.

D_{1b} deformation event, Domains 3 and 4

In Domains 3 and 4 elements of the first generation fold-fault system are rarely observed. Only two F_1 folds are observed in Domain 3 and none in Domain 4. Section K-K' (Insert II) displays a broken F_1 fold on the southern limb of a F_2 synclinal antiform. This particular fold indicates that the deformation event represented in D_{1b} developed northerly-verging structural systems. In Domain 3 several panels of moderate to steep north-dipping, but south face sandstone beds in the Blow Me Down Brook formation provide further evidence of the early fold-thrust system. The dispersion pattern of the poles to bedding in Domains 3 and 4 suggest that large-scale, mushroom-type interference patterns are present in these domains. However, Bay of Islands covers a large portion of these domains and away from the shoreline, outcrop is scarce. Therefore

a detailed analysis of the $F_1 \backslash F_2$ interference patterns is not possible in the western portions of the map area.

The geometry and style of observed F_1 folds in the area indicates the fold system was north-verging. The discrepancy between the style and orientation of the F_1 fold systems between the eastern and western domains of the map area suggests that they formed in different tectonic settings and that in Domain 3, the F_1 folds were formed by a fold-thrust event which was spatially unrelated to the initial, D_1 deformation in this area. Section 8.2.2 discusses the hypothesis of early fold systems transported within the upper thrust sheets of the allochthon.

8.2.2 D_2 deformation

D_{2a} deformation event, Domains 1, 2, and 5

In Domains 1, 2, and 5 the second phase of deformation resulted in the development of a large, internally faulted antiformal culmination (Figure 8.2). The culmination is interpreted as a regional scale structure within the F_2 fold-thrust system, and is associated with out-of-sequence duplex structures in the core of the culmination. Re-imbrication of the F_1 fold-thrust structures combined with the formation of a variety of faults, including forethrusts, backthrusts, and accommodation faults (e.g., Mitra, 2002) are associated with F_2 folding and generated a geometrically complex structural system. East of the study area in Humber Arm, the western limb of the Cook's Brook syncline is characterized by a westerly-verging F_2 fold system, which is similar to the F_2 fold system in Domain 1 (Bosworth, 1984; Waldron et al., 2002). The Cook's Brook syncline and the

broken antiformal culmination in Frenchman's Cove may form a syngenetic F_2 synform-antiform pair, suggesting that the F_2 fold system in Domains 1, 2, and 5 is a significant regional scale structure within this portion of the Humber Arm Allochthon (Figure 8.2).

Tight, strongly asymmetric, overturned F_2 folds associated with thrust faults are the predominant structural features formed in D_{2a}. Tight folding of the S_1 cleavage and bedding on micro- to macroscopic scales locally resulted in the strong transposition of early planar fabrics during the F_2 folding event. This phase of transposition led to dismemberment of bedding, and cleavage, bedding-perpendicular tension veins, development of discrete scaly cleavage domains due to heterogeneous reworking of the S_1 cleavage, formation of bedding-perpendicular tension veins, and progressive tightening of fold interlimb angles. These F_2 fabrics overprint similar F_1 fabrics and generate structures with chaotic appearance. Extreme segmentation of the lithological successions in relatively small fault panels characterizes the F_2 fold-thrust system, and is the result of intensely developed break-thrusts and accommodation faults developed in the core of the antiformal culmination (Figure 8.2). Throughout Domains 1, 2, and 5, F_2 synforms and antiforms are isolated within thin imbricate slices created by the F_2 break-thrusts. In the core of the culmination F_2 fold trains are strongly broken and dismembered by the formation of F_2 thrust faults and duplex structures.

A prominent feature of the F_2 fold-thrust system is the switch from northwest- to southeast-vergence between domains 1 and 2 (Insert II, Section E-E'). The opposing vergence of the F_2 fold-thrust systems in Domains 1 and 2 are interpreted to represent the development of fold systems on the eastern and western flanks of the regional scale

antiformal culmination, respectively (Figure 8.2). This geometry implies that the culmination was associated with a divergent axial surface fan in its early stages of development, when the parasitic fold systems amplified on the limbs. A similar, folding-associated cleavage fan characterizes that portion of the allochthon situated between the study area and Cornerbrook (Stevens, 1965; Waldron, 1985; Bosworth, 1985). In the study area, intense regional east-west shortening led to over tightening of the antiform, in the incompetent lithologies, resulting in steepening and transposition of all structural elements, and internal fragmentation by faulting.

D_{2b} deformation event, Domains 3 and 4

The second generation structures in Domains 3 and 4 are developed in thick-bedded sandstone successions of the Blow Me Down Brook. The folds are commonly open to close asymmetric polyclinal kink-style folds and form macro- to regional-scale fold trains. The contrast in fold styles between the eastern and western portions of the study area, are the related to the mechanical stratigraphy. The competent thick-bedded sandstone successions in Domains 3 and 4 formed folds with large initial wavelengths, and abundant slickenfibers packages on the bedding surfaces indicates that flexural slip was played an important role in the formation of the fold system. However, the F_2 fold system is east-west trending and northerly to northwesterly-verging, approximately a 30° to 40° difference from the trend of the second generation fold systems in Domains 1, 2, and 5. The contrasts in structural style and orientation of the F_2 fold-thrust systems in Domains 4 and 5 indicates that the F_2 fold system is not syngenetic with the F_2 folds

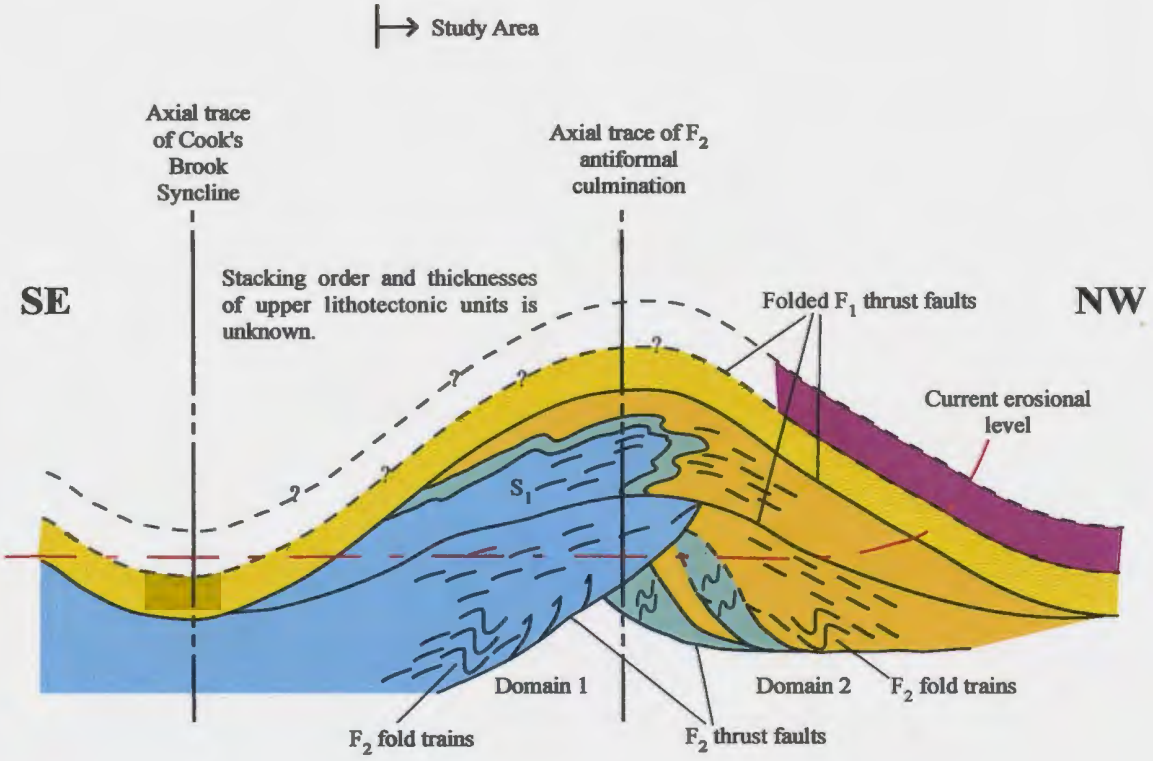

Figure 8.2 Schematic sections depicting the evolution of the F_2 antiformal culmination in D_2. Note the high density of F_2 thrust faults and accommodation faults in the core of the culmination, which re-imbricate the folded F_1 duplex structures (not to scale). Detailed, accurate cross-sections are presented on Insert II, sections A to H. General form of the Cook's Brook syncline is adapted from other workers (Stevens, 1965; Waldron et al., 2003).

systems in the eastern portion of the map area. This implies that a different mechanism of folding formed the F_2 fold system in the western domains.

The upper slice of the allochthon was emplaced during the D_1 deformation event along the roof thrust of regional F_1 duplex structures containing telescoped deep-water continental margin successions (Figure 8.2). The presence of folded Blow Me Down Brook formation sandstone successions structurally overlying a portion of the Humber Arm Supergroup southeast of Frenchman's Cove supports the hypothesis that a once regionally extensive thrust sheet containing the Blow Me Down Brook formation was present in the central portions of the allochthon (Waldron et al., 2003). Two models can be considered to account for the northerly-vergence of the F_2 fold-thrust system in Domain 3. The first model postulates that the fold-thrust system may is not spatially related to the D_{2a} deformation event. This requires that the fold-thrust system developed in a separate, unknown tectonic environment and was preserved during transport and emplacement of the thrust sheet in the highest structural levels of the allochthon. A second model postulates that this northerly-verging fold-thrust system developed as the result of a local, gravity-induced décollement on the western flank of the F_2 antiformal culmination, causing the Blow Me Down Ophiolite Massif to slide off the flank towards the northwest. As the regional culmination amplified, the flank became tilted enough so that the ophiolite sheet could reactivate the basal thrust fault between the ophiolite and the Blow Me Down Brook formation. This model suggests that the F_2 fold-thrust system in Domains 3 and 4 developed in direct response to this late movement of the ophiolite massif and is not a regionally extensive structural system.

Selecting a mechanism to form the F_2 fold system is not an easy problem to solve. The contrasts in style and mechanical stratigraphy across domain boundaries make it impossible to correlate the eastern and western fold systems. The choice of models may not be resolved without detailed and refined radiometric ages of the generations of structures. However, the low temperature conditions during deformation in Domains 3 and 4 formed brittle structures with weak fabric development and datable metamorphic minerals are not present in the western portions of study area.

8.2.3 D_3 deformation

The third phase of deformation in the Frenchman's Cove-York Harbour area is marked by the development of an east-verging fold-thrust system (Figure 8.3). The antiformal culmination formed during D_2 lies in the footwall and is truncated by this major, out-of-sequence fault system; creating complex footwall cut-off geometries typical of out-of-sequence fault systems (Morley, 1988). In the hanging wall, a westerly-dipping imbricate fan associated with east-verging F_3 fault-propagation folds deforms thick-bedded sandstone successions of the Blow Me Down Brook formation (Insert II, sections I to J).

The F_3 folds have a limited areal extent and are only observed in Domain 3a. The folds are close to tight, asymmetric, broken fault-propagation folds. The easterly-vergence of the fold system is consistent with the reverse thrust sense of the west-dipping faults. The footwall of the F_3 thrust system contains the complex geology of the F_2 antiformal culmination, which is clearly truncated by the F_3 fault system (Insert I). In the hanging wall of the fault is a well developed imbricate fan (possibly eroded F_3 duplex

structures), which can be mapped on Wood's Island and west of Shoal Point. The structurally lowest imbricate sheets contain the Frenchman's Cove and Wood's Island volcanics (Figure 8.3). South of Frenchman's Cove a duplex structure of volcanic rocks is shown on the geological map (Insert I). These volcanic rocks have been exhumed from the core of the F_2 antiformal culmination by F_3 thrust faults. The volcanics are interpreted to have been part of a folded F_1 duplex structure and were incorporated into the easterly-verging F_3 fold-thrust system. This implies that some of the west-dipping faults bounding the volcanic horses are in-fact folded, west-verging F_1 thrust faults. An example of a folded, west-verging F_1 shear zone is located on Wood's Island at the base of the volcanic horse. Other occurrences of igneous rocks are present along strike of the F_3 thrust system, and are associated with east-verging thrust faults.

The F_3 fold-thrust system is an out-of-sequence fault system that truncates early generations of structures, both in the hanging wall and footwall (Figure 8.3 and Insert III, Section N-N'). However, the timing of the fold-thrust system is difficult to determine. It may be an out of the syncline accommodation fault that formed late in the development of the F_2 antiformal culmination. In this scenario the fault would have formed to accommodate for the inability of the mechanically stiff Blow Me Down Ophiolite Massif to fold in the core of a possible synform to the west. Alternatively, the F_3 fold-thrust system may be a thin-skinned response of the Humber Arm Allochthon to the Devonian-aged Acadian Orogeny, similar to the triangle zone in the vicinity of the Port-au-Port Peninsula (Waldron and Stockmal, 1994; Waldron et al., 1998).

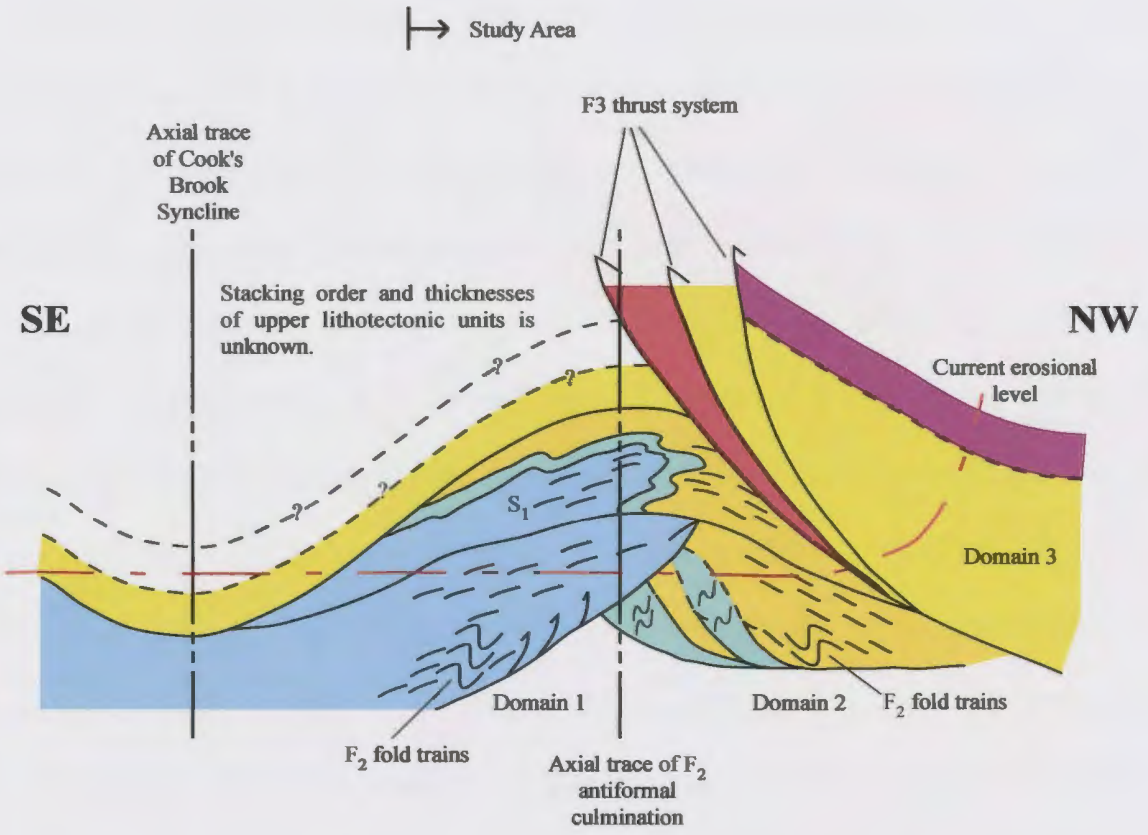

Figure 8.3 Schematic sections depicting the out-of-sequence F_3 fold-thrust system truncating the F_2 antiformal culmination during D_3. The F_3 faults inherit the volcanic rocks by re-imbricating D_1 duplex structures, which are re-folded by the F_2 fold system (not to scale). See Insert II, sections I to J and Insert III, Section N-N', Detail C for accurate and detailed sections of the F_3 fold-thrust system. General form of the Cook's Brook syncline is adapted from other workers (Stevens, 1965; Waldron et al., 2003).

8.2.4 D_4 deformation

The D_4 deformation event is recognized as a late faulting event that overprints earlier deformation events in the Frenchman's Cove - York Harbour area. The shoreline exposure is two dimensional and the faults cannot be traced along strike due to poor inland outcrop exposure, limiting the understanding of this young fault system. It is characterized by northerly striking, steep to sub-vertical faults, which typically display several sets of slickenlines with inconsistent overprinting relationships and variable senses of slip. However a strong component of strike-slip is observed on many of these fault surfaces, this is demonstrated by the slip linear plot presented in Figure 7.6a. Further evidence for significant strike-slip displacement along this young fault population is found in the western portion of Domain 2a. The coastal exposure is dissected by a series of steep, northerly trending faults on which slickenfibers indicate the sense of displacement of the oblique slip faults was predominantly sinistral strike-slip with a small component of reverse-sense displacement. Lower hemisphere, equal area plots of bedding and cleavage in Domain 2a were used to analyse the F_2 fold system, which trends north-south within the domain. The trend of the F_2 fold system was 37° west of the regional trend of the F_2 fold systems in Domains 1 and 2b. The pattern of the pole distribution which defines the fold systems in Domain 2a is identical to the pole plots of bedding in Domain 2b. Furthermore, reconstruction of F_2 antiforms and synforms preserved in F_2 imbricate slices show that the style, geometry, and vergence of the F_2 fold system in Domain 2a is compatible with the F_2 fold system in Domains 1, 2b, and 5. The presence of sinistral-reverse faults overprinting the domain and the similarity in style and

geometry of the F_2 fold system to regional F_2 fold systems, indicates that Domain 2a was subjected to a rigid body rotation. The sense of block rotation to generate the current orientation of the F_2 fold system in Domain 2a is sinistral relative to the F_2 fold system in Domain 2b. However, this sense of rotation is consistent with the sense of displacement of post F_3 faults observed within Domain 2a.

The truncation of an F_3 thrust fault in Domain 3a is the only substantive timing relationship available for the fault system (Insert III, Section J-J', 675 m). This indicates that the fault system is post F_3, but does not provide an absolute time frame for the development of the fault system. Bosworth (1985) documented the presence of a population of northeast-striking normal faults that overprint early structures east of Frenchman's Cove. This fault population records strike-slip displacement of unknown sense and quantity. Bosworth (1985) speculates that the fault system may be related to Carboniferous strike-slip fault systems. The population of faults observed in domains 3 and 5 are similar in orientation and style to Bosworth's (1985) fault set. Although the faults analysed in this study are not definitively normal faults they do display evidence of a significant strike-slip component. The presence of a regional strike-slip fault system is supported by the presence of the Carboniferous-aged Deer Lake and Bay St. George sedimentary basins, and associated pop-up structures near Stephenville (Waldron et al., 1998; Palmer et al., 2002). The D_4 fault system observed in Humber Arm may be related to these young strike-slip fault systems. The regional strike-slip systems are considered to have a dextral sense of displacement, which is incompatible with the fault system in the Frenchman's Cove - York Harbour area. However, the relationship between the

regional scale and local scale strike-slip faults is poorly constrained and the fault in Frenchman's Cove may be an antithetic structure (e.g. R'-shear) within the regional strike-slip systems. A detailed kinematic analysis of the post F_3 fault system in Humber Arm is required, to determine the overall orientation and sense of displacement of the young fault system in with respect to the Devonian- or Carboniferous-aged regional strike-slip fault systems.

8.3 Mélange vs. dismemberment and mixing during polyphase deformation

The origin and significance of deformed belts with chaotic-appearing structures and fabrics is a long standing question in interpreting the evolution of the Humber Arm Allochthon. In the Bay of Islands previous workers in the area had classified and mapped most of the eastern portion of the map area as mélange, incorporating Domains 2, 5, and small portions of Domains 1 and 3 (e.g., Stevens, 1965 and 1970; Bruckner, 1966; Waldron, 1985; Williams and Cawood, 1988; Wojtal, 2001). As discussed in Chapter 2, early workers considered the chaotic mélange zone to have formed as an olistostrome during emplacement of successive structural slices by gravity sliding along sub-horizontal detachment surfaces (Stevens, 1965; Bruckner, 1966; Williams, 1975). The mélange in Frenchman's Cove is interpreted by these early workers to be the sub-horizontal contact between the intermediate (sedimentary) slices of the allochthon and the Blow Me Down Ophiolite Massif.

Waldron et al. (1988) examined the mélange in Frenchman's Cove, focusing largely on the significance of the extensional structures, which are common in the mélange (see also Stevens, 1965; Waldron, 1985); concluding that these structures

formed in a progressive bulk shear (i.e., co-axial) environment during multiple phases of gravity-spreading in the Taconic accretionary wedge. The concept of structural slicing, introduced by Bosworth (1984) in the mélange at Frenchman's Cove, mimics the geometry of large scale thrust systems on the outcrop to microscopic scale and progressively dismembers bedding, resulting in formation of the polyhedral blocks (purportedly seen at Frenchman's Cove), as opposed to lozenge-shaped boudins. The process of structural slicing occurs in a progressive simple shear (i.e., non-coaxial) environment and such a regime and is more consistent with the style of the F_1 and F_2 fold-thrust systems observed in Frenchman's Cove. Neither of the mechanisms proposed by Waldron et al. (1988) or Bosworth (1985) satisfactorily describes all of the structures and fabrics seen in the mélange, nor are they compatible with the strain paths proposed for the origin of the structures.

This thesis presents a model of polyphase deformation in which the fabrics and structural features observed at Frenchman's Cove are the result of successive, complex, progressive heterogeneous deformations involving mainly non-coaxial strain paths. Small scale extensional structures are not uncommon features in many fold belts (e.g., Ramsay and Huber, 1987). Chapter six describes how local strain fields developed in fold hinges form bedding-perpendicular veins and shale injection structures. Progressive folding of pre-deformed strata with high competency contrasts results in fold geometries that allow the generation of small-scale extensional structures by attenuation of fold limbs; as proposed in section 8.1. The translation and rotation during non-cohesive (brittle) flow along faults associated with the F_1 and F_2 fold systems in D_{1a} and D_{2a} are

also important factors. The first and second order thrust systems form imbricate fans and/or duplex structures in the strata on a range of scales. Structural slicing dismembers strata at the outcrop and smaller scales in conjunction with the macro-scale F_1 and F_2 thrust systems; resulting in broken formation and mixing of lithologies at all scales of observation (Bosworth, 1984). In Frenchman's Cove the D_1 and D_2 phases of deformation both generated the style of structures described here. Overprinting of the D_2 phase of deformation and transposition of D_1 structures resulted in the intense broken formation and complex fold-thrust systems observed in Frenchman's Cove. These structural fabrics in domains 1, 2, and 5 have previously been mapped as mélange. However, it is only the sedimentary units which are disrupted in the Frenchman's Cove-York Harbour area, forming broken formation (e.g., Raymond, 1984).

Wojtal (2001) presented a study of the "Companion" mélange in Frenchman's Cove, which analysed the development of fault arrays in three-dimensional general strain fields during non-coaxial shearing. Wojtal (2001) states that: "...the paucity of unfaulted antiform-synform pairs yields few data (n=23) giving the sense of overturning of folds."; concluding that kinematics of the faults provides the only method of analysing finite strain in the deformed rocks of this area. A series of lower hemisphere, equal area projections present structural data collected from many of the same outcrop locations visited during this study. However, Wojtal's (2001) data set appears to preferentially measure steeply-dipping planar elements, both within the area referred to as Domain 2 by this study, and along the western shoreline exposures north of the Blow Me Down Brook Ophiolite Massif (Domain 3 in this study). The structural data presented in Chapter 5 of

this thesis roughly corresponds to Wojtal's (2001) presented data, but demonstrates a greater variety of bedding and S_1 cleavage orientations, which delineate the pi-girdles of F_2 fold systems in each of the five tectono-stratigraphic domains. Wojtal (2001) attempts to remove the effects of F_2 (his F_2 fold generation) by applying a rotation to the "layering," and rotating all of the layering elements to a sub-horizontal orientation. It appears that this was done about a rotation axis corresponding to the fold axis of his F_2 generation of folds. He identifies an easterly-verging kink fold west of Frenchman's Cove as representing his F_2 generation of folds. This identified fold is located within Domain 3a of this study and is a component of the out-of-sequence F_3 fold-thrust system, and demonstrably overprints the F_2 fold-thrust systems in Domains 2 and 3 (Inserts I and II). It is the opinion of this author, that based on the miscorrelation of fold generations and associated fault systems in the area, the conclusions reached by Wojtal (2001) regarding the kinematics of deformation in the area are invalid.

Only a narrow interval of what this study considers to represent true mélange, containing igneous blocks, is present on Wood's Island. Two hypotheses are presented to consider the formation of this mélange:

The first hypothesis correlates the mélange zone with the east-verging F_3 fault system in D_3. In this scenario the zone is interpreted as a relatively deep rooted splay of the eastwards-propagating F_3 thrust fault system. The propagation, from a deep seated detachment zone, of new thrust faults in the F_3 imbricate fan would transect and cut up section through the core of the F_2 antiformal culmination, developed during D_2. The trajectory of the younger faults would allow for the incorporation of many of the rock

types present in the allochthon, and generate a zone of mélange within the F_3 thrust faults. This interpretation is consistent with the association of igneous rocks and the D_3 phase of deformation (Insert I).

The second hypothesis correlates the mélange zone with post F_3 faulting in D_4. The western boundary of the mélange zone is defined by a steep reverse-sense shear zone that is oblique to the footwall fabrics. The orientation of the shear zone is coincident with the population of northeast striking post F_3 faults. The oblique and strike-slip lineations on these faults suggest that they may have formed in the young strike-slip fault system overprinting the Humber Arm Allochthon. The sub-vertical cleavage developed in the mélange zone is sub-parallel to the boundary shear zone; an orientation which is incompatible with development in early sub-horizontal faults (Bosworth, 1985). The shear zone and cleavage are both compatible with formation in a sub-vertical high strain zone within a strike-slip fault system. Strike-slip systems have internal fault geometries that are capable of significant uplift and mixing of exotic lithologies (Karig, 1980; Sylvester, 1988). A young, D_4, strike-slip system superimposed on the Humber Arm Allochthon would be capable of generating zones of mélange containing the "exotic" lithologies seen on Wood's Island.

Formation of the mélange in D_3 or D_4 provides the fault systems with a much wider variety of "exotic" lithologies to incorporate into the mélange. During D_1 the igneous rocks, comprising volcanic suites and the Blow Me Down Ophiolite Massif were emplaced within the upper structural slices of the allochthon. During the development of the F_1 recumbent fold system there would not have been a large volume of igneous rock

available to dismember and incorporate into F_1 shear zones. However, by D_3 all of the principal components of the allochthon were assembled in D_1 nappe-type structures and folded by regional scale F_2 folds. Therefore the younger, out-of-sequence D_3 and D_4 structural systems would be able to sample and incorporate igneous rocks from a variety of structural levels within the allochthon.

8.4 Proposed tectonic setting

The style of structures, sequencing of generations and the overall structural architecture of the Frenchman's Cove - York Harbour area is consistent with the formation in an accretionary wedge. A developing accretionary wedge in the foreland of an orogenic system will contain all of the structural elements and lithotectonic units observed in the Humber Arm Allochthon. The geometry of an accretionary wedge and its internal rheology give it particular properties that control the distribution and styles of deformation. In general, a wedge behaves in a ductile fashion, maintaining its coherency during progressive deformation (Platt, 1986). Therefore, the toe of the wedge is deformed in a brittle fashion, forming foreland propagating fold-thrust systems (Platt, 1986). Towards the deeper portions of the wedge pressure and temperature increase, causing progressively more ductile styles of deformation within the wedge (Platt, 1986). As an accretionary wedge evolves it will deform internally in order to maintain a constant taper angle, referred to as the critical angle (Platt, 1986). Accretion of material at the toe decreases the critical angle causing the wedge to internally shorten, effectively increasing the angle of the taper. This causes out-of-sequence, foreland propagating faults and backthrusts to accommodate the shortening and increases the thickness of the wedge. If

the taper of the wedge becomes too steep it will collapse, forming extensional structures to thin the wedge and restore the critical angle (Platt, 1986). Underplating is a common process in accretionary wedges where material from the subducted plate is accreted to the base of the wedge. This mechanism was proposed by Malpas and Stevens (1979) to explain the incorporation of the Bay of Islands Ophiolite Complex within the allochthon. The underplated material is progressively exhumed towards the upper structural levels of the wedge; presumably by thrust faults during internal shortening events (Platt, 1986).

The structural style of the tectono-stratigraphic domains within the study area suggests they developed towards the toe of an accretionary wedge. The more ductile deformation conditions demonstrated by the D_1 structural systems indicate that this event occurred deeper in the wedge, before being exhumed into a shallower, less ductile environment. Development of duplex structures and emplacement of the ophiolite complex suggest that D_1 occurred near the basal detachment of the wedge, a structural position where underplated material could easily be incorporated into the duplex structure. D_2 represents progressive foreland propagating deformation and may also represent exhumation towards shallower portions of the wedge. D_3 and D_4 are considered to be out-of-sequence fold-fault systems, which developed in response to periods when the accretionary wedge was internally deformed in order to restore the critical taper.

Cowan (1985) classified mélange and correlated its formation to different environments of an accretionary wedge. His Type I and II mélanges consist of dismembered and broken formation, comparable to the fabrics observed in Domains 1, 2, and 5. Type I and II mélanges correlate to the toe, the top of the wedge, and imbricate

fans and duplex structures formed near the base of the wedge (Cowan, 1985), similar to the positions of D_1 and D_2. This thesis demonstrates the strain paths associated with simple shear generate multiple, superposed fold generations and simultaneously develop broken formation and other small scale structural features, typically associated with mélange (e.g., Waldron, 1985). Standard models of mélange formation, Cowan's (1985) included, invoke bulk pure shear (coaxial) to generate an early event of layer parallel extension, ignoring multiple, superposed fold generations and associated faults, which generate the same structures and fabrics during the development of the fold generations (e.g., Waldron, 1985; Waldron et al., 1988; Wojtal, 2001).

The toe of an accretionary wedge is an attractive tectonic setting for the style and sequence of deformation observed in the study area. An accretionary wedge is inherently a polydeformed terrane, within one orogenic event; and the wedge provides a mechanism for incorporating and emplacing the Bay of Islands Ophiolite Complex in the upper structural levels of the allochthon.

8.5 Conclusions

This thesis presents a detailed study of the complex structural geology at the trailing edge of the Blow Me Down Ophiolite Massif. Detailed mapping in the Frenchman's Cove - York Harbour area has identified fine-scale fault bounded panels, containing discreet lithostratigraphic units, which can be grouped into five larger scale tectono-stratigraphic domains (Insert I). Careful analysis of the style, orientation patterns and overprinting relationships of structures contained within these domains demonstrates that four phases of deformation have affected this area. These local deformation events

may be correlated with regional orogenic events which affect the Humber Zone starting with the Taconic Orogeny in the middle Ordovician and ending during the Alleghanian Orogeny in the Carboniferous.

Mélange in this area is constrained to discreet, steeply-dipping high-strain zones within the allochthon and demonstrably does not form continuous, sub-horizontal sheets at the basal contact of the ophiolite massif, as suggested by previous workers (e.g. Stevens, 1970; Williams, 1975; Waldron, 1985). The development of mélange containing igneous blocks is the result of the polyphase deformation history of the area. Emplacement of the Blow Me Down Ophiolite Massif in the upper levels of D_1 duplex and nappe structures generated the overall structural layering of the Humber Arm Allochthon; subsequently, during out-of-sequence thrust events, igneous blocks were incorporated in these fault zones by footwall/hanging wall plucking. Therefore, the occurrence of igneous blocks in narrow, discreet zones of mélange is considered to demarcate the younger fault systems formed during D_3 and D_4.

Broken formations are ubiquitous in domains 1, 2, and 5, and consist of dismembered components of the Humber Arm Supergroup. Previous workers have correlated these deformed lithological units with mélange in this area. Although it is possible that the broken formation resulted from processes generally associated with mélange formation (e.g. Waldron, 1985), there is a wide variety of possible strain paths through which the fabrics of the dismembered belts may develop. In this thesis the broken formation is considered to have formed as the result of polyphase folding, combined with fine-scale thrusting. The structural features (e.g. shale injection, tension

gashes perpendicular to bedding, rootless fold hinges) observed in the belts of broken formation are consistent with development in tangential longitudinal strain fields formed during the folding of layered strata which exhibit high competency contrasts between layers. Because of the limited areal extent of mélange with exotic blocks in this area and the spatial association of these mélange zones with D_3 and D_4 fault systems, it is concluded that significant development of mélange did not occur during the early phases of deformation in this portion of the allochthon. The broken formations observed in domains 1, 2, and 5 are primarily the result of polyphase folding with all the associated small scale processes (limb disruption and hinge isolation during transposition) operating during non-coaxial deformations. Notably, the development of scaly cleavage with slickensided surfaces attests to the important role that progressive non-coaxial deformation played in the development of the belts of broken formation.

Determining the structural architecture and tectonic history of a complex terrane is a difficult task. Individual deformation events and associated structural systems must be constrained by integrating detailed structural and stratigraphic datasets. Without the proper documentation of the structural styles, orientation patterns, and overprinting relationships on a local scale it is not possible to accurately delineate the geometry of the regionally important structural systems. Furthermore, deformation events delineated on the basis of spurious correlations would undoubtedly have been miscorrelated across major structural domain boundaries.

Based on the analysis of structural overprinting relationships and fold interference patterns, this thesis identifies five distinctly different tectonic transport directions in the

Frenchman's Cove - York Harbour area (see Chapter 5.4). Local variations in the asymmetry of the fold inference patterns, formed during the superposition of the F_1 fold systems by the northwest-verging F_2 fold systems, demonstrate that tectonic transport directions were more varied during D_1 than the uniform, west-verging tectonic displacements suggested by previous workers. Using interference patterns two tectonic transport directions can be demonstrated for the F_1 fold system at Frenchman's Cove, namely to the west and northwest.

The large, mechanically competent Blow Me Down Ophiolite Massif exerted a strong edge effect in the evolution of the regional structures, increasing the degree of structural complexity of the D_3 and D_4 structural systems around its margins. The east-verging D_3 structural system is most prominent along the trailing edge of the ophiolite massif where it imbricates D_1 and D_2 structural features. A wide range of lithological units from within the allochthon, including igneous blocks, are incorporated into F_3 faults, which previous workers considered to be large sheets of mélange demarcating sub-horizontal thrust faults along the boundaries of each structural slice. However, the distribution of mélange in this area is strongly controlled by the out-of-sequence F_3 fold-fault system, and it is the late dismemberment of the allochthon's structural slices which resulted in the formation of discreet, fault-bounded mélange zones later in its tectonic evolution.

In D_4 a strike slip fault system with apparent sinistral displacement overprints the Frenchman's Cove area of the allochthon. Sub-vertical high strain zones related to this fault system may further contribute to the late development and compartmentalization of

mélange in this particular portion of the allochthon. The relationship of this fault system to the regional strike slip fault systems developed elsewhere in the external Humber Zone during the Devonian and Carboniferous is poorly understood, but it does highlight that the external Humber Arm Allochthon is affected by the younger Appalachian orogenic events.

In order to understand the tectonic history of the Humber Arm Allochthon and emplacement of the Bay of Islands Ophiolite Complex it is critical that regional geological models be derived from detailed tectono-stratigraphic studies. Detailed studies of the fundemental structural contacts are important to correctly identify the style, geometry, and sequence of structural systems developed during polyphase deformation of this complex terrane. The increased resolution of the structural studies will generate more comprehensive datasets for the poorly understood younger strike slip fault systems which overprint the Humber Arm Allochthon.

References cited

Aceñolaza, F.G. and Durand, F.R. 1973. Trazas Fósiles del basamento cristalino argentino. Boletin de la Asociacion Geologica de Córdoba, 1: 45-56.

Baker, D.F. 1979. Geology and geochemistry of an alkali volcanic suite (Skinner Cove Formation) in the Humber Arm Allochthon, Newfoundland. M.Sc. thesis, Memorial University of Newfoundland, St. John's, NL, pp. 314.

Batten, D.J. 1982. Palynofacies, palaeoenvironments and petroleum. Journal of Micropalaeontology, 1: 107-114.

Batten, D.J. 1996. Chapter 26a: Palynofacies and paleoenvironmental interpretation. *In* Palynology: principles and applications; American Association of Stratigraphic Palynologists Foundation. Volume 3. *Edited by* J. Jansonious and D.C. McGregor. pp. 1011-1063.

Bird, J.M. and Dewey, J.F. 1970. Lithosphere plate-continental margin tectonics and the evolution of the Appalachian Orogen. Bulletin of the Geological Society of America, 81: 1031-1060.

Bostock, H.H., Cumming, L.M., Williams, H., and Smyth, W.R. 1983. Geology of the Strait of Belle Isle area, northwestern insular Newfoundland, southern Labrador and adjacent Quebec. Geological Survey of Canada, Ottawa, pp. 145.

Bosworth, W. 1984. The relative roles of boudinage and "structural slicing" in the disruption of layered rock sequences. Journal of Structural Geology, 92: 447-456.

Bosworth, W. 1985. East-directed imbrication and oblique-slip faulting in the Humber Arm Allochthon of western Newfoundland: structural and tectonic significance. Canadian Journal of Earth Science, 22, 1351:1360.

Botsford, J. 1988. Stratigraphy and sedimentology of Cambro-Ordovician deep water sediments, Bay of Islands, western Newfoundland. Ph.D. thesis, Memorial University of Newfoundland, St. John's, NL.

Bouma, A.H. 1962. Sedimentology of some flysch deposits; a graphic approach to facies interpretation. Elsevier, Amsterdam, pp. 168.

Borradaile, G.J., Bayly, M.B., and Powell, C.M.A. 1982. Atlas of deformational and metamorphic rock fabrics. Springer, Berlin, Heidelberg, New York, pp. 551.

Bruckner, W.D. 1966. Stratigraphy and structure of west-central Newfoundland. *In* Guidebook, geology of parts of Atlantic Provinces, Annual Meeting. *Edited by* Poole, W.H. Geological Association of Canada, Mineralogical Association of Canada, pp. 137-151.

Burden, E., Calon, T., Normore, L. and Strowbridge, S. 2001. Stratigraphy and structure of sedimentary rocks in the Humber Arm Allochthon, southwestern Bay of Islands, Newfoundland. *In* Current Research. Newfoundland Department of Mines and Energy Geological Survey, Report 2001-1, pp. 15-22.

Byrne, T. 1984. Early deformation in melange terranes of the Ghost Rocks Formation, Kodiak Islands, Alaska. *In* Melanges: Their Nature, Origin, and Significance. *Edited by* L.A Raymond. The Geological Society of America: Special Paper 198, pp 21 – 51.

Calon, T., Buchanan, C., Burden, E.B., Feltham, G., and Young, J. 2002. Stratigraphy and structure of sedimentary rocks in the Humber Arm Allochthon, southwestern Bay of Islands, Newfoundland. *In* Current Research. Newfoundland Department of Mines and Energy Geological Survey, Report 2002-1, pp. 35-45.

Cawood, P.A. and Botsford, J.W. 1991. Facies and structural contrasts across Bonne Bay cross-strike discontinuity, western Newfoundland. American Journal of Science, 291: 737-759.

Cawood, P.A. and Nemchin, A.A. 2001. Paleogeographic development of the east Laurentian margin: Constraints from U-Pb dating of detrital zircons in the Newfoundland. Geological Society of America Bulletin, 113, 9: 1234-1246.

Cawood, P.A. and Suhr, G. 1992. Generation and obduction of ophiolites: constraints from the Bay of Islands Complex, western Newfoundland. Tectonics, 11, 4: 884-897.

Cawood, P.A., McCausland, P.J.A., and Dunning, G.R. 2001. Opening Iapetus: constraints from the Laurentian margin in Newfoundland. Geological Society of America Bulletin, 113, 4: 443-453.

Cawood, P.A., van Gool, J.A.M., and Dunning, G.R. 1996. Geological development of eastern Humber and western Dunnage zones: Cornerbrook-Glover Island region, Newfoundland. Canadian Journal of Earth Sciences, 33: 182-198.

Charvet, J. and Ogawa, Y. 1994. Arc-trench tectonics. *In* Continental deformation. *Edited by* Paul J. Hancock. Pergamon Press, Tarrytown, NY, pp 180-190.

Church, W.R. and Stevens, R.K. 1971. Early Paleozoic ophiolite complexes of the Newfoundland Appalachians as mantle-oceanic crust sequences. Journal of Geophysical Research, 76:1460-1466.

Cloos, M., 1984. Flow melanges and the structural evolution of accretionary wedges. *In* Melanges: Their Nature, Origin, and Significance. *Edited by* L.A. Raymond. The Geological Society of America: Special Paper 198, pp 71 – 79.

Comeau, R.L. 1973. Transported Slices of the Coastal Complex, Bay of Islands-Western Newfoundland. M.Sc. thesis, Memorial University of Newfoundland, St. John's, NL, pp. 105.

Cooper, J.R. 1936. Geology of the southern half of the Bay of Islands igneous complex. *In* Newfoundland Department of Natural Resources, Geology Section, Bulletin Number 4.

Cowan, D.S. 1985. Structural styles in Mesozoic and Cenozoic melanges in the western Cordillera of North America. Geological Society of America Bulletin, 96: 451 – 462.

Dewey, J.F. 1969. Evolution of the Appalachian\Caledonian Orogen. Nature, 222: 124-129.

Dewey, J.F. and Bird, J.M. 1971. Origin and emplacement of the ophiolite suite: Appalachian ophiolites in Newfoundland. Journal of Geophysical Research, 76: 3179-3206.

Dewey, J.F. and Kidd, W.S.F. 1974. Continental collisions in the Appalachian\Caledonian orogenic belt: variations related to complete and incomplete suturing. Geology, 2:543-546.

Downie, C. 1981. Lower Cambrian acritarchs from Scotland, Norway, Greenland, and Canada. Transactions of the Royal Society of Edinburgh: Earth Sciences, 72: 257-285.

Eisenack, A. 1958. Microfossilien aus dem Ordovizium des Baltikums. I, Markositschicht, Dictyonema-Scheifer, Glaukonitsand, Glaukonilkalk. Senckenbergiana Lethaea, 39: 389-305.

Forbes, E., 1848. On *Oldhamia*, a new genus of Silurian fossils. Geological Survey of Dublin, Journal 4.

Godfrey, S. 1982. Rock Groups, Structural Slices and Deformation in the Humber Arm Allocthon at Serpentine Lake, Western Newfoundland. M.Sc. thesis, Memorial University of Newfoundland, St. John's, NL, pp. 182.

Greenly, E. 1919. The geology of Anglesey. Great Britain Geological Survey Memoir, 1, pp. 980.

Hobbs, B.E., Means, W.D., and Williams, P.F. 1976. An outline of structural geology. Wiley and Sons, New York, NY, pp. 571.

Howley, J.P. 1907. Geological map of Newfoundland.

Hsu, K.J. 1974. Melange and their distinction from olistostromes. *In* Modern and Ancient Geosynclinal Sedimentation. *Edited by* R.H. Dott jr. and R.H. Shaver. Society of Economic Paleontologists and Mineralogists Special Publication No. 19, pp 321 – 333.

James, N.P. Botsford, J.W., and Williams, S.H. 1987. Allochthonous slope sequence at Lobster Cove Head: evidence for a complex Middle Ordovician platform margin in western Newfoundland. Canadian Journal of Earth Science, 24: 1199-1211.

Jacobi, R.D., 1984. Modern submarine sediment slides. *In* Melanges: Their Nature, Origin, and Significance. *Edited by* L.A. Raymond. The Geological Society of America: Special Paper 198, pp 81 - 102.

Karig, D.E., 1980. Material transport within accretionary prisms and the "knocker" problem. Journal of Geology, 88: 27- 39.

Kay, M. 1945. Paleogeographic and palinspastic maps. Bulletin of the American Association of Petroleum Geologists, 29: 426-450.

Kay, M. 1951. North American Geosynclines. The Geological Society of America, Memoir 48, pp. 143.

Kindle, C.H. and Whittington, H.B. 1958. Stratigraphy of the Cow Head region, western Newfoundland. Geological Society of America Bulletin, 69: 315-342.

Krogh, T.E. 1982. Improved accuracy of U-Pb zircon ages by the creation of more concordant systems using an air abrasion technique. Geochimica et Cosmochimica Acta, 46: 637-649.

Lavoie, D., Burden, E.T., and Lebel, D. 2003. Stratigraphic framework for the Cambrian-Ordovician rift and passive margin successions from southern Quebec to western Newfoundland. Canadian Journal of Earth Sciences, 40, 2: 177-205.

Lilly, H.D. 1963. Geology of the Hughes Brook-Goose Arm Area, west Newfoundland. Memorial University of Newfoundland, Geology Report no. 2, St. John's, NL.

Lilly, H.D. 1967. Some notes on stratigraphy and structural styles in central-west Newfoundland. Geological Association of Canada, Special Paper No. 4, 201-212.

Lindholm, R.M. and Casey, J.F. 1989. Regional significance of the Blow Me Down Brook Formation, western Newfoundland: New fossil evidence for an Early Cambrian. Geological Society of America Bulletin, 101: 1-13.

Logan, W.E.. 1863. Report on the Geology of Canada. Geological Survey of Canada, Ottawa, ON, pp. 983.

Malpas, J. and Stevens, R.K. 1979. The origin and emplacement of the ophiolite suite with examples from western Newfoundland. *In* Ophiolites of the Canadaian Appalachians and Soviet Urals. *Edited by* J. Malpas and R.W. Talkington. Memorial University of Newfoundland, Department of Geology, Report No. 8, Contribution to I.G.C.P. Project 39, pp. 21-42.

Marshak, S. and Mitra, G. 1988. Basic methods of structural geology. Prentice Hall Inc. Englewood Cliffs, NJ, pp 446.

Martin, F. 1978. Lower Paleozoic Chitinozoa and Acritarcha from Newfoundland. *In* Current research, Part B, Geological Survey of Canada, no.78-1B, pp.73-81.

McCausland, P.J.A. and Hodych, J.P. 1998. Paleomagnetism of the 550 MA Skinner Cove volcanics of western Newfoundland and the opening of the Iapetus Ocean. Earth and Planetary Science Letters, 163: 15-29.

McCausland, P.J.A., Hodych, J.P., and Dunning, G.R. 1997. Evidence from western Newfoundland for the final break-up of Rodinia? U-Pb age and paleolatitude of the Skinner Cove Volcanics. *In* Geological Association of Canada 1997 Annual Meeting, Abstract Volume, 1997, pp. A-99.

Meschede, M. 1986. A method of discriminating between different types of mid-ocean ridge basalts and continental tholeiites with the Nb-Zr-Y diagram. Chemical Geology, 56: 207-218.

Mitra, S. 1990. Fault-propagation folds: geometry, kinematic evolution, and hydrocarbon traps. The American Association of Petroleum Geologists Bulletin, 74, 6: 921-945.

Mitra, S. 2002. Fold-accommodation faults. The American Association of Petroleum Geologists Bulletin, 86, 4: 671-693.

Morley, C.K. 1988. Out-of-sequence thrusts. Tectonics, 7, 3: 539-561.

Murray, A. and Howley, J.P. 1881. Geological Survey of Newfoundland from 1864-1880. Stanford, London, UK, pp. 372-409.

Needham, D.T. 1987. Asymmetric extensional structures and their implications for the generation of mélanges. Geology Magazine, 124, 4: 311-318.

Palmer, S.E., Burden, E., and Waldron, J.W.F. 2001. Stratigraphy of the Curling Group (Cambrian), Humber Arm Allocthon, Bay of Islands. *In* Current Research. Newfoundland Department of Mines and Energy Geological Survey, Report 2001-1, pp. 105-112.

Petit, J.P. 1987. Criteria for the sense of movement on fault surfaces in brittle rocks. Journal of Structural Geology, 9, 5: 597-608.

Platt, J.P. 1986. Dynamics of orogenic wedges and the uplift of high-pressure metamorphic rocks. Geological Society of America Bulletin, 97: 1037-1053.

Quinn, L. 1988. Distribution and significance of Ordovician flysch units in western Newfoundland. *In* Current research. Part B, Eastern and Atlantic Canada, Paper - Geological Survey of Canada, 88-1B: 119-126.

Quinn, L. 1992. Foreland and trench slope basin sandstones of the Goose Tickle Group and Lower Head Formation, western Newfoundland. Ph.D. thesis, Memorial University of Newfoundland, St. John's, NL, pp. 574.

Quinn L. 1995. Middle Ordovician foredeep fill in western Newfoundland. *In* Current Perspectives in the Appalachian - Caledonian Orogen: Geological Association of Canada, Special Paper 41. *Edited by* J.P. Hibbard, C.R. van Staal, and P.A. Cawood. Geological Association of Canada, pp. 43-64.

Ramsay, J.G. 1967. Folding and Fracturing of rocks. McGraw-Hill Book Co., New York, pp. 568.

Ramsay, J.G. and Huber, M.I. 1987. The techniques of modern structural geology, volume 2: folds and fractures. Academic Press Inc., London, UK, pp. 700.

Ramsay, J.G., Casey, M., and Kligfield, R. 1983. Role of shear in development of the Helvetic fold-thrust belt of Switzerland. Geology, 11: 439-442.

Raymond, L.A., 1984. Classification of melanges. *In* Melanges: Their Nature, Origin, and Significance. *Edited by* L.A. Raymond. The Geological Society of America: Special Paper 198, pp 7 – 19.

Reading, H.G. 1986. Sedimentary Environments and Facies, Second Edition. Blackwell Scientific Publications, Oxford, UK, pp. 615.

Riba, O. 1976. Syntectonic unconformities of the Alto Cardener, Spanish Pyrenees: A genetic interpretation. Sedimentary Geology, 15: 213-233.

Rodgers, J. and Neale, E.R.W. 1963. Possible "Taconic" Klippen in western Newfoundland. American Journal of Science, 261: 213-230.

Saleeby, J., 1979. Kaweah serpentine melange, southwest Sierra Nevada foothills, California. Geological Society of America Bulletin, 90: 29 – 46.

Schillereff, S. and Williams, H. 1979. Geology of Stephenville map area, Newfoundland. *In* Current Research (Part A). Geological Survey of Canada, Paper 79-1a: 327-332.

Schuchert. C. and Dunbar, C.O. 1934. Stratigraphy of Western Newfoundland, The Geological Society of America, Memoir 1, pp. 123.

Seilacher, A. 1967. Bathymetry of trace fossils. Marine Geology, 5: 413-429.

Smith, C.H. 1958. Bay of Islands Igneous complex, western Newfoundland. M.Sc. thesis, Memorial University of Newfoundland, St. John's, NL

Stevens, R.K. 1965. Geology of the Humber Arm area, west Newfoundland. MSc. Thesis, Memorial University of Newfoundland, St. John's, NL, pp. 121.

Stevens, R.K. 1970. Cambro-Ordovician flysch sedimentation and tectonics in west Newfoundland and their possible bearing on a proto - Atlantic Ocean. *In* Flysch sedimentology in North America. *Edited by* J. Lajoie. The Geological Association of Canada, Special Paper Number 7, pp 165-177.

Sylvester, A.G. 1988. Strike-slip faults. Geological Society of America Bulletin, 100: 1666-1703.

Waldron, J.W.F. 1985. Structural history of continental margin sediments beneath the Bay of Islands Ophiolite, Newfoundland. Canadian Journal of Earth Sciences, 22, 11: 1618-1632.

Waldron, J.W.F., and Stockmal, G.S. 1991. Mid-Paleozoic thrusting at the Appalachian deformation front: Port au Port Peninsula, western Newfoundland. Canadian Journal of Earth Sciences, 28: 1992-2002.

Waldron, J.W.F., Anderson, S.D., Cawood, P.A., Goodwin, L.B., Hall, J.H., Jamieson, R.A., Palmer, S.E., Stockmal, G.S., and Williams, P.F. 1998. Evolution of the Appalachian Laurentian margin: Lithoprobe results in western Newfoundland. Canadian Journal of Earth Sciences, 35: 1271-1287.

Waldron, J.W.F., Henry, A.D., and Bradley, J.C. 2002. Structure and polyphase deformation of the Humber Arm Allochthon and related rocks west of Corner Brook, Newfoundland. *In* Current Research. Newfoundland Department of Mines and Energy Geological Survey, Report 2002-1, pp. 47-52.

Waldron, J.W.F., Henry, A.D., Bradley, J.C., and Palmer, S.E. 2003. Development of a folded thrust stack; Humber Arm Allochthon, Bay of Islands, Newfoundland Appalachians. *In* The Appalachian forelands and platform NATMAP project, geological bridges of eastern Canada. *Edited by* D. Lavoie, M. Malo, and A. Tremblay. Canadian Journal of Earth Sciences, 40, 2: 237-253.

Waldron, J.W.F., Turner, D., and Stevens, R.K. 1988. Stratal disruption and development of melange, Western Newfoundland: effect of high fluid pressure in an accretionary terrain. Journal of Structural Geology, 10, 8: 861-973.

Walthier, T.N. 1949. Geology and mineral deposits of the area between Corner Brook and Stephenville, western Newfoundland. *In* Geology and Mineral deposits of the area between Lewis Hills and Bay St. George, western Newfoundland. Newfoundland Geological Survey, Bulletin 35.

Weitz, J.L. 1953. Geology of the Bay of Islands area, western Newfoundland. Ph.D. thesis, Yale University, New Haven, Conn.

Williams, H. 1964. The Appalachians in northeastern Newfoundland - a two-sided symmetrical system. American Journal of Science, 262: 1137-1158.

Williams, H. 1971. Mafic - ultramafic complexes in western Newfoundland Appalachians and the evidence for their transportation: A review and interim report. The Geological Association of Canada: Proceedings, 24, 1: 9-25.

Williams, H. 1973. Bay of Islands Map-Area, Newfoundland, (12G). Report and Map 1355A. *In* Geological Survey of Canada: Paper 72-34, pp. 1-7.

Williams, H. 1975. Structural Succession, Nomenclature, and Interpretation of Transported Rocks in Western Newfoundland. Canadian Journal of Earth Sciences, 12: 1874-1894.

Williams, H. 1979. Appalachian orogen in Canada. Canadian Journal of Earth Sciences, 16: 792-807.

Williams, H. 1982. Geology of the Canadian Applachians. *In* Perspectives in regional geological synthesis. *Edited by* A.R. Palmer. The Geological Society of America, D-NAG special publication 1, pp. 57-66.

Williams, H. and Cawood, P.A.. 1989. Geology, Humber Arm Allochthon, Newfoundland. Geological Survey of Canada, Map 1678A.

Williams, H. and Godfrey, S.C. 1980. Geology of Stephenville map area, Newfoundland. *In* Current Research (Part A). Geological Survey of Canada, Paper 80-1a: 217-221.

Williams, H. and Hiscott, R.N. 1987. Definition of the Iapetus rift-drift transition in western Newfoundland. Geology, 15: 1044-1047.

Williams, H. and Stevens, R.K. 1974. The ancient continental margin of eastern North America. *In* North American ophiolites. *Edited by* R.G. Coleman and W.P. Irwin. Oregon Department of Geology and Mineral Industries, Bulletin 95, pp. 1-11.

Williams, P.F. 1977. Foliation: a review and discussion. Tectonophysics, 39:305-328

Wilson, J.T. 1966. Did the Atlantic Ocean close and reopen? Nature, 211: 676.

Winchester, J.A. and Floyd, P.A. 1977. Geochemical discrimination of different magma series and their differentiation products using immobile elements. Chemical Geology, 20: 325-343.

Wojtal, S. and Mitra, G. 1988. Nature of deformation in some fault rocks from Appalachian thrusts. *In* Geometries and Mechanisms of Thrusting, with special reference to the Appalachians. *Edited by* G. Mitra and S. Wojtal. The Geological Society of America: Special Paper 222, pp. 17-34.

Wojtal, S. 2001, The nature and origin of asymmetric arrays of shear surfaces in fault zones. *In* The Nature and Tectonic Significance of Fault Zone Weakening. *Edited by* Holdsworth, R.E., Strachan, R.A., Magloughlin, J., and Knipe, R.J. Geological Society, London, Special Publication, 186, pp. 171-193.

Appendix A

Sample lists

Sample descriptions and locations

Project:	Station:	Northing:	Easting:	Geochem:	◉
FCYH	S0306	5438086.50	411800.91	Thin Section:	◉
Sample#:	S0306-01	Geochem		Oriented:	○
TS#:	NA			Oriented:	○

Sample description\results **Dip: Dip Dir:**

Sample processed for XRF by Dr. J. Hodych. Analysis is presented Appendix C.

Project:	Station:	Northing:	Easting:	Geochem:	○
FCYH	FB-03-02-245	5438185.00	411736.00	Thin Section:	◉
Sample#:	FB-03-02-245-01	Hand Sample		Oriented:	○
TS#:	245-01a	Not Oriented		Oriented:	○

Sample description\results **Dip: Dip Dir:**

Contact between Blow Me Down Brook formation and the Wood's Island volcanics.

Project:	Station:	Northing:	Easting:	Geochem:	○
FCYH	FB-03-02-245	5438185.00	411736.00	Thin Section:	◉
Sample#:	FB-03-02-245-01	Hand Sample		Oriented:	○
TS#:	245-01b	Not Oriented		Oriented:	○

Sample description\results **Dip: Dip Dir:**

Contact between Blow Me Down Brook formation and the Wood's Island volcanics.

Project:	Station:	Northing:	Easting:	Geochem:	○
FCYH	FB-03-02-245	5438185.00	411736.00	Thin Section:	◉
Sample#:	FB-03-02-245-02	Hand Sample		Oriented:	○
TS#:	245-02	Not Oriented		Oriented:	○

Sample description\results **Dip: Dip Dir:**

Sheared contact between Blow Me Down Brook formation and the Wood's Island Volcanics.

Sample descriptions and locations

Project:	Station:	Northing:	Easting:	Geochem:	○
FCYH	S0303	5438197.00	411715.78	Thin Section:	◉
Sample#:	S0303-001	Oriented Sample		Oriented:	◉
TS#:	S0303-001a	(XZ) perp to foliation		Oriented:	○

Sample description\results **Dip:** **Dip Dir:**

Sheared contact between Blow Me Down Brook formation sandstone and the Wood's Island volcanics.

Project:	Station:	Northing:	Easting:	Geochem:	○
FCYH	S0303	5438197.00	411715.78	Thin Section:	◉
Sample#:	S0303-001	Oriented Sample		Oriented:	◉
TS#:	S0303-001b	(XZ) perp to foliation		Oriented:	○

Sample description\results **Dip:** **Dip Dir:**

Shear bands within the sheared contact between Blow Me Down Brook formation sandstone and the Wood's Island volcanics.

Project:	Station:	Northing:	Easting:	Geochem:	○
FCYH	A1102	5434892.00	412919.13	Thin Section:	◉
Sample#:	A1102-001	Palynology		Oriented:	○
TS#:	2002-024	Not Oriented		Oriented:	○

Sample description\results **Dip:** **Dip Dir:**

Non-diagnostic acritarch assemblage.

Project:	Station:	Northing:	Easting:	Geochem:	○
FCYH	A1201	5442942.00	398218.47	Thin Section:	◉
Sample#:	A1201.002	Palynology		Oriented:	○
TS#:	2002-025	Not Oriented		Oriented:	○

Sample description\results **Dip:** **Dip Dir:**

Barren

Sample descriptions and locations

Project:	Station:	Northing:	Easting:	Geochem: ○
FCYH	A1204	5442924.50	398098.47	Thin Section: ◉
Sample#: A1204-001		Palynology		Oriented: ○
TS#: 2002-026		Not Oriented		Oriented: ○
Sample description\results				Dip: Dip Dir:
Barren				

Project:	Station:	Northing:	Easting:	Geochem: ○
FCYH	A2401	5432993.50	415838.50	Thin Section: ◉
Sample#: A2401		Palynology		Oriented: ○
TS#: 2001-215		Not Oriented		Oriented: ○
Sample description\results				Dip: Dip Dir:
Barren				

Project:	Station:	Northing:	Easting:	Geochem: ○
FCYH	A2501	5433389.00	415645.00	Thin Section: ◉
Sample#: A2501-001		Palynology		Oriented: ○
TS#: 2001-218		Not Oriented		Oriented: ○
Sample description\results				Dip: Dip Dir:
Barren				

Project:	Station:	Northing:	Easting:	Geochem: ○
FCYH	A2503	5433525.50	415573.97	Thin Section: ◉
Sample#: A2503-001		Palynology		Oriented: ○
TS#: 2001-216		Not Oriented		Oriented: ○
Sample description\results				Dip: Dip Dir:
Barren				

Sample descriptions and locations

Project:	Station:	Northing:	Easting:	Geochem: ○
FCYH	A2510	5434303.00	415361.47	Thin Section: ◉
Sample#: A2510-001		Palynology		Oriented: ○
TS#: 2001-217		Not Oriented		Oriented: ○
Sample description\results				Dip: Dip Dir:
Barren				

Project:	Station:	Northing:	Easting:	Geochem: ○
FCYH	A2604	5434431.00	415191.00	Thin Section: ◉
Sample#: A2604-001		Palynology		Oriented: ○
TS#: 2001-219		Not Oriented		Oriented: ○
Sample description\results				Dip: Dip Dir:
Barren				

Project:	Station:	Northing:	Easting:	Geochem: ○
FCYH	A2607	5434649.50	413350.81	Thin Section: ◉
Sample#: A2607-001		Palynology		Oriented: ○
TS#: 2002-027		Not Oriented		Oriented: ○
Sample description\results				Dip: Dip Dir:
Barren				

Project:	Station:	Northing:	Easting:	Geochem: ○
FCYH	A2607	5434649.50	413350.81	Thin Section: ◉
Sample#: A2607-002		Palynology		Oriented: ○
TS#: 2001-220		Not Oriented		Oriented: ○
Sample description\results				Dip: Dip Dir:
Barren				

Sample descriptions and locations

Project:	Station:	Northing:	Easting:	Geochem: ○
FCYH	A2705	5434686.00	414968.38	Thin Section: ◉
Sample#: A2705-001		Palynology		Oriented: ○
TS#: 2001-221		Not Oriented		Oriented: ○

Sample description\results **Dip:** **Dip Dir:**

Barren

Project:	Station:	Northing:	Easting:	Geochem: ○
FCYH	A2709	5434566.50	414683.78	Thin Section: ◉
Sample#: A709-001		Palynology		Oriented: ○
TS#: 2001-222		Not Oriented		Oriented: ○

Sample description\results **Dip:** **Dip Dir:**

Barren

Project:	Station:	Northing:	Easting:	Geochem: ○
FCYH	A2713	5434504.50	414476.75	Thin Section: ◉
Sample#: A2713-001		Palynology		Oriented: ○
TS#: 2001-223		Not Oriented		Oriented: ○

Sample description\results **Dip:** **Dip Dir:**

Barren

Project:	Station:	Northing:	Easting:	Geochem: ○
FCYH	A3001	5434774.00	413214.66	Thin Section: ◉
Sample#: A3001-001		Palynology		Oriented: ○
TS#: 2002-028		Not Oriented		Oriented: ○

Sample description\results **Dip:** **Dip Dir:**

Barren

Sample descriptions and locations

Project:	Station:	Northing:	Easting:	Geochem: ○
FCYH	A3001	5434774.00	413214.66	Thin Section: ◉
Sample#: A3001-003		Palynology		Oriented: ○
TS#: 2001-224		Not Oriented		Oriented: ○

Sample description\results **Dip:** **Dip Dir:**

Barren

Project:	Station:	Northing:	Easting:	Geochem: ○
FCYH	A3001	5434774.00	413214.66	Thin Section: ◉
Sample#: A3001-004		Palynology		Oriented: ○
TS#: 2002-029		Not Oriented		Oriented: ○

Sample description\results **Dip:** **Dip Dir:**

Barren

Project:	Station:	Northing:	Easting:	Geochem: ○
FCYH	A3002	5434819.00	413175.16	Thin Section: ◉
Sample#: A3002-001		Palynology		Oriented: ○
TS#: 2002-030		Not Oriented		Oriented: ○

Sample description\results **Dip:** **Dip Dir:**

Barren

Project:	Station:	Northing:	Easting:	Geochem: ○
FCYH	A3003	5434874.00	413142.41	Thin Section: ◉
Sample#: A3003-001		Palynology		Oriented: ○
TS#: 2001-225		Not Oriented		Oriented: ○

Sample description\results **Dip:** **Dip Dir:**

Non-diagnostic acritarch assemblage.

Sample descriptions and locations

Project:	Station:	Northing:	Easting:	Geochem: ○
FCYH	A3003	5434874.00	413142.41	Thin Section: ◉
Sample#: A3003-002		Palynology		Oriented: ○
TS#: 2001-226		Not Oriented		Oriented: ○

Sample description\results **Dip: Dip Dir:**

Non-diagnostic acritarch assemblage.

Project:	Station:	Northing:	Easting:	Geochem: ○
FCYH	A3101	5434891.50	412943.97	Thin Section: ◉
Sample#: A3101-001		Palynology		Oriented: ○
TS#: 2001-227		Not Oriented		Oriented: ○

Sample description\results **Dip: Dip Dir:**

Barren

Project:	Station:	Northing:	Easting:	Geochem: ○
FCYH	A3101	5434891.50	412943.97	Thin Section: ◉
Sample#: A3101-002		Palynology		Oriented: ○
TS#: 2001-228		Not Oriented		Oriented: ○

Sample description\results **Dip: Dip Dir:**

Barren

Project:	Station:	Northing:	Easting:	Geochem: ○
FCYH	FB-03-02-268	5437703.00	413010.00	Thin Section: ◉
Sample#: FB-03-02-268-01		Palynology		Oriented: ○
TS#: 2002-175		Not Oriented		Oriented: ○

Sample description\results **Dip: Dip Dir:**

Barren. Highly Cooked

Sample descriptions and locations

Project:	Station:	Northing:	Easting:	Geochem: ○
FCYH	FB-03-02-271	5437683.00	413176.00	Thin Section: ◉
Sample#: FB-03-02-271-02	Palynology			Oriented: ○
TS#: 2002-176	Not Oriented			Oriented: ○

Sample description\results **Dip:** **Dip Dir:**

Broken Lunelidyia - Upper Tremadoc

Project:	Station:	Northing:	Easting:	Geochem: ○
FCYH	FB-03-02-278	5437440.00	413436.00	Thin Section: ◉
Sample#: FB-03-02-278-01	Palynology			Oriented: ○
TS#: 2002-177	Not Oriented			Oriented: ○

Sample description\results **Dip:** **Dip Dir:**

Baltisporidium crinitium forms - Tremadoc - Arenig

Project:	Station:	Northing:	Easting:	Geochem: ○
FCYH	FB-03-02-278	5437440.00	413436.00	Thin Section: ◉
Sample#: FB-03-02-278-02	Palynology			Oriented: ○
TS#: 2002-178	Not Oriented			Oriented: ○

Sample description\results **Dip:** **Dip Dir:**

Baltisporidium crinitum forms - Tremadoc - Arenig

Project:	Station:	Northing:	Easting:	Geochem: ○
FCYH	FB-03-02-281	5437384.00	413585.00	Thin Section: ◉
Sample#: FB-03-02-281-01	Palynology			Oriented: ○
TS#: 2002-179	Not Oriented			Oriented: ○

Sample description\results **Dip:** **Dip Dir:**

Lunalidyia - Upper Tremadoc

Sample descriptions and locations

Project:	Station:	Northing:	Easting:	Geochem:
FCYH	FB-03-02-289	5437307.00	413919.00	Thin Section: ◉

Sample#: FB-03-02-289-01 Palynology **Oriented:** ○

TS#: 2002-180 Not Oriented **Oriented:** ○

Sample description\results **Dip:** **Dip Dir:**

Cooked beyond recognition. More so than normal BMDB

Project:	Station:	Northing:	Easting:	Geochem:
FCYH	S0102	5434940.00	413055.06	Thin Section: ◉

Sample#: S0102-001 Palynology **Oriented:** ○

TS#: 2002-031 Not Oriented **Oriented:** ○

Sample description\results **Dip:** **Dip Dir:**

Non-diagnostic acritarch assemblage.

Project:	Station:	Northing:	Easting:	Geochem:
FCYH	S0201	5434762.50	413245.88	Thin Section: ◉

Sample#: S0201-001 Palynology **Oriented:** ○

TS#: 2002-032 Not Oriented **Oriented:** ○

Sample description\results **Dip:** **Dip Dir:**

Barren

Project:	Station:	Northing:	Easting:	Geochem:
FCYH	S0201	5434762.50	413245.88	Thin Section: ◉

Sample#: S0201-004 Palynology **Oriented:** ○

TS#: 2002-033 Not Oriented **Oriented:** ○

Sample description\results **Dip:** **Dip Dir:**

Barren

Sample descriptions and locations

Project:	Station:	Northing:	Easting:	Geochem: ○
FCYH	S0201	5434762.50	413245.88	Thin Section: ◉
Sample#: S0201-006		Palynology		Oriented: ○
TS#: 2001-234		Not Oriented		Oriented: ○

Sample description\results **Dip:** **Dip Dir:**

Barren

Project:	Station:	Northing:	Easting:	Geochem: ○
FCYH	S0202	5434736.00	413295.16	Thin Section: ◉
Sample#: S0202-001		Palynology		Oriented: ○
TS#: 2001-229		Not Oriented		Oriented: ○

Sample description\results **Dip:** **Dip Dir:**

Non-diagnostic assemblage

Project:	Station:	Northing:	Easting:	Geochem: ○
FCYH	S0204	5434700.00	413319.44	Thin Section: ◉
Sample#: S0204-001		Palynology		Oriented: ○
TS#: 2001-230		Not Oriented		Oriented: ○

Sample description\results **Dip:** **Dip Dir:**

Non-diagnostic assemblage

Project:	Station:	Northing:	Easting:	Geochem: ○
FCYH	S0204	5434700.00	413319.44	Thin Section: ◉
Sample#: S0204-002		Palynology		Oriented: ○
TS#: 2002-034		Not Oriented		Oriented: ○

Sample description\results **Dip:** **Dip Dir:**

Barren

Sample descriptions and locations

Project:	Station:	Northing:	Easting:	Geochem: ○
FCYH	S0206	5434612.00	413420.38	Thin Section: ◉
Sample#: S0206-001		Palynology		Oriented: ○
TS#: 2001-231		Not Oriented		Oriented: ○

Sample description\results **Dip:** **Dip Dir:**

Barren

Project:	Station:	Northing:	Easting:	Geochem: ○
FCYH	S0310	5438223.50	411984.91	Thin Section: ◉
Sample#: S0310-002		Palynology		Oriented: ○
TS#: 2001-232		Not Oriented		Oriented: ○

Sample description\results **Dip:** **Dip Dir:**

Non-diagnostic acritarch assemblage.

Project:	Station:	Northing:	Easting:	Geochem: ○
FCYH	S0401	5434457.00	414359.84	Thin Section: ◉
Sample#: S0401-001		Palynology		Oriented: ○
TS#: 2001-234		Not Oriented		Oriented: ○

Sample description\results **Dip:** **Dip Dir:**

Barren

Project:	Station:	Northing:	Easting:	Geochem: ○
FCYH	S0403	5438237.50	412363.41	Thin Section: ◉
Sample#: S0403-001		Palynology		Oriented: ○
TS#: 2001-235		Not Oriented		Oriented: ○

Sample description\results **Dip:** **Dip Dir:**

Barren

Sample descriptions and locations

Project:	Station:	Northing:	Easting:	Geochem: ○
FCYH	S0403	5438237.50	412363.41	Thin Section: ◉
Sample#: S0403-002		Palynology		Oriented: ○
TS#: 2001-236		Not Oriented		Oriented: ○

Sample description\results **Dip:** **Dip Dir:**

Barren

Project:	Station:	Northing:	Easting:	Geochem: ○
FCYH	S0404	5438222.00	412385.78	Thin Section: ◉
Sample#: S0404-001		Palynology		Oriented: ○
TS#: 2002-035		Not Oriented		Oriented: ○

Sample description\results **Dip:** **Dip Dir:**

Barren

Project:	Station:	Northing:	Easting:	Geochem: ○
FCYH	S0405	5438208.00	412415.50	Thin Section: ◉
Sample#: S0405-001		Palynology		Oriented: ○
TS#: 2001-237		Not Oriented		Oriented: ○

Sample description\results **Dip:** **Dip Dir:**

Non-diagnostic acritarch assemblage.

Project:	Station:	Northing:	Easting:	Geochem: ○
FCYH	S0405	5438208.00	412415.50	Thin Section: ◉
Sample#: S0405-002		Palynology		Oriented: ○
TS#: 2001-238		Not Oriented		Oriented: ○

Sample description\results **Dip:** **Dip Dir:**

Non-diagnostic acritarch assemblage.

Appendix B

Field stations

List of field stations and co-ordinates

Projection UTM **Datum:** NAD27 **Zone** 21

Project	Stations	Northing	Easting	Altitude (m)	Lithology
FCYH	300602-01	5432016.00	414003.00	180	MAP
FCYH	300602-02	5431722.00	413808.00	202	MAP
FCYH	300602-03	5431841.00	413523.00	244	VOLC
FCYH	300602-04	5431857.00	413892.00	181	BMDB
FCYH	300602-05	5431855.00	413930.00	193	BMDB
FCYH	300602-06	5432441.00	414227.00	122	IT
FCYH	300602-07	5433261.00	413728.00	107	IT
FCYH	300602-08	5433421.00	413763.00	67	IT
FCYH	300602-09	5433500.00	413745.00	51	IT
FCYH	300602-10	5433773.00	413787.00	40	IT
FCYH	300602-11	5433801.00	413849.00	71	MAP
FCYH	A0101	5434916.00	412755.81	1	BMDB
FCYH	A0102	5434922.00	412785.88	4	BMDB
FCYH	A0103	5434925.00	412801.28	0	BMDB
FCYH	A0201	5434916.00	412831.09	2	BMDB
FCYH	A0202	5434923.00	412857.50	2	BMDB
FCYH	A0701	5434908.50	412874.81	1	BMDB
FCYH	A0801	5435071.50	411426.31	2	BMDB
FCYH	A1101	5434908.00	412898.19	1	BMDB
FCYH	A1102	5434892.00	412919.13	11	BMDB
FCYH	A1103	5434892.00	412939.59	0	BMDB
FCYH	A1104	5434758.00	413101.13	60	
FCYH	A1105	5434711.50	413153.03	61	
FCYH	A1106	5434665.00	413212.94	62	
FCYH	A1107	5434631.50	413242.38	63	
FCYH	A1108	5434567.50	413335.63	48	
FCYH	A1701	5434912.50	413023.19	1	
FCYH	A1702	5434903.00	413144.34	1	
FCYH	A2401	5432993.50	415838.50	0	CBF
FCYH	A2402	5433047.50	415799.88	0	CBF
FCYH	A2403	5433111.50	415770.88	0	CBF
FCYH	A2404	5433150.50	415761.94	1	CBF
FCYH	A2405	5433196.50	415737.06	0	CBF
FCYH	A2406	5433331.00	415666.75	0	CBF
FCYH	A2407	5433245.50	415720.28	0	CBF
FCYH	A2501	5433389.00	415645.00	0	MAP
FCYH	A2502	5433497.50	415591.84	0	MAP
FCYH	A2503	5433525.50	415573.97	0	MAP
FCYH	A2504	5433555.00	415539.38	0	MAP
FCYH	A2505	5433627.00	415491.47	0	MAP
FCYH	A2506	5433713.00	415473.06	0	CBF

List of field stations and co-ordinates

Projection UTM **Datum:** NAD27 **Zone** 21

Project	Stations	Northing	Easting	Altitude (m)	Lithology
FCYH	A2507	5433803.50	415451.06	0	CBF
FCYH	A2508	5433922.50	415428.75	0	CBF
FCYH	A2509	5434221.00	415391.66	0	
FCYH	A2510	5434303.00	415361.47	0	CBF
FCYH	A2511	5434652.50	414810.03	0	MAP
FCYH	A2512	5434688.00	414834.69	0	MAP
FCYH	A2601	5434339.00	415326.22	0	MAP
FCYH	A2602	5434370.50	415291.63	0	MAP
FCYH	A2603	5434398.00	415241.63	0	MAP
FCYH	A2604	5434431.00	415191.00	0	MAP
FCYH	A2605	5434453.50	415162.84	0	MAP
FCYH	A2606	5434719.50	414865.13	0	MAP
FCYH	A2607	5434649.50	413350.81	0	RBA
FCYH	A2701	5434496.00	415148.88	0	MAP
FCYH	A2702	5434531.50	415095.34	0	MAP
FCYH	A2703	5434578.50	415071.22	0	MAP
FCYH	A2704	5434642.50	415022.53	0	MAP
FCYH	A2705	5434686.00	414968.38	0	MAP
FCYH	A2706	5434739.50	414938.50	0	MAP
FCYH	A2707	5434789.50	414870.59	0	MAP
FCYH	A2708	5434580.50	414727.09	0	MAP
FCYH	A2709	5434566.50	414683.78	0	RBA
FCYH	A2710	5434587.50	414631.47	0	RBA
FCYH	A2711	5434579.00	414597.00	0	RBA
FCYH	A2712	5434530.00	414530.50	0	MAP
FCYH	A2713	5434504.50	414476.75	0	MAP
FCYH	A2714	5434478.00	414440.53	0	MAP
FCYH	A2715	5434452.50	414459.88	12	MAP
FCYH	A3001	5434774.00	413214.66	0	IT
FCYH	A3002	5434819.00	413175.16	0	IT
FCYH	A3003	5434874.00	413142.41	0	BMDB
FCYH	A3004	5434924.50	413125.69	0	BMDB
FCYH	A3005	5434966.00	413096.38	0	
FCYH	A3101	5434891.50	412943.97	0	MAP
FCYH	AD038	5440224.50	411298.81	0	BMDB
FCYH	AD039	5440251.50	411246.94	0	BMDB
FCYH	AD046	5440305.50	411045.63	0	BMDB
FCYH	AD052	5439334.50	410344.22	0	BMDB
FCYH	AD057	5439162.00	410049.53	0	BMDB
FCYH	AD058	5438938.00	410294.41	0	BMDB
FCYH	AD059	5438604.00	410653.41	0	BMDB

List of field stations and co-ordinates

Projection UTM **Datum:** NAD27 **Zone** 21

Project	Stations	Northing	Easting	Altitude (m)	Lithology
FCYH	AD062	5438251.00	411525.00	0	BMDB
FCYH	AD063	5438259.50	411485.59	0	BMDB
FCYH	AD064	5438247.00	411429.56	0	BMDB
FCYH	AD065	5438288.50	411315.41	0	BMDB
FCYH	AD066	5438290.50	411294.66	0	BMDB
FCYH	AD067	5438290.50	411253.16	0	BMDB
FCYH	EB-01-235	5438222.00	411665.00	0	BMDB
FCYH	EB-01-236	5438224.00	411969.00	7	BMDB
FCYH	FB-03-02-164	5434660.00	413352.00	3	
FCYH	FB-03-02-165	5434712.00	413295.00	8	
FCYH	FB-03-02-184	5432886.00	414220.00	94	
FCYH	FB-03-02-185	5432929.00	414251.00	87	BMDB
FCYH	FB-03-02-186	5432825.00	414381.00	96	MAP
FCYH	FB-03-02-187	5432830.00	414412.00	117	
FCYH	FB-03-02-188	5432794.00	414437.00	110	MAP
FCYH	FB-03-02-189	5432732.00	414527.00	101	
FCYH	FB-03-02-190	5432698.00	414549.00	99	MAP
FCYH	FB-03-02-191	5432653.00	414584.00	112	IT
FCYH	FB-03-02-192	5432690.00	414231.00	121	IT
FCYH	FB-03-02-193	5432718.00	414256.00	115	
FCYH	FB-03-02-194	5432791.00	414273.00	115	
FCYH	FB-03-02-195	5433342.00	414133.00	109	CBF
FCYH	FB-03-02-196	5433436.00	414146.00	116	MAP
FCYH	FB-03-02-197	5433436.00	414171.00	123	MAP
FCYH	FB-03-02-198	5433431.00	414202.00	122	CBF
FCYH	FB-03-02-199	5433534.00	414258.00	129	
FCYH	FB-03-02-200	5433625.00	414244.00	120	CBF
FCYH	FB-03-02-201	5433667.00	414238.00	82	
FCYH	FB-03-02-202	5433714.00	414241.00	49	CBF
FCYH	FB-03-02-203	5433765.00	414264.00	51	
FCYH	FB-03-02-204	5433929.00	414207.00	58	MAP
FCYH	FB-03-02-205	5434327.00	413602.00	62	
FCYH	FB-03-02-206	5434328.00	413594.00	0	MAP
FCYH	FB-03-02-207	5434235.00	413590.00	0	CBF
FCYH	FB-03-02-208	5434054.00	413644.00	0	BMDB
FCYH	FB-03-02-209	5434911.00	412755.00	0	BMDB
FCYH	FB-03-02-210	5434919.00	412796.00	0	BMDB
FCYH	FB-03-02-211	5434928.00	412834.00	0	BMDB
FCYH	FB-03-02-212	5434906.00	412910.00	0	BMDB
FCYH	FB-03-02-213	5434892.00	412958.00	0	CBF
FCYH	FB-03-02-214	5434958.00	413074.00	0	BMDB

List of field stations and co-ordinates

Projection UTM **Datum:** NAD27 **Zone** 21

Project	Stations	Northing	Easting	Altitude (m)	Lithology
FCYH	FB-03-02-215	5434669.00	413345.00	0	RBA
FCYH	FB-03-02-216	5434845.00	413161.00	0	IT
FCYH	FB-03-02-217	5434246.00	415390.00	0	CBF
FCYH	FB-03-02-218	5434345.00	415322.00	6	CBF
FCYH	FB-03-02-219	5434379.50	415273.69	0	MAP
FCYH	FB-03-02-220	5434496.00	415141.00	1	MAP
FCYH	FB-03-02-221	5434597.00	415064.41	0	MAP
FCYH	FB-03-02-222	5433873.00	412396.00	57	BMDB
FCYH	FB-03-02-223	5433875.00	412480.00	61	BMDB
FCYH	FB-03-02-224	5433880.00	412323.00	66	BMDB
FCYH	FB-03-02-225	5433867.00	412241.00	70	BMDB
FCYH	FB-03-02-226	5433968.00	412075.00	46	BMDB
FCYH	FB-03-02-227	5434327.00	411308.00	79	BMDB
FCYH	FB-03-02-228	5434363.00	411188.00	65	BMDB
FCYH	FB-03-02-229	5434488.00	411046.00	58	BMDB
FCYH	FB-03-02-230	5434574.00	410991.00	64	BMDB
FCYH	FB-03-02-231	5434426.00	411234.00	57	BMDB
FCYH	FB-03-02-232	5434456.00	411263.00	61	BMDB
FCYH	FB-03-02-233	5434518.00	411287.00	70	BMDB
FCYH	FB-03-02-234	5434552.00	411301.00	107	BMDB
FCYH	FB-03-02-235	5434582.00	411287.00	115	BMDB
FCYH	FB-03-02-236	5434617.00	411257.00	107	BMDB
FCYH	FB-03-02-237	5434653.00	411216.00	109	BMDB
FCYH	FB-03-02-238	5434819.00	411221.00	112	BMDB
FCYH	FB-03-02-239	5434841.00	411196.00	65	BMDB
FCYH	FB-03-02-240	5434863.00	411142.00	62	BMDB
FCYH	FB-03-02-241	5434906.00	411184.00	55	BMDB
FCYH	FB-03-02-242	5434940.00	411216.00	39	BMDB
FCYH	FB-03-02-243	5435040.00	411198.00	27	BMDB
FCYH	FB-03-02-244	5434726.00	410829.00	27	BMDB
FCYH	FB-03-02-244a	5434809.00	410811.00	32	BMDB
FCYH	FB-03-02-244b	5434712.00	410822.09	25	BMDB
FCYH	FB-03-02-245	5438185.00	411736.00	15	BMDB
FCYH	FB-03-02-246	5438156.00	411734.00	4	VOLC
FCYH	FB-03-02-247	5438099.00	411860.00	8	VOLC
FCYH	FB-03-02-248	5438304.00	412174.00	10	BMDB
FCYH	FB-03-02-249	5438294.00	412212.00	3	CBF
FCYH	FB-03-02-250	5438281.00	412259.00	6	CBF
FCYH	FB-03-02-251	5438242.00	412297.00	12	BMDB
FCYH	FB-03-02-252	5438248.00	412353.00	0	BMDB
FCYH	FB-03-02-253	5438236.00	412374.00	0	BMDB

List of field stations and co-ordinates

Projection UTM **Datum:** NAD27 **Zone** 21

Project	Stations	Northing	Easting	Altitude (m)	Lithology
FCYH	FB-03-02-254	5438191.00	412429.00	0	BMDB
FCYH	FB-03-02-255	5438206.00	412447.00	0	BMDB
FCYH	FB-03-02-256	5438202.00	412481.00	0	
FCYH	FB-03-02-257	5438157.00	412552.00	0	
FCYH	FB-03-02-258	5438100.00	412606.00	6	BMDB
FCYH	FB-03-02-259	5438051.00	412641.00	7	BMDB
FCYH	FB-03-02-260	5438010.00	412691.00	3	
FCYH	FB-03-02-261	5437964.00	412738.00	0	BMDB
FCYH	FB-03-02-262	5437897.00	412769.00	0	MAP
FCYH	FB-03-02-263	5437870.00	412839.00	8	
FCYH	FB-03-02-264	5437837.00	412885.00	11	MAP
FCYH	FB-03-02-265	5437823.00	412920.00	0	MAP
FCYH	FB-03-02-266	5437797.00	412951.00	1	BMDB
FCYH	FB-03-02-267	5437760.00	412979.00	4	BMDB
FCYH	FB-03-02-268	5437703.00	413010.00	0	CBF
FCYH	FB-03-02-269	5437697.00	413057.00	0	CBF
FCYH	FB-03-02-270	5437714.00	413121.00	3	CBF
FCYH	FB-03-02-271	5437683.00	413176.00	0	CBF
FCYH	FB-03-02-272	5437650.00	413224.00	0	MAP
FCYH	FB-03-02-273	5437593.00	413263.00	3	RBA
FCYH	FB-03-02-274	5437555.00	413293.00	0	RBA
FCYH	FB-03-02-275	5437533.00	413325.00	9	RBA
FCYH	FB-03-02-276	5437491.00	413355.00	9	RBA
FCYH	FB-03-02-277	5437482.00	413407.00	0	MAP
FCYH	FB-03-02-278	5437440.00	413436.00	0	RBA
FCYH	FB-03-02-279	5437376.00	413495.00	0	RBA
FCYH	FB-03-02-280	5437367.00	413527.00	0	CBF
FCYH	FB-03-02-281	5437384.00	413585.00	0	CBF
FCYH	FB-03-02-282	5437384.00	413644.00	2	CBF
FCYH	FB-03-02-283	5437373.00	413679.00	0	CBF
FCYH	FB-03-02-284	5437372.00	413704.00	4	CBF
FCYH	FB-03-02-285	5437404.00	413776.00	6	CBF
FCYH	FB-03-02-286	5437386.00	413836.00	6	MAP
FCYH	FB-03-02-287	5437363.00	413868.00	0	BMDB
FCYH	FB-03-02-288	5437350.00	413881.00	0	BCA
FCYH	FB-03-02-289	5437307.00	413919.00	11	BMDB
FCYH	FB-03-02-290	5437266.00	413964.00	0	BMDB
FCYH	FB-03-02-291	5437273.00	414018.00	0	
FCYH	FB-03-02-292	5437259.00	414068.00	0	BMDB
FCYH	FB-03-02-293	5437210.00	414118.00	0	RBA
FCYH	FB-03-02-294	5437173.00	414174.00	0	MAP

List of field stations and co-ordinates

Projection UTM **Datum:** NAD27 **Zone** 21

Project	Stations	Northing	Easting	Altitude (m)	Lithology
FCYH	FB-04-02-295	5437156.00	414239.00	0	MLG
FCYH	FB-04-02-296	5437153.00	414270.00	1	MLG
FCYH	FB-04-02-297	5437148.00	414290.00	0	MLG
FCYH	FB-04-02-298	5437165.00	414398.00	0	BMDB
FCYH	FB-04-02-299	5437215.00	414291.00	13	VOLC
FCYH	FB-04-02-300	5437207.00	414493.00	13	BMDB
FCYH	FB-04-02-301	5437355.00	414481.00	3	MLG
FCYH	FB-04-02-302	5437484.00	414441.00	6	BMDB
FCYH	FB-04-02-303	5437564.00	414417.00	8	MLG
FCYH	FB-04-02-304	5437632.00	414395.00	7	BMDB
FCYH	FB-04-02-305	5437673.00	414383.00	9	BMDB
FCYH	FB-04-02-306	5437694.00	414377.00	8	BMDB
FCYH	FB-04-02-307	5439401.00	410233.00	0	BMDB
FCYH	FB-04-02-308	5439424.00	410214.00	1	BMDB
FCYH	FB-04-02-309	5439431.00	410187.00	18	BMDB
FCYH	FB-04-02-310	5439265.00	410068.00	2	BMDB
FCYH	FB-04-02-311	5435698.00	403143.00	0	BMDB
FCYH	FB-04-02-312	5435751.00	403131.00	0	BMDB
FCYH	FB-04-02-313	5435851.00	403113.00	2	BMDB
FCYH	FB-04-02-314	5435637.00	403062.00	3	BMDB
FCYH	FB-04-02-315	5435656.00	403105.00	4	BMDB
FCYH	FB-04-02-316	5435673.00	403121.00	1	BMDB
FCYH	FB-04-02-317	5435637.00	403048.00	2	BMDB
FCYH	FB-04-02-318	5435520.00	402690.00	0	BMDB
FCYH	FB-04-02-319	5435502.00	402633.00	1	BMDB
FCYH	FB-04-02-320	5435510.00	402605.00	0	BMDB
FCYH	FB-04-02-321	5435533.00	402515.00	0	BMDB
FCYH	FB-04-02-322	5435533.00	402493.00	0	BMDB
FCYH	FB-04-02-323	5435533.00	402457.25	0	BMDB
FCYH	FB-04-02-324	5435530.00	402445.00	2	BMDB
FCYH	FB-04-02-325	5435499.00	402383.00	2	BMDB
FCYH	FB-04-02-326	5435494.00	402347.00	4	BMDB
FCYH	FB-04-02-327	5435478.00	402303.00	7	BMDB
FCYH	FB-04-02-328	5435434.00	402226.00	1	BMDB
FCYH	FB-04-02-329	5435420.00	402201.00	1	BMDB
FCYH	FB-04-02-330	5435409.00	402184.00	1	BMDB
FCYH	FB-04-02-331	5434067.00	401825.00	0	BMDB
FCYH	FB-04-02-332	5434109.00	401857.00	12	BMDB
FCYH	FB-04-02-455	5432675.00	413547.00	139	MAP
FCYH	FB-04-02-456	5432348.00	413450.00	145	VOLC
FCYH	FB-04-02-457	5432295.00	413444.00	186	VOLC

List of field stations and co-ordinates

Projection UTM **Datum:** NAD27 **Zone** 21

Project	Stations	Northing	Easting	Altitude (m)	Lithology
FCYH	FB-04-02-458	5432209.00	413404.00	192	VOLC
FCYH	FB-04-02-459	5431997.00	413179.00	259	VOLC
FCYH	FB-04-02-460	5432010.00	412945.00	267	BMDB
FCYH	FB-04-02-461	5432033.00	412905.00	180	BMDB
FCYH	FB-04-02-462	5432068.00	412915.00	189	BMDB
FCYH	FB-04-02-463	5432097.00	412914.00	194	BMDB
FCYH	FB-04-02-464	5432122.00	412905.00	193	BMDB
FCYH	FB-04-02-465	5432158.00	412884.00	182	MLG
FCYH	FB-04-02-466	5432261.00	412841.00	178	
FCYH	FB-04-02-467	5432692.00	412569.00	134	BMDB
FCYH	FB-04-02-468	5432811.00	412472.00	104	BMDB
FCYH	FB-04-02-469	5432899.00	412465.00	103	BMDB
FCYH	FB-04-02-470	5432961.00	412395.00	103	BMDB
FCYH	FB-04-02-471	5432986.00	412297.00	103	BMDB
FCYH	FB-04-02-472	5433013.00	412289.00	108	BMDB
FCYH	FB-04-02-473	5433032.00	412277.00	111	BMDB
FCYH	FB-04-02-474	5433057.00	412270.00	111	BMDB
FCYH	FB-04-02-475	5433070.00	412270.00	108	BMDB
FCYH	FB-04-02-476	5433112.00	412248.00	103	BMDB
FCYH	FB-04-02-477	5433174.00	412219.00	104	BMDB
FCYH	FB-04-02-478	5433192.00	412215.00	97	BMDB
FCYH	FB-04-02-479	5433308.00	412169.00	87	BMDB
FCYH	FB-05-02-480	5433864.00	413641.00	51	RBA
FCYH	FB-05-02-481	5433794.00	413629.00	56	RBA
FCYH	FB-05-02-482	5433659.00	413569.00	69	RBA
FCYH	FB-05-02-483	5433563.00	413478.00	76	IT
FCYH	FB-05-02-484	5433539.00	413461.00	73	BMDB
FCYH	FB-05-02-485	5433510.00	413425.00	71	BMDB
FCYH	FB-05-02-486	5433470.00	413399.00	102	MLG
FCYH	FB-05-02-524	5441928.00	410918.00	9	BMDB
FCYH	FB-05-02-525	5441222.00	410943.00	6	VOLC
FCYH	FB-05-02-526	5439810.00	409715.72	0	BMDB
FCYH	FB-05-02-527	5439833.50	409693.28	0	BMDB
FCYH	FB-05-02-528	5439846.00	409683.19	0	BMDB
FCYH	FB-05-02-529	5439865.00	409671.97	0	BMDB
FCYH	FB-05-02-530	5439890.00	409503.63	0	BMDB
FCYH	FB-05-02-531	5439810.00	409489.03	0	BMDB
FCYH	FB-05-02-532	5439695.50	409454.22	0	BMDB
FCYH	FB-05-02-533	5439727.00	409505.84	0	BMDB
FCYH	FB-05-02-534	5439771.00	409632.69	0	BMDB
FCYH	FB-05-02-535	5439821.50	409781.94	0	BMDB

List of field stations and co-ordinates

Projection UTM **Datum:** NAD27 **Zone** 21

Project	Stations	Northing	Easting	Altitude (m)	Lithology
FCYH	FB-05-02-536	5441839.00	409656.25	0	BMDB
FCYH	FB-05-02-537	5441460.00	409784.19	0	BMDB
FCYH	FB-05-02-538	5441411.50	409833.56	0	BMDB
FCYH	FB-05-02-539	5441311.00	409866.72	0	BMDB
FCYH	FB-05-02-540	5441158.00	410009.75	0	BMDB
FCYH	FB-05-02-541	5440496.00	410563.28	0	BMDB
FCYH	FB-05-02-542	5440552.50	410461.94	0	BMDB
FCYH	FB-05-02-543	5440748.50	410393.81	0	BMDB
FCYH	ILNDCOVE	5435874.50	405862.13	2	BMDB
FCYH	J0201	5434929.00	412853.13	12	BMDB
FCYH	J0202	5434908.50	412795.09	6	BMDB
FCYH	J0203	5434862.50	412678.13	7	BMDB
FCYH	J0204	5434894.00	412605.03	6	BMDB
FCYH	J0205	5434886.00	412540.53	5	BMDB
FCYH	J0206	5434854.50	412502.13	4	BMDB
FCYH	J0207	5434834.00	412432.97	8	BMDB
FCYH	J0208	5434806.50	412364.50	11	BMDB
FCYH	J0209	5434801.50	412340.47	6	BMDB
FCYH	J0210	5434848.00	412252.88	1	BMDB
FCYH	J0211	5433605.50	412891.69	35	BMDB
FCYH	J0401	5433574.00	412725.38	37	BMDB
FCYH	J0403	5433528.50	412871.53	69	BMDB
FCYH	J0404	5433565.00	412937.09	79	BMDB
FCYH	J0405	5433692.50	412775.97	78	BMDB
FCYH	J0406	5434809.50	411940.91	22	BMDB
FCYH	J0407	5434875.00	411902.34	1	BMDB
FCYH	J0408	5434891.00	411918.25	2	BMDB
FCYH	J0409	5434891.00	411887.25	2	BMDB
FCYH	J0410	5435034.00	411689.47	2	BMDB
FCYH	J0411	5435048.00	411575.63	9	BMDB
FCYH	J0412	5435058.00	411502.81	2	BMDB
FCYH	J0413	5435066.50	411445.22	1	BMDB
FCYH	J0501	5435095.00	411351.50	1	BMDB
FCYH	J0502	5435109.50	411330.53	2	BMDB
FCYH	J0503	5435099.50	411257.31	1	BMDB
FCYH	J0504	5435102.00	411234.56	2	BMDB
FCYH	J0601	5435107.50	411196.72	1	BMDB
FCYH	J0602	5435107.00	411151.56	1	BMDB
FCYH	J0603	5435111.00	411117.88	0	BMDB
FCYH	J0604	5435066.00	411002.38	0	BMDB
FCYH	J0605	5435057.50	410974.63	0	BMDB

List of field stations and co-ordinates

Projection UTM **Datum:** NAD27 **Zone** 21

Project	Stations	Northing	Easting	Altitude (m)	Lithology
FCYH	J0606	5435054.50	410943.88	2	BMDB
FCYH	J0607	5435017.50	410898.72	2	BMDB
FCYH	J0608	5435027.50	410885.81	1	BMDB
FCYH	J0609	5435032.50	410878.34	0	BMDB
FCYH	J0610	5435026.00	410841.13	2	BMDB
FCYH	J0611	5435022.50	410816.31	1	BMDB
FCYH	J0612	5435044.50	410799.63	1	BMDB
FCYH	J0613	5435033.00	410771.91	2	BMDB
FCYH	J0614	5435022.00	410705.09	2	BMDB
FCYH	J0615	5435021.00	410597.75	2	BMDB
FCYH	J0616	5435010.50	410568.88	1	BMDB
FCYH	J0701	5435546.50	408878.28	1	BMDB
FCYH	J0702	5435548.50	408876.91	0	BMDB
FCYH	J0703	5435399.00	409003.78	1	BMDB
FCYH	J0704	5435363.50	409036.09	1	BMDB
FCYH	J0705	5435346.00	409105.19	1	BMDB
FCYH	J0706	5435348.50	409225.06	2	BMDB
FCYH	J0707	5435331.00	409261.91	0	BMDB
FCYH	J0708	5435302.00	409278.38	1	BMDB
FCYH	J0709	5435219.00	409515.94	2	BMDB
FCYH	J0710	5435165.00	409565.47	2	BMDB
FCYH	J0711	5435152.00	409605.38	2	BMDB
FCYH	J0712	5435113.50	409637.63	2	BMDB
FCYH	J0713	5435058.00	409650.66	27	BMDB
FCYH	J0801	5435653.50	403098.03	1	BMDB
FCYH	J0802	5435649.50	403070.13	2	BMDB
FCYH	J0803	5435671.50	403064.66	0	BMDB
FCYH	J0804	5435627.50	403042.72	2	BMDB
FCYH	J0807	5435610.00	402978.84	0	BMDB
FCYH	J0808	5435622.50	402947.88	2	BMDB
FCYH	J0809	5435615.00	402935.16	3	BMDB
FCYH	J0810	5435609.50	402922.00	2	BMDB
FCYH	J0901	5435685.00	403137.88	1	BMDB
FCYH	J0902	5435672.50	403129.88	0	BMDB
FCYH	J0903	5435658.50	403107.63	2	BMDB
FCYH	J0904	5435647.00	403060.09	1	BMDB
FCYH	J0905	5435629.50	403009.88	2	BMDB
FCYH	J0906	5435503.00	402683.16	2	BMDB
FCYH	J0907	5435517.00	402620.72	1	BMDB
FCYH	J0908	5435539.00	402493.19	1	BMDB
FCYH	J0909	5435545.50	402474.38	1	BMDB

List of field stations and co-ordinates

Projection UTM **Datum:** NAD27 **Zone** 21

Project	Stations	Northing	Easting	Altitude (m)	Lithology
FCYH	J0910	5435541.00	402463.41	1	BMDB
FCYH	J0911	5435534.50	402441.31	0	BMDB
FCYH	J0912	5435537.50	402428.19	3	BMDB
FCYH	J0913	5435524.00	402411.22	2	BMDB
FCYH	J0914	5435523.00	402405.38	1	BMDB
FCYH	J0915	5435476.00	402300.56	1	BMDB
FCYH	J0916	5435476.50	402278.88	1	BMDB
FCYH	J0917	5435457.00	402253.69	0	BMDB
FCYH	J0918	5435448.50	402223.44	0	BMDB
FCYH	J0919	5435428.00	402192.47	1	BMDB
FCYH	J1001	5435091.50	409992.38	1	BMDB
FCYH	J1002	5435074.00	409957.00	0	BMDB
FCYH	J1003	5435061.50	409957.63	0	BMDB
FCYH	J1106	5435065.50	410008.69	1	BMDB
FCYH	J1107	5435059.00	410004.97	2	BMDB
FCYH	J1108	5435051.50	410046.66	2	BMDB
FCYH	J1109	5435049.50	410075.06	3	BMDB
FCYH	J1110	5435031.00	410082.88	3	BMDB
FCYH	J1111	5435035.00	410104.63	2	BMDB
FCYH	J1112	5435037.00	410125.25	3	BMDB
FCYH	J1113	5435030.00	410141.09	7	BMDB
FCYH	J1501	5434913.50	413033.59	4	MLG
FCYH	J1502	5434927.50	413066.63	0	MLG
FCYH	J1503	5434964.00	413067.69	0	MLG
FCYH	J1504	5434967.00	413087.03	2	MLG
FCYH	J1505	5434967.00	413091.19	2	MLG
FCYH	J1506	5434887.50	413135.91	2	MLG
FCYH	J1507	5434889.50	413137.63	3	MLG
FCYH	J1508	5434817.00	413173.59	4	IT
FCYH	J1509	5434778.50	413217.00	3	IT
FCYH	J1601	5435925.50	406932.63	3	BMDB
FCYH	J1602	5435955.00	406832.81	1	BMDB
FCYH	J1702	5439079.50	401014.88	2	
FCYH	J1703	5439037.50	401009.75	10	
FCYH	J1704	5439056.50	401041.47	12	
FCYH	J1801	5435959.00	406788.38	1	BMDB
FCYH	J1802	5435959.00	406788.00	0	BMDB
FCYH	J1803	5435959.00	406788.00	0	
FCYH	J1804	5435959.00	406788.00	0	BMDB
FCYH	J1806	5435959.00	406788.00	0	BMDB
FCYH	J2401	5432823.00	411069.81	19	BMDB

List of field stations and co-ordinates

Projection UTM **Datum:** NAD27 **Zone** 21

Project	Stations	Northing	Easting	Altitude (m)	Lithology
FCYH	J2402	5433007.50	411087.09	44	BMDB
FCYH	J2403	5433027.00	411128.34	68	BMDB
FCYH	J2404	5433081.50	411137.25	62	BMDB
FCYH	J2405	5433106.00	411123.75	65	BMDB
FCYH	J2406	5433109.00	411084.31	65	BMDB
FCYH	J2407	5433119.00	411060.38	53	BMDB
FCYH	J2408	5433242.00	410976.09	63	BMDB
FCYH	J2409	5433312.50	411014.50	51	BMDB
FCYH	J2410	5433356.00	410919.44	48	BMDB
FCYH	J2411	5433454.00	410832.59	70	BMDB
FCYH	J2501	5430982.50	412230.38	109	
FCYH	J2502	5430871.50	412575.94	121	VOLC
FCYH	J2801	5434708.00	413317.38	11	RBA
FCYH	JN1702	5438460.00	401018.25	2	
FCYH	JN1901	5434682.50	410442.34	16	BMDB
FCYH	JN1902	5434290.00	410530.50	0	BMDB
FCYH	JN1903	5434175.00	410549.25	0	BMDB
FCYH	JN1904	5434007.50	410570.50	0	BMDB
FCYH	JN2101	5435608.50	406284.06	54	BMDB
FCYH	JN2102	5435856.50	405800.81	2	BMDB
FCYH	JN2103	5435871.00	405860.09	2	BMDB
FCYH	JN2104	5435872.00	405909.72	0	BMDB
FCYH	JN2105	5435879.50	405994.59	3	BMDB
FCYH	JN2106	5435916.50	406161.34	0	BMDB
FCYH	JN2107	5435927.00	406398.38	1	BMDB
FCYH	JN2108	5435999.50	406538.69	3	BMDB
FCYH	JN2109	5436012.50	406568.13	1	BMDB
FCYH	JN2201	5435984.00	406630.94	1	BMDB
FCYH	JN2202	5435980.50	406766.91	2	BMDB
FCYH	JN2203	5435935.00	407016.63	2	BMDB
FCYH	JN2501	5435882.50	405987.13	2	BMDB
FCYH	JN2502	5435925.00	407046.28	4	BMDB
FCYH	JN2503	5435924.00	407031.78	7	BMDB
FCYH	JN2701	5435874.50	405862.13	2	BMDB
FCYH	JN3001	5435931.00	407029.63	2	BMDB
FCYH	JN3002	5435928.50	407015.13	3	BMDB
FCYH	JN3003	5435933.00	406953.91	1	BMDB
FCYH	S0101	5434907.50	412999.72	0	
FCYH	S0102	5434940.00	413055.06	0	BMDB
FCYH	S0103	5434965.00	413080.28	0	
FCYH	S0104	5434325.00	414284.00	0	

List of field stations and co-ordinates

Projection UTM **Datum:** NAD27 **Zone** 21

Project	Stations	Northing	Easting	Altitude (m)	Lithology
FCYH	S0201	5434762.50	413245.88	0	RBA
FCYH	S0202	5434736.00	413295.16	0	RBA
FCYH	S0203	5434716.00	413306.53	0	RBA
FCYH	S0204	5434700.00	413319.44	0	RBA
FCYH	S0205	5434629.00	413391.41	0	CBF
FCYH	S0206	5434612.00	413420.38	3	CBF
FCYH	S0207	5434486.00	414440.66	0	
FCYH	S0208	5434495.50	414402.09	0	
FCYH	S0209	5434483.50	414375.59	0	
FCYH	S0301	5438233.50	411637.50	2	BMDB
FCYH	S0302	5438209.50	411689.69	0	BMDB
FCYH	S0303	5438197.00	411715.78	0	VOLC
FCYH	S0304	5438153.00	411736.97	1	VOLC
FCYH	S0305	5438122.00	411749.63	1	VOLC
FCYH	S0306	5438086.50	411800.91	0	VOLC
FCYH	S0307	5438112.50	411858.28	0	VOLC
FCYH	S0308	5438155.50	411941.47	0	BMDB
FCYH	S0309	5438191.00	411950.09	0	BMDB
FCYH	S0310	5438223.50	411984.91	6	BMDB
FCYH	S0311	5438263.50	412014.03	0	BMDB
FCYH	S0401	5434457.00	414359.84	0	MAP
FCYH	S0402	5434409.50	414343.03	0	
FCYH	S0403	5438237.50	412363.41	0	MAP
FCYH	S0404	5438222.00	412385.78	0	MAP
FCYH	S0405	5438208.00	412415.50	0	BMDB
FCYH	S0406	5438186.50	412435.63	0	BMDB
FCYH	S0407	5438252.00	412300.09	0	BMDB
FCYH	S0408	5438309.00	412130.13	0	BMDB
FCYH	S0409	5434362.00	414317.44	0	MAP
FCYH	TC-Seal	5437114.00	404840.25	0	BMDB
FCYH	TC-SS-00-07	5438480.00	401170.00	0	VOLC
FCYH	TC-SS-00-08	5438490.00	401190.00	0	MAP
FCYH	TC-SS-00-16	5439080.00	401060.00	0	CBF
FCYH	TC-SS-00-17	5439130.00	401080.00	0	BMDB
FCYH	TC-SS-00-18	5439140.00	401090.00	0	BMDB
FCYH	TC-SS-00-19	5439270.00	401130.00	0	BMDB
FCYH	TC-SS-00-50	5438520.00	401250.00	0	EI
FCYH	TC-SS-00-51	5438530.00	401300.00	0	EI
FCYH	TC-SS-00-61	5437050.00	405100.00	0	BMDB
FCYH	TC-SS-00-61a	5437060.00	405180.00	0	BMDB
FCYH	TC-SS-00-61b	5437080.00	405220.00	0	BMDB

List of field stations and co-ordinates

Projection UTM **Datum:** NAD27 **Zone** 21

Project	Stations	Northing	Easting	Altitude (m)	Lithology
FCYH	TC-SS-00-61c	5437170.00	405210.00	0	BMDB
FCYH	TC-SS-00-61d	5437180.00	405110.00	0	BMDB
FCYH	TC-SS-00-62	5437150.00	405030.00	0	BMDB
FCYH	TC-SS-00-62a	5437070.00	404960.00	0	BMDB
FCYH	TC-SS-00-62b	5437210.00	404890.00	0	BMDB
FCYH	TC-SS-00-63	5437220.00	404740.00	0	BMDB
FCYH	TC-SS-00-64	5437060.00	404730.00	0	BMDB
FCYH	TC-SS-00-65	5437030.00	404890.00	0	BMDB
FCYH	TC-SS-00-66	5437010.00	404570.00	0	BMDB
FCYH	TC-SS-00-66a	5437000.00	404510.00	0	BMDB
FCYH	TC-SS-00-66b	5437000.00	404490.00	0	BMDB
FCYH	TC-SS-00-66c	5437020.00	404460.00	0	BMDB
FCYH	TC-SS-00-67	5433470.00	401100.00	0	
FCYH	TC-SS-00-68	5433080.00	401400.00	0	

Appendix C

Geochemistry analysis

MUN-XRF Trace T020220T

pressed pellet: 5.0000 g sample + 0.7000 g Phenolic Resin (Sept. 1992)

Station	Sample#	Rock	Na2O wt%	MgO wt%	Al2O3 wt%	SiO2 wt%	P2O5 wt%	S ppm	Cl ppm	K2O wt%
S0306	S0306-01	Volcanic	4.3400002	10.74	13.2	49.619999	0.095	51	63	0.06

Station	Sample#	Rock	CaO wt%	Sc ppm	TiO2 wt%	V ppm	Cr ppm	MnO wt%	Fe203T wt%	Ni ppm
S0306	S0306-01	Volcanic	7.1300001	32	0.96	268	264	0.181	10.89	48

Station	Sample#	Rock	Cu ppm	Zn ppm	Ga ppm	As ppm	Rb ppm	Sr ppm	Y ppm	Zr ppm
S0306	S0306-01	Volcanic	23	36	17	-1	0.3	129.5	19.200001	53.400002

Station	Sample#	Rock	Nb ppm	Ba ppm	Ce ppm	Pb ppm	Th ppm	U ppm	Total
S0306	S0306-01	Volcanic	1.3	-1	-1	8	-1	-1	97.37

Note: total is calculated as all oxides (i.e. elemental values converted to oxide values for total only.)

ert I

of the
ork Harbour area,
ewfoundland

Chris Buchanan